DISCLAIMER

SRC Technical Notes are informal memos intended for internal communication and documentation of work in progress. These notes are not necessarily definitive and have not undergone a pre-publication review. If you rely on this note for purposes other than its intended use, you assume all risk associated with such use.

University of Wisconsin-Synchrotron Radiation Center TECHNICAL NOTE	**File No.** SRC-218	**Page** 1 of 66
Subject: **Two-stage bunch compression with resistive impedance approximation of coherent synchrotron radiation**	**Author(s):** **R. A. Bosch**	
	Date: **June 8, 2007**	

Two-stage bunch compression, where each stage compresses a chirped beam in a magnetic chicane, may be utilized in the design of a driver for a free-electron laser (FEL). For the high currents required of an FEL, compressor performance may be adversely affected by the wake of coherent synchrotron radiation (CSR). When the CSR wake is dominated by edge radiation downstream of the chicane magnets, it may be approximated as the wake from resistive impedance. For a typical bunch-compressor chicane magnet, this approximation applies for wavelengths exceeding 1 micron.

For a preliminary two-stage bunch compressor design that compresses by a factor of twenty, longitudinal tracking with resistive impedance approximates the longitudinal phase space obtained from three-dimensional tracking with computed CSR. By approximating CSR as resistive impedance, longitudinal CSR effects may be studied analytically, and tracking with "CSR" may be performed without modeling the transverse dynamics.

With this approximation, we develop formulas that describe when part of the bunch becomes upright in phase space, producing a large current spike and energy depression. The formulas correctly predict good performance when Gaussian bunches with peak current of 50 A and rms bunch length σ_z of 1 mm are compressed, and that the bunch tail becomes upright in phase space when parabolic bunches with peak current of 50 A and σ_z of 0.4 mm are compressed. The formulas also show how the compressor design may be modified to prevent the upright bunch behavior with the shorter bunch length.

We obtain analytic formulas for the jitter in the bunch arrival time resulting from bunch-to-bunch variation in current, energy and chirp. The formulas determine the permitted variations that give arrival-time jitter less than 15 fs in the preliminary design. Bunch-to bunch peak current variation should be less than 6.5 A, which is 13% of the peak current. The bunch-to-bunch energy variation should be less than 5.6 keV, which is 4.5×10^{-5} times the bunch energy when entering the compressor. The bunch-to-bunch chirp variation should be less than 3.3×10^{7} eV/m, which is 3% of the design chirp.

Analytic small-signal gain formulas for microbunching describe the output current and energy modulations that result from given input current and energy modulations, including the suppression at short wavelengths by the bunch's energy spread. Large output modulations of the bunch current may be caused by relatively small input energy modulations. Heating the uncompressed bunches by a laser heater so that the energy spread is 5-10 keV is predicted to suppress microbunching for initial wavelengths less than 100 microns. In this case, initial energy modulations at wavelengths around 100 microns should be smaller than ~500 eV to prevent large current modulations in the compressed bunches.

1. INTRODUCTION

Two-stage bunch compression, where each stage compresses a chirped beam in a magnetic chicane, may be utilized in an FEL driver [1]. The wake of coherent synchrotron radiation (CSR) in the chicane magnets may adversely affect the macroscopic current profile of the compressed bunch and/or cause microbunching [2, 3, 4, 5]. In this note, we consider wavelengths for which a chicane magnet's CSR may be approximated by resistive impedance $\sim Z_0$ resulting from coherent edge radiation downstream of the magnet [6], where $Z_0 = 377\ \Omega$. This approximation applies for wavelengths where the edge-radiation formation length exceeds that of ordinary synchrotron radiation within small-angle chicane bending magnets. For a magnet in which the electron orbit has radius of curvature 1 m and the electron energy exceeds 125 MeV, this approximation applies for wavelengths $\lambda > 1\,\mu\text{m}$. For shorter wavelengths, the CSR impedance Z_{CSR} depends weakly on wavelength (for ordinary synchrotron radiation, $|Z_{\text{CSR}}| \propto \lambda^{-1/3}$ [4]). Therefore, resistive wakes may also roughly approximate wavelengths shorter than 1 μm.

Consider a bunch compressor chicane in which a chirped beam is under compressed and affected by CSR from edge radiation. The bunch is fully compressed upon its exit from the 2nd-to-last magnet of the chicane, so that the coherent edge radiation wake from the last two bending magnets dominates. If we approximate the impedance from each of these magnets as Z_0, their combined impedance of $\sim 2Z_0$ acts upon the bunch after its compression. The precise value of the impedance depends upon the bunchlength, radius of curvature within the bending magnet, relativistic factor γ, and the vacuum chamber dimensions [6]. For the bunch compressor modeled in this report, we find that a resistive impedance of $3Z_0 = 1131\ \Omega$ approximates particle tracking with computed CSR.

A preliminary two-stage bunch compressor design compresses a bunch with peak current of 50 A by a factor of twenty to obtain a peak current of 1 kA. Longitudinal tracking without wakes using the code LiTrack [7] is shown in fig. 1 for a trapezoidal bunch of 100,000 particles with flattop of 2 mm, peak current of 50 A and Gaussian energy spread of 1 keV. At the head and tail, the bunch current drops linearly to zero over a distance of 1 mm. The bunch is accelerated from initial energy of 4 MeV to 144 MeV in TESLA 1.3-GHz superconducting cavities, with the bunch center at a linac phase 15° earlier than the peak. Passage through superconducting 3.9-GHz harmonic cavities approximately linearizes the chirp while decreasing the energy of the bunch center to 125 MeV. At energy $E_1 = 125$ MeV, the first bunch compressor chicane BC1 has transfer matrix element $R_{56}^{(1)} = -0.0977$ m, compressing the chirped bunch by the ratio $C_1 = 5$. The bunch is then accelerated in 1.3-GHz cavities to energy of 600 MeV, with the bunch center at a linac phase 4.5° earlier than peak. At energy $E_2 = 600$ MeV, the second bunch compressor chicane BC2 has transfer matrix element $R_{56}^{(2)} = -0.07349$ m, compressing the chirped bunch by the ratio $C_2 = 4$. The fully compressed bunch is then accelerated in 1.3-GHz cavities to energy of 1700 MeV, with the bunch center at a linac phase 38° later than peak in order to dechirp the bunch. The bunch-compressor parameters are given in Table I.

In fig. 2, the fully compressed bunch at 1700 MeV is shown when a resistive impedance of strength $3Z_0$ is modeled after each bunch compressor using a modified version of LiTrack. In figs. 2(a) and 2(b), the initial Gaussian energy spreads are 1 keV and 3 keV, respectively. The bunch is apparently affected by microbunching that has grown from numerical noise. Fig. 2(c) shows tracking when the initial energy spread is 10 keV. With this large energy spread, the microbunching is suppressed, so that the central portion of the bunch has uniform energy and current. For a trapezoidal bunch affected by resistive impedance, the head, flattop portion, and tail form line segments in phase space.

Figure 3 shows tracking of a Gaussian bunch with peak current of 50 A and rms bunchlength of 1 mm, for initial energy spreads of 1, 3 and 10 keV.

In fig. 4, we show computed lattice functions when this bunch compressor design is implemented with FODO focusing in the linacs, using 5° bending magnets in BC1 and 2.5° bending magnets in BC2. For this computation, we used the MAD-with-acceleration code [8], modified by DESY to model the transverse focusing in a standing wave cavity [9]. In fig. 5, we show bunch properties at 1.7 GeV from tracking by the code "elegant" [10] of a trapezoidal bunch of 100,000 particles with flattop current of 50 A and normalized emittance of 1 μm. The initial longitudinal bunch distributions are the same as those tracked in fig. 2. Coherent synchrotron radiation is modeled in the chicane bending magnets and downstream drift regions with the "use_stupakov" method.

In fig. 6, we show bunch properties at 1.7 GeV when Gaussian bunches with peak current of 50 A and σ_z = 1 mm are tracked with CSR by the "elegant" code.

A comparison of figs. 2–3 with figures 5–6 indicates that the CSR effects observed in "elegant" tracking are approximated by the resistive wakes in our modified-LiTrack tracking.

2. NOTATION

Consider a bunch compressor in which a cold chirped beam is compressed in two chicanes (BC1 and BC2) and affected by CSR from edge radiation, approximated by resistive impedance after each chicane. At the entrance of the first bunch compressor BC1, let $z = ct_{\text{arrival}}$ parameterize the bunch with $z = 0$ for the reference particle and $z > 0$ at the tail, where c is the speed of light. Let $\varepsilon(z)$ describe the energy distribution and $I(z)$ the magnitude of the bunch current. The magnitude of the electron charge is e.

BC1 compresses at energy E_1, where the bunch has linear energy chirp $d\varepsilon/dz = S_1$. After the bunch exits BC1 and traverses the impedance R_1, let z_1 parameterize the bunch, with energy profile $\varepsilon_1(z_1)$ and current magnitude profile $I_1(z_1)$. The bunch compression results from the transfer matrix element $R_{56}^{(1)} = \partial z_1 / \partial\{[\varepsilon(z) - E_1]/E_1\}$. Letting $T_1 \equiv R_{56}^{(1)}/E_1$, the compression ratio C_1 obeys $C_1^{-1} = 1 + T_1 S_1$ and $C_1 = 1 - C_1 T_1 S_1$, where $C_1 > 0$ for undercompression and $C_1 < 0$ for overcompression in which the head and tail of the bunch are exchanged. For compression in a chicane, $R_{56}^{(1)}$ is negative, so $T_1 < 0$ and $S_1 > 0$.

The linac section between bunch compressor BC1 and bunch compressor BC2 imparts energy $E_2 - E_1$ and additional energy chirp S_2. Let $\varepsilon_L(z_1)$ describe the energy profile after this linac section, with total chirp (for a zero-current bunch) $d\varepsilon_L/dz_1 = S_2 + C_1 S_1$.

BC2 compresses at energy E_2. After the bunch exits BC2 and traverses the impedance R_2, let z_2 parameterize the bunch, with energy profile $\varepsilon_2(z_2)$ and current magnitude profile $I_2(z_2)$. The bunch compression results from the transfer matrix element $R_{56}^{(2)} = \partial z_2 / \partial\{[\varepsilon_L(z_1) - E_2]/E_2\}$. Letting $T_2 \equiv R_{56}^{(2)}/E_2$, the compression ratio C_2 obeys $C_2^{-1} = 1 + T_2(S_2 + C_1 S_1)$ and $C_2 = 1 - C_2 T_2(S_2 + C_1 S_1)$, where $C_2 > 0$ for undercompression and $C_2 < 0$ for overcompression. For compression in a chicane, $R_{56}^{(2)}$ is negative, so $T_2 < 0$.

3. CURRENT VARIATION

Let us first consider the effect of varying bunch current $I(z)$ at the entrance of the bunch compressor, where the chirped beam has energy $\varepsilon(z) = E_1 + S_1 z$. The compression is described by the transformation

$$z_1(z) = z + (R_{56}^{(1)} / E_1)(\varepsilon(z) - E_1) = z(1 + T_1 S_1) = z / C_1 \tag{1}$$

so that the inverse is $z(z_1) = C_1 z_1$. After compression, the current profile is

$$I_1(z_1) = I(z(z_1)) / (dz_1 / dz) = C_1 I(C_1 z_1) \tag{2}$$

After passing through the resistive wake of BC1, the energy profile is

$$\varepsilon_1(z_1) = \varepsilon(z(z_1)) - eR_1 I_1(z_1) = E_1 + S_1 C_1 z_1 - eR_1 C_1 I(C_1 z_1) \tag{3}$$

The bunch then passes through the linac section between BC1 and BC2, so that

$$\varepsilon_{\mathrm{L}}(z_1) = E_2 + (S_2 + S_1 C_1) z_1 - eR_1 C_1 I(C_1 z_1) \tag{4}$$

The effect of BC2 is

$$\begin{aligned} &z_2(z_1) = z_1 + (R_{56}^{(2)} / E_2)(\varepsilon_{\mathrm{L}}(z_1) - E_2) = z_1 / C_2 - T_2 eR_1 C_1 I(C_1 z_1), \\ &z_2(z) = z / C_1 C_2 - T_2 eR_1 C_1 I(z) \\ &dz_2 / dz = [1 - C_1^2 C_2 T_2 eR_1 I'(z)] / C_1 C_2 \end{aligned} \tag{5}$$

When $dz_2 / dz = 0$, part of the bunch is upright in phase space after BC2. This occurs where

$$I'(z) = I'_{\mathrm{crit}} = (C_1^2 C_2 T_2 eR_1)^{-1} = E_2 / (C_1^2 C_2 R_{56}^{(2)} eR_1) \tag{6}$$

If $I'(z) \neq I'_{\mathrm{crit}}$ for any value of z, $z_2(z)$ is invertible to obtain $z(z_2)$, and the current after BC2 and impedance R_2 is

$$I_2(z_2) = I(z(z_2)) / (dz_2 / dz) = C_1 C_2 I(z(z_2)) / [1 - C_1^2 C_2 T_2 eR_1 I'(z(z_2))] \ . \tag{7}$$

The bunch's energy profile after the resistive wake R_2 is

$$\begin{aligned} &\varepsilon_2(z_2) = \varepsilon_{\mathrm{L}}(z_1(z_2)) - eR_2 I_2(z_2) \\ &= E_2 + (S_1 + S_2 / C_1) z(z_2) - eR_1 C_1 I(z(z_2)) - eR_2 C_1 C_2 I(z(z_2)) / [1 - C_1^2 C_2 T_2 eR_1 I'(z(z_2))] \end{aligned} \tag{8}$$

4. ENERGY VARIATION

Now consider the effect of an energy variation $\Delta E(z)$ for a bunch with constant current. At the bunch compressor entrance, $I(z) = I_0$ and $\varepsilon(z) = E_1 + S_1 z + \Delta E(z)$. The BC1 compression obeys

$$z_1(z) = z + (R_{56}^{(1)} / E_1)(\varepsilon(z) - E_1) = z / C_1 + T_1 \Delta E(z), \tag{9}$$

with derivative

$$z_1'(z) = C_1^{-1}[1 + C_1 T_1 \Delta E'(z)]. \tag{10}$$

Part of the bunch is upright after the first compressor, for arbitrary current and impedance, when

$$\Delta E'(z) = -1 / C_1 T_1 = -E_1 / C_1 R_{56}^{(1)}. \tag{11}$$

The function $z_1(z)$ is invertible if its derivative is nonzero for all values of z, in which case we let $z(z_1)$ denote the inverse. After compression in BC1,

$$I_1(z_1) = \frac{I(z(z_1))}{dz_1/dz} = \frac{C_1 I_0}{1 + C_1 T_1 \Delta E'(z(z_1))} \tag{12}$$

After passing through the resistive wake of BC1,

$$\varepsilon_1(z_1) = \varepsilon(z(z_1)) - eR_1 I_1(z_1) = E_1 + S_1 z(z_1) + \Delta E(z(z_1)) - \frac{eR_1 C_1 I_0}{1 + C_1 T_1 \Delta E'(z(z_1))} \tag{13}$$

The bunch then passes through the linac section between BC1 and BC2, so that

$$\begin{aligned} \varepsilon_L(z_1) &= E_2 + S_2 z_1 + S_1 z(z_1) + \Delta E(z(z_1)) - \frac{eR_1 C_1 I_0}{1 + C_1 T_1 \Delta E'(z(z_1))} \\ &= E_2 + S_2\left(\frac{z(z_1)}{C_1} + T_1 \Delta E(z(z_1))\right) + S_1 z(z_1) + \Delta E(z(z_1)) - \frac{eR_1 C_1 I_0}{1 + C_1 T_1 \Delta E'(z(z_1))} \end{aligned} \tag{14}$$

The effect of BC2 is $z_2(z_1) = z_1 + (R_{56}^{(2)}/E_2)(\varepsilon_L(z_1) - E_2) = z_1 + T_2(\varepsilon_L(z_1) - E_2)$, so that

$$\begin{aligned} z_2(z) &= \frac{1}{C_1 C_2}\left[z + (C_1 T_1 + C_1^2 C_2 T_2)\Delta E(z) - \frac{C_1^2 C_2 T_2 eR_1 I_0}{1 + C_1 T_1 \Delta E'(z)} \right], \\ dz_2/dz &= \frac{1}{C_1 C_2}\left[1 + (C_1 T_1 + C_1^2 C_2 T_2)\Delta E'(z) + \frac{C_1^3 C_2 T_1 T_2 eR_1 I_0 \Delta E''(z)}{[1 + C_1 T_1 \Delta E'(z)]^2} \right]. \end{aligned} \tag{15}$$

When the RHS of eq. (15) is zero, an upright bunch occurs after BC2. The function $z_2(z)$ is invertible if its derivative is nonzero for all values of z, in which case we let $z(z_2)$ denote the inverse. The current profile after BC2 is

$$I_2(z_2) = \frac{I(z(z_2))}{dz_2/dz} = \frac{C_1 C_2 I_0}{1 + (C_1 T_1 + C_1^2 C_2 T_2)\Delta E'(z(z_2)) + \frac{C_1^3 C_2 T_1 T_2 eR_1 I_0 \Delta E''(z(z_2))}{[1 + C_1 T_1 \Delta E'(z(z_2))]^2}}. \tag{16}$$

After the resistive wake of BC2, the energy profile is

$$\begin{aligned} \varepsilon_2(z_2) &= E_2 + (S_1 + S_2/C_1) z(z_2) + (1 + S_2 T_1)\Delta E(z(z_2)) - \frac{eR_1 C_1 I_0}{1 + C_1 T_1 \Delta E'(z(z_2))} \\ &- \frac{eR_2 C_1 C_2 I_0}{1 + (C_1 T_1 + C_1^2 C_2 T_2)\Delta E'(z(z_2)) + \frac{C_1^3 C_2 T_1 T_2 eR_1 I_0 \Delta E''(z(z_2))}{[1 + C_1 T_1 \Delta E'(z(z_2))]^2}} \end{aligned} \tag{17}$$

5. UPRIGHT BUNCHES

Consider a trapezoidal bunch with flattop region where $I(z) = I_0$, in which the current at the head and tail drop linearly to zero over a distance Δz. According to eq. (6), the tail will be upright in phase space after BC2 (causing a current spike) for $\Delta z = \Delta z_{crit} = |R_{56}^{(2)} C_1^2 C_2 eR_1 I_0 / E_2|$. When the current spike passes through the resistive impedance of BC2, a large energy depression occurs, spoiling the trailing end of the flattop. This behavior is illustrated in fig. 7 by LiTrack results for our preliminary bunch-compressor design, where $\Delta z_{crit} = 0.69$ mm for an initial flattop current of 50 A and $R_1 = 3Z_0$.

For a Gaussian bunch with peak current I_0, eq. (6) predicts that an upright bunch tail region will occur when $\sigma_z \le \sigma_{z\_crit} = e^{-1/2} |R_{56}^{(2)} C_1^2 C_2 e R_1 I_0 / E_2|$, which equals 0.42 mm when I_0 = 50 A and $R_1 = 3Z_0$. Preliminary FEL parameters call for a bunch with I_0 = 50 A and σ_z = 1 mm, which comfortably exceeds σ_{z_crit} = 0.42 mm. Modified-LiTrack and "elegant" tracking (shown in figs 3 and 6) confirm that these bunches may be compressed without the bunch tail becoming upright.

Revised FEL parameters call for a parabolic bunch with peak current of 50 A and σ_z = 0.4 mm. For a parabolic bunch, an upright bunch tail region is predicted by eq. (6) when $\sigma_z \le \sigma_{z\_crit} = (2/\sqrt{5}) |R_{56}^{(2)} C_1^2 C_2 e R_1 I_0 / E_2|$, where σ_{z_crit} = 0.62 mm when I_0 = 50 A and $R_1 = 3Z_0$. For σ_z = 0.4 mm, tracking with modified-LiTrack in fig. 8 and "elegant" tracking in fig. 9 both confirm that the bunch tail becomes upright in phase space, resulting in a current spike. Consequently, the preliminary bunch compressor performance is not optimal for the revised bunch length of 0.4 mm. For example, when the compression of parabolic bunches is improved by tweaking the compressor parameters to compensate CSR wakes, moderate current spikes at the bunch head and/or tail remain.

For a fixed total bunch compression $C_1 C_2$, smaller values of Δz_{crit} and σ_{z_crit} may be obtained by decreasing the magnitude of the compression in BC1, decreasing $|R_{56}^{(2)}|$, or increasing E_2, thereby decreasing the relative energy chirp into BC2 resulting from the CSR impedance R_1. Such a modification would allow the compression of shorter bunches with a peak current of 50 A.

When the flattop portion of a trapezoidal bunch has a current modulation $I(z) = I_0 + \Delta I \cos(kz)$, eq. (6) predicts that upright bunch regions occur for $\Delta I = |E_2 / (C_1^2 C_2 k R_{56}^{(2)} e R_1)|$. This is illustrated in LiTrack results for an initial modulation with wavelength of 0.3333 mm in fig. 10(a)–(b). The effect is reduced when the bunch entering BC1 has a large Gaussian energy spread, as shown in fig. 10(c)–(d).

When part of a bunch has an excessively large chirp error $|\Delta E'(z)|$, eqs. (11) and (15) indicate that dz_1/dz and/or dz_2/dz may become zero, resulting in upright bunch segments. Upright bunch segments from excessive chirp at the head and tail are shown in fig. 11. The magnitude of $\Delta E'(z)$ that may be tolerated without causing an upright bunch after BC1 may be increased by decreasing $|C_1|$ or $|R_{56}^{(1)}|$ or by increasing E_1, so that a given $\Delta E'(z)$ causes less relative energy chirp into BC1. For a given total compression $C_1 C_2$, larger magnitudes of $\Delta E'(z)$ and $\Delta E''(z)$ may be tolerated without causing an upright bunch after BC2 when $|C_1|$, $|R_{56}^{(1)}|$ and $|R_{56}^{(2)}|$ are small while E_1 and E_2 are large.

Upright bunch behavior may also result from a periodic energy modulation of the form $\Delta E(z) = \Delta E \cos(kz)$. When wakefields are neglected, eq. (15) predicts upright bunch behavior after BC2 when $\Delta E = |(C_1 R_{56}^{(1)} / E_1 + C_1^2 C_2 R_{56}^{(2)} / E_2) k|^{-1}$. For the preliminary bunch compressor design studied here, an energy modulation with wavelength of 0.3333 mm is predicted to produce upright bunch behavior when ΔE = 3.28 keV, in agreement with modified-LiTrack modeling in figs. 12(a)–(b). For an approximate CSR wake $R_1 = 3Z_0$, eq. (15) predicts upright bunch behavior for ΔE = 948 eV, in agreement with modified-LiTrack modeling shown in figs. 12(c)–(d).

The upright bunch predictions for current and energy modulations (calculated for $R_1 = R_2 = 3Z_0$) are in approximate agreement with three-dimensional "elegant" tracking with computed CSR wakes.

6. JITTER

To seed compressed bunches with a laser, we would like the jitter in the bunch arrival time, Δt_2, to be smaller than 15 fs. Equations (5) and (15) may be used to provide estimates on the permitted bunch-to-bunch variation in current, energy and chirp such that $\Delta t_2 < 15$ fs.

From eq. (5), $\partial z_2(z)/\partial I(z) = -C_1 T_2 e R_1 = -C_1 (R_{56}^{(2)}/E_2) e R_1$, where $z_2 = ct_2$. To achieve arrival time jitter less than Δt_2, the bunch-to-bunch current variation ΔI must obey

$$\Delta I < |\, c\Delta t_2 E_2 / (R_{56}^{(2)} e R_1 C_1)\,| \tag{18}$$

For $\Delta t_2 = 15$ fs, ΔI must be less than 6.5 A (for $R_1 = 3Z_0$). Therefore, $\Delta I / I_0 < 13\%$ is required.

From eq. (15), $\partial z_2(z)/\partial \Delta E(z) = (C_1 C_2)^{-1}(C_1 T_1 + C_1^2 C_2 T_2)$. To achieve jitter less than Δt_2, the bunch-to-bunch energy variation ΔE at the entrance of BC1 must therefore obey

$$\Delta E < |\, c\Delta t_2 C_1 C_2 / (C_1 T_1 + C_1^2 C_2 T_2)\,| = |\, c\Delta t_2 C_1 C_2 / (C_1 R_{56}^{(1)}/E_1 + C_1^2 C_2 R_{56}^{(2)}/E_2)\,| \tag{19}$$

For $\Delta t_2 = 15$ fs, ΔE must be less than 5.6 keV, so that $\Delta E / E_1 < 4.5\times 10^{-5}$ is required. For single-stage compression, eq. (9) indicates that, to achieve jitter less than Δt, ΔE must obey $\Delta E < |\, c\Delta t / T_1\,| = |\, c\Delta t E_1 / R_{56}^{(1)}\,|$. For example, a single-stage compressor at energy E_1 of 500 MeV with $R_{56}^{(1)} = -0.1$ m requires that ΔE must be less than 22.5 keV, so that $\Delta E / E_1 < 4.5\times 10^{-5}$ is again required.

The bunch arrival time is insensitive to ΔE when $C_1 T_1 + C_1^2 C_2 T_2 = C_1 R_{56}^{(1)}/E_1 + C_1^2 C_2 R_{56}^{(2)}/E_2 = 0$, which requires over compression in one of the stages. [In this case, the total compression is also insensitive to chirp variation, since $\partial(C_1 C_2)/\partial S_1 = -C_1 C_2 (C_1 T_1 + C_1^2 C_2 T_2)$.] However, over compression may cause undesirable CSR and space-charge wakes where the bunch head and tail are exchanged.

From eq. (15), $\partial z_2(z)/\partial \Delta E'(z) = C_1^2 T_1 T_2 e R_1 I_0$ for $|\, C_1 T_1 \Delta E'(z)\,| << 1$. To achieve jitter less than Δt_2, the bunch-to-bunch chirp variation $\Delta E'$ must therefore obey

$$\Delta E' < c\Delta t_2 / (C_1^2 T_1 T_2 e R_1 I_0) = c\Delta t_2 E_1 E_2 / (C_1^2 R_{56}^{(1)} R_{56}^{(2)} e R_1 I_0) \tag{20}$$

For $\Delta t_2 =$ 15 fs, $\Delta E'$ must be less than 3.3×10^7 eV/m (for $R_1 = 3Z_0$). The design chirp is $d\varepsilon/dz = S_1 = 9.9\times 10^8$ eV/m, so that $\Delta E'/S_1 < 3\%$ is required.

7. MICROBUNCHING SMALL-SIGNAL GAIN

For an input current variation $I(z) = I_0 + \Delta I \cos(kz)$, passage through BC1 and its impedance gives, from eqs. (2) and (3):

$$\begin{aligned} I_1(z_1) &= C_1[I_0 + \Delta I \cos(kC_1 z_1)] \\ \varepsilon_1(z_1) &= E_1 + S_1 C_1 z_1 - e R_1 C_1 [I_0 + \Delta I \cos(kC_1 z_1)] \end{aligned} \tag{21}$$

In complex notation, $I(z) = \mathrm{Re}\{I_0[1+(\Delta I/I_0)e^{ikz}]\}$, while $I_1(z_1) = \mathrm{Re}\{C_1 I_0[1+(\Delta I/I_0)e^{ikC_1 z_1}]\}$. Thus, the microbunching small-signal gain of BC1, in complex notation, obeys

$$\frac{\Delta I / I_{\mathrm{out}}}{\Delta \mathrm{I}/\mathrm{I}_{\mathrm{in}}} = 1 \quad , \quad \frac{\Delta E / E_{\mathrm{out}}}{\Delta \mathrm{I}/\mathrm{I}_{\mathrm{in}}} = \frac{-C_1 e R_1 I_0}{E_1} \quad , \tag{22}$$

where $E_{\rm out} = E_1$ is the design energy of the compressor.

For an input energy variation $\Delta E(z) = \Delta E \cos(kz)$, eq. (9) gives $z(z_1) = C_1 z_1 - C_1 T_1 \Delta E \cos(kC_1 z_1)$ to first order in ΔE, so that eqs. (12) and (13) give

$$I_1(z_1) = C_1 I_0 [1 + C_1 T_1 k \Delta E \sin(kC_1 z_1)]$$
$$\varepsilon_1(z_1) = E_1 - eR_1 C_1 I_0 + S_1 C_1 z_1 + C_1 \Delta E \cos(kC_1 z_1) - C_1^2 eR_1 I_0 T_1 k \Delta E \sin(kC_1 z_1) \tag{23}$$

In complex notation, the small-signal gain of BC1 obeys

$$\frac{\Delta I / I_{\rm out}}{\Delta E / E_{\rm in}} = -iC_1 k R_{56}^{(1)}, \quad \frac{\Delta E / E_{\rm out}}{\Delta {\rm E}/{\rm E}_{in}} = C_1 + iC_1^2 eR_1 I_0 k R_{56}^{(1)} / E_1 \tag{24}$$

Thus, for BC1

$$\begin{pmatrix} \Delta I / I \\ \Delta E / E \end{pmatrix}_{\rm out} = \begin{pmatrix} 1 & -iC_1 k R_{56}^{(1)} \\ -eR_1 C_1 I_0 / E_1 & C_1 + iC_1^2 eR_1 I_0 k R_{56}^{(1)} / E_1 \end{pmatrix} \begin{pmatrix} \Delta I / I \\ \Delta E / E \end{pmatrix}_{\rm in} \tag{25}$$

The linac section between BC1 and BC2 is described by

$$\begin{pmatrix} \Delta I / I \\ \Delta E / E \end{pmatrix}_{\rm out} = \begin{pmatrix} 1 & 0 \\ 0 & E_1 / E_2 \end{pmatrix} \begin{pmatrix} \Delta I / I \\ \Delta E / E \end{pmatrix}_{\rm in} \tag{26}$$

while, for BC2, using the fact that the current and wavenumber have been increased by the factor C_1

$$\begin{pmatrix} \Delta I / I \\ \Delta E / E \end{pmatrix}_{\rm out} = \begin{pmatrix} 1 & -iC_2 (C_1 k) R_{56}^{(2)} \\ -eR_2 C_2 (C_1 I_0) / E_2 & C_2 + iC_2^2 eR_2 (C_1 I_0)(C_1 k) R_{56}^{(2)} / E_2 \end{pmatrix} \begin{pmatrix} \Delta I / I \\ \Delta E / E \end{pmatrix}_{\rm in} \tag{27}$$

The transformation through two bunch compressors is given by multiplying the matrices in eqs. (25), (26) and (27). We thereby obtain, for two-stage compression of a cold beam,

$$\frac{\Delta I / I_{\rm out}}{\Delta I / I_{\rm in}} = 1 + iC_1^2 C_2 eR_1 I_0 k R_{56}^{(2)} / E_2 \tag{28}$$

$$\frac{\Delta E / E_{\rm out}}{\Delta {\rm I}/{\rm I}_{\rm in}} = -C_1 C_2 e(R_1 + R_2) I_0 / E_2 - iC_1^3 C_2^2 e^2 R_1 R_2 I_0^2 k R_{56}^{(2)} / E_2^2 \tag{29}$$

$$\frac{\Delta I / I_{\rm out}}{\Delta E / E_{\rm in}} = C_1^3 C_2 eR_1 I_0 k^2 R_{56}^{(1)} R_{56}^{(2)} / E_2 - iC_1 k R_{56}^{(1)} - iC_1^2 C_2 k R_{56}^{(2)} E_1 / E_2 \tag{30}$$

$$\begin{aligned} \frac{\Delta E / E_{\rm out}}{\Delta E / E_{\rm in}} &= C_1 C_2 E_1 / E_2 - C_1^4 C_2^2 e^2 R_1 R_2 I_0^2 k^2 R_{56}^{(1)} R_{56}^{(2)} / E_2^2 \\ &+ iC_1^2 C_2 e(R_1 + R_2) I_0 k R_{56}^{(1)} / E_2 + iC_1^3 C_2^2 eR_2 I_0 k R_{56}^{(2)} E_1 / E_2^2 \end{aligned} \tag{31}$$

Equations (28)–(31) may also be obtained directly from eqs. (7), (8), (16) and (17). The RHS of eqs. (28)–(31) diverge as $k \to \infty$, which is an unphysical result from neglecting the beam's energy spread.

In Appendix A, a symmetric energy distribution $f(\delta)$ is considered, where δ is the energy deviation from that of a cold beam with current or energy modulation. For single-stage compression, the growth of the current and average-energy modulations obey

$$\frac{\Delta I / I_{\text{out}}}{\Delta \text{I}/\text{I}_{\text{in}}} = F_1 \quad , \quad \frac{\Delta E / E_{\text{out}}}{\Delta \text{I}/\text{I}_{\text{in}}} = \frac{-F_1 C_1 e R_1 I_0}{E_1} - \frac{iG_1 C_1}{E_1} \tag{32}$$

$$\frac{\Delta I / I_{\text{out}}}{\Delta E / E_{\text{in}}} = -iF_1 C_1 k R_{56}^{(1)}, \quad \frac{\Delta E / E_{\text{out}}}{\Delta \text{E}/\text{E}_{in}} = F_1 C_1 - \frac{G_1 C_1^2 k R_{56}^{(1)}}{E_1} + \frac{iF_1 C_1^2 e R_1 I_0 k R_{56}^{(1)}}{E_1} \tag{33}$$

where

$$F_1 = \int \cos(kC_1 T_1 \delta) f(\delta) d\delta, \quad G_1 = \int \sin(kC_1 T_1 \delta) \delta f(\delta) d\delta \ . \tag{34}$$

For a Gaussian energy distribution $f(\delta)$, the modification of single-stage microbunching gain $(\Delta I / I)_{\text{out}} / (\Delta E / E)_{\text{in}}$ by the factor F_1 has been previously found in Ref. [3].

Appendix A shows that the growth rates for 2-stage compression become

$$\frac{\Delta I / I_{\text{out}}}{\Delta I / I_{\text{in}}} = F_3 + iF_1 F_2 C_1^2 C_2 e R_1 I_0 k R_{56}^{(2)} / E_2 \tag{35}$$

$$\begin{aligned} \frac{\Delta E / E_{\text{out}}}{\Delta \text{I}/\text{I}_{\text{in}}} &= -C_1 C_2 e (F_1 F_2 R_1 + F_3 R_2) I_0 / E_2 + F_1 G_2 C_1^3 C_2^2 e R_1 I_0 k R_{56}^{(2)} / E_2^2 \\ &- iF_1 F_2 C_1^3 C_2^2 e^2 R_1 R_2 I_0^2 k R_{56}^{(2)} / E_2^2 - iG_3 C_1 C_2 / E_2 \end{aligned} \tag{36}$$

$$\frac{\Delta I / I_{\text{out}}}{\Delta E / E_{\text{in}}} = F_1 F_2 C_1^3 C_2 e R_1 I_0 k^2 R_{56}^{(1)} R_{56}^{(2)} / E_2 - iF_3 C_1 k R_{56}^{(1)} - iF_3 C_1^2 C_2 k R_{56}^{(2)} E_1 / E_2 \tag{37}$$

$$\begin{aligned} \frac{\Delta E / E_{\text{out}}}{\Delta E / E_{\text{in}}} &= F_3 C_1 C_2 E_1 / E_2 - F_1 F_2 C_1^4 C_2^2 e^2 R_1 R_2 I_0^2 k^2 R_{56}^{(1)} R_{56}^{(2)} / E_2^2 \\ &- G_3 C_1^2 C_2 k R_{56}^{(1)} / E_2 - G_3 C_1^3 C_2^2 k R_{56}^{(2)} E_1 / E_2^2 \\ &+ iF_1 F_2 C_1^2 C_2 e R_1 I_0 k R_{56}^{(1)} / E_2 + iF_3 C_1^2 C_2 e R_2 I_0 k R_{56}^{(1)} / E_2 + iF_3 C_1^3 C_2^2 e R_2 I_0 k R_{56}^{(2)} E_1 / E_2^2 \\ &- iF_1 G_2 C_1^4 C_2^2 e R_1 I_0 k^2 R_{56}^{(1)} R_{56}^{(2)} / E_2^2 \end{aligned} \tag{38}$$

where

$$F_2 = \int \cos(kC_1^2 C_2 T_2 \delta) f(\delta) d\delta, \quad G_2 = \int \sin(kC_1^2 C_2 T_2 \delta) \delta \, f(\delta) d\delta \tag{39}$$

and

$$F_3 = \int \cos[k(C_1 T_1 + C_1^2 C_2 T_2)\delta] f(\delta) d\delta \ , \ G_3 = \int \sin[k(C_1 T_1 + C_1^2 C_2 T_2)\delta] \delta \, f(\delta) d\delta \, . \tag{40}$$

For an initial Gaussian energy distribution $f(\delta)$ with rms energy spread of σ_E [11],

$$\begin{aligned} F_1 &= \exp[-(kC_1 R_{56}^{(1)} \sigma_E / E_1)^2 / 2], \\ F_2 &= \exp[-(kC_1^2 C_2 R_{56}^{(2)} \sigma_E / E_2)^2 / 2], \\ F_3 &= \exp\{-[k(C_1 R_{56}^{(1)} / E_1 + C_1^2 C_2 R_{56}^{(2)} / E_2)\sigma_E]^2 / 2\}, \\ G_1 &= (kC_1 R_{56}^{(1)} / E_1)\sigma_E^2 \exp[-(kC_1 R_{56}^{(1)} \sigma_E / E_1)^2 / 2] \\ G_2 &= (kC_1^2 C_2 R_{56}^{(2)} / E_2)\sigma_E^2 \exp[-(kC_1^2 C_2 R_{56}^{(2)} \sigma_E / E_2)^2 / 2] \\ G_3 &= k(C_1 R_{56}^{(1)} / E_1 + C_1^2 C_2 R_{56}^{(2)} / E_2)\sigma_E^2 \exp\{-[k(C_1 R_{56}^{(1)} / E_1 + C_1^2 C_2 R_{56}^{(2)} / E_2)\sigma_E]^2 / 2\} \end{aligned} \tag{41}$$

Figures 13–15 show the microbunching gain of our 2-stage bunch compressor design for Gaussian energy distributions with σ_E = 1,3 or 10 keV, calculated for $R_1 = R_2 = 3Z_0$.

When the initial energy spread results from a laser heater that is matched to the transverse beam size, the distribution $f(\delta)$ is approximately a semicircular distribution [5]

$$f(\delta) = \frac{2}{\pi\delta_{\max}}\sqrt{1-\left(\frac{\delta}{\delta_{\max}}\right)^2} \tag{42}$$

where [12] $\delta_{\max} = 2\sigma_E$. In this case [13],

$$\begin{aligned}
F_1 &= (kC_1R_{56}^{(1)}\sigma_E/E_1)^{-1}J_1(2kC_1R_{56}^{(1)}\sigma_E/E_1)\\
F_2 &= (kC_1^2C_2R_{56}^{(2)}\sigma_E/E_2)^{-1}J_1(2kC_1^2C_2R_{56}^{(2)}\sigma_E/E_2)\\
F_3 &= [k(C_1R_{56}^{(1)}/E_1 + C_1^2C_2R_{56}^{(2)}/E_2)\sigma_E]^{-1}J_1[2k(C_1R_{56}^{(1)}/E_1 + C_1^2C_2R_{56}^{(2)}/E_2)\sigma_E]\\
G_1 &= (kC_1R_{56}^{(1)}/2E_1)^{-1}J_2(2kC_1R_{56}^{(1)}\sigma_E/E_1)\\
G_2 &= (kC_1^2C_2R_{56}^{(2)}/2E_2)^{-1}J_2(2kC_1^2C_2R_{56}^{(2)}\sigma_E/E_2)\\
G_3 &= [k(C_1R_{56}^{(1)}/E_1 + C_1^2C_2R_{56}^{(2)}/E_2)/2]^{-1}J_2[2k(C_1R_{56}^{(1)}/E_1 + C_1^2C_2R_{56}^{(2)}/E_2)\sigma_E]
\end{aligned} \tag{43}$$

Figures 16–18 show the microbunching gain for semicircular energy distributions with σ_E = 1,3 or 10 keV, calculated for $R_1 = R_2 = 3Z_0$.

For a Gaussian energy spread or energy spread from a laser heater, a large relative current modulation $\Delta I/I_{\text{out}}$ may result from a small $\Delta E/E_{\text{in}}$. The gain at short wavelengths is suppressed by energy spread. Heating the uncompressed bunches by a laser heater so that the energy spread is 5-10 keV is predicted to suppress microbunching for initial wavelengths less than 100 microns. In this case, initial energy modulations at wavelengths around 100 μm should be smaller than ~1 keV to prevent large current modulations from CSR in the compressed bunches. Since microbunching gain may be increased by a factor of ~2 from linac wakefields [4], we estimate that the initial energy modulations at wavelengths around 100 μm should be smaller than ~500 eV.

8. SUMMARY

We have considered two-stage bunch compression, where each stage compresses a chirped beam in a magnetic chicane. For high bunch currents, compressor performance may be adversely affected by the wake of coherent synchrotron radiation (CSR). We modeled the case where the CSR wake is dominated by edge radiation downstream of the chicane magnets, so that it may be approximated by the wake from resistive impedance. Tracking studies confirm that resistive impedance is a valid approximation.

For this case, we performed analytic modeling of CSR effects. Formulas were obtained to determine when a portion of the bunch becomes upright in phase space, producing a large current spike and energy depression. The formulas show how a compressor design may be modified to prevent the upright bunch regions. Examples were provided by tracking of a preliminary bunch-compressor design.

We also obtained formulas for the jitter in the bunch arrival time resulting from bunch-to-bunch variation in current, energy and chirp. The formulas were applied to determine the permitted variations that give arrival-time jitter less than 15 fs.

The small-signal gain of microbunching was derived for periodic modulations, including the gain suppression at short wavelengths from the bunch's energy spread. The gain formulas describe the output current and energy modulations that result from given input current and energy modulations. For our

preliminary bunch-compressor design, the gain was computed for a Gaussian energy spread and for the energy distribution produced by laser heating. A large output current modulation may be caused by a relatively small input energy modulation. The formulas were applied to determine the permitted size of initial energy modulations that do not produce large modulations in the output current.

APPENDIX A. MICROBUNCHING WITH ENERGY SPREAD

A. Current modulation

Consider an initial symmetric distribution of energies $f(\delta)$, where δ is the initial energy deviation from that of an ideal cold beam. The current density in phase space is $I(z,\delta) = I(z) f(\delta)$, where $I(z)$ is the bunch current. For an initial current modulation,

$$I(z) = I_0 + \Delta I \cos(kz) . \tag{A1}$$

At the entrance of BC1, let $\varepsilon(z,\delta)$ equal the energy at coordinate (z,δ), while the average energy at longitudinal position z is denoted $\varepsilon(z)$. We therefore have

$$\varepsilon(z,\delta) = E_1 + S_1 z + \delta , \qquad \varepsilon(z) = \int \varepsilon(z,\delta) f(\delta) d\delta = E_1 + S_1 z \tag{A2}$$

The compression in BC1 gives the transformation

$$z_1(z,\delta) = z + T_1[\varepsilon(z,\delta) - E_1] = z / C_1 + T_1 \delta \tag{A3}$$

with inverse

$$z(z_1,\delta) = C_1 z_1 - C_1 T_1 \delta \tag{A4}$$

After BC1, the current density in coordinates (z_1,δ) is

$$I_1(z_1,\delta) = I(z(z_1,\delta),\delta)/(\partial z_1 / \partial z) = C_1\{I_0 + \Delta I \cos[k(C_1 z_1 - C_1 T_1 \delta)]\} f(\delta) . \tag{A5}$$

The current after BC1 equals

$$I_1(z_1) = \int I_1(z_1,\delta) d\delta = C_1[I_0 + F_1 \Delta I \cos(kC_1 z_1)], \tag{A6}$$

where

$$F_1 = \int \cos(kC_1 T_1 \delta) f(\delta) d\delta \ . \tag{A7}$$

After passing through the resistive impedance, using the relation $C_1 = 1 - S_1 C_1 T_1$ gives the energy in coordinates (z_1,δ)

$$\varepsilon_1(z_1,\delta) = \varepsilon(z(z_1,\delta),\delta) - eR_1 I_1(z_1) = E_1 + S_1 C_1 z_1 + C_1 \delta - eR_1 C_1 [I_0 + F_1 \Delta I \cos(kC_1 z_1)] \tag{A8}$$

The average energy of electrons at coordinate z_1, $\varepsilon_1(z_1)$, obeys $\varepsilon_1(z_1) I_1(z_1) = \int d\delta \varepsilon_1(z_1,\delta) I_1(z_1,\delta)$. To first order in ΔI, this gives

$$\varepsilon_1(z_1) = E_1 + S_1 C_1 z_1 - eR_1 C_1 [I_0 + F_1 \Delta I \cos(kC_1 z_1)] + G_1 C_1 (\Delta I / I_0) \sin(kC_1 z_1) \tag{A9}$$

where

$$G_1 = \int \sin(kC_1 T_1 \delta) \delta \, f(\delta) d\delta \tag{A10}$$

Thus, for single-stage compression, eq. (22) is modified by the energy spread to become

$$\frac{\Delta I / I_{\rm out}}{\Delta {\rm I}/{\rm I}_{\rm in}} = F_1 \quad , \quad \frac{\Delta E / E_{\rm out}}{\Delta {\rm I}/{\rm I}_{\rm in}} = \frac{-F_1 C_1 e R_1 I_0}{E_1} - \frac{i G_1 C_1}{E_1} \tag{A11}$$

After the linac section between BC1 and BC2, using the relation $C_1 = 1 - S_1 C_1 T_1$ gives

$$\begin{aligned} \varepsilon_{\rm L}(z_1,\delta) &= \varepsilon_1(z_1,\delta) + E_2 - E_1 + S_2 z_1 \\ &= E_2 + (S_1 C_1 + S_2) z_1 + C_1 \delta - e R_1 C_1 [I_0 + F_1 \Delta I \cos(k C_1 z_1)] \end{aligned} \tag{A12}$$

The compression in BC2 gives the transformation

$$z_2(z_1,\delta) = z_1 + T_2[\varepsilon_L(z_1,\delta) - E_2] = z_1 / C_2 + C_1 T_2 \delta - C_1 T_2 e R_1 [I_0 + F_1 \Delta I \cos(k C_1 z_1)] \tag{A13}$$

The inverse to first order in ΔI is

$$z_1(z_2,\delta) = C_2 z_2 - C_1 C_2 T_2 \delta + C_1 C_2 T_2 e R_1 \{I_0 + F_1 \Delta I \cos[k(C_1 C_2 z_2 + C_1^2 C_2 T_2 e R_1 I_0 - C_1^2 C_2 T_2 \delta)]\} \tag{A14}$$

We can relate z_2 and z by using eq. (A3),

$$z_2(z,\delta) = z / C_1 C_2 + (T_1 / C_2 + T_2 C_1)\delta - C_1 T_2 e R_1 \{I_0 + F_1 \Delta I \cos[k(z + C_1 T_1 \delta)]\} \tag{A15}$$

with derivative

$$\partial z_2 / \partial z(z,\delta) = (C_1 C_2)^{-1} \{1 + F_1 C_1^2 C_2 T_2 e R_1 k \Delta I \sin[k(z + C_1 T_1 \delta)]\} . \tag{A16}$$

When this derivative equals zero, an upright bunch region occurs after BC2. The energy spread modifies the threshold value of ΔI by the factor F_1^{-1}.

The inverse of $z_2(z,\delta)$ is, to first order in ΔI

$$\begin{aligned} z(z_2,\delta) &= C_1 C_2 z_2 + C_1^2 C_2 T_2 e R_1 I_0 - (C_1 T_1 + C_1^2 C_2 T_2)\delta \\ &+ F_1 C_1^2 C_2 T_2 e R_1 \Delta I \cos[k(C_1 C_2 z_2 + C_1^2 C_2 T_2 e R_1 I_0 - C_1^2 C_2 T_2 \delta)] \end{aligned} \tag{A17}$$

The current density after BC2 in coordinates (z_2,δ) is, to first order in ΔI

$$\begin{aligned} I_2(z_2,\delta) &= \frac{I[z(z_2,\delta),\delta]}{\partial z_2 / \partial z} = \frac{C_1 C_2 \{I_0 + \Delta I \cos[k z(z_2,\delta)]\} f(\delta)}{1 + F_1 C_1^2 C_2 T_2 e R_1 k \Delta I \sin\{k[z(z_2,\delta) + C_1 T_1 \delta]\}} \\ &= C_1 C_2 f(\delta) I_0 \begin{pmatrix} 1 + (\Delta I / I_0)\cos\{k[C_1 C_2 z_2 + C_1^2 C_2 T_2 e R_1 I_0 - (C_1 T_1 + C_1^2 C_2 T_2)\delta]\} \\ - F_1 C_1^2 C_2 T_2 e R_1 k \Delta I \sin[k(C_1 C_2 z_2 + C_1^2 C_2 T_2 e R_1 I_0 - C_1^2 C_2 T_2 \delta)] \end{pmatrix} . \end{aligned} \tag{A18}$$

To first order in ΔI,

$$\begin{aligned} I_2(z_2) &= \int I_2(z_2,\delta) d\delta = C_1 C_2 I_0 \{1 + (\Delta I / I_0) F_3 \cos[k(C_1 C_2 z_2 + C_1^2 C_2 T_2 e R_1 I_0)] \\ &- F_1 F_2 C_1^2 C_2 T_2 e R_1 k \Delta I \sin[k(C_1 C_2 z_2 + C_1^2 C_2 T_2 e R_1 I_0)]\} \end{aligned} , \tag{A19}$$

where

$$F_2 = \int \cos(k C_1^2 C_2 T_2 \delta) f(\delta) d\delta , \quad F_3 = \int \cos[k(C_1 T_1 + C_1^2 C_2 T_2)\delta] f(\delta) d\delta . \tag{A20}$$

Using the relation $C_2 = 1 - (S_1 C_1 + S_2) T_2 C_2$ gives the energy in coordinates (z_2,δ) to first order in ΔI

$$\begin{aligned}
&\varepsilon_2(z_2,\delta) = \varepsilon_L(z_1(z_2,\delta),\delta) - eR_2 I_2(z_2) \\
&= E_2 - eR_1C_1I_0 - eR_2C_1C_2I_0 + (S_1C_1 + S_2)(C_2z_2 + C_1C_2T_2eR_1I_0) + C_1C_2\delta \\
&- F_1C_1C_2eR_1\Delta I\cos[k(C_1C_2z_2 + C_1^2C_2T_2eR_1I_0 - C_1^2C_2T_2\delta)] \\
&- F_3C_1C_2eR_2\Delta I\cos[k(C_1C_2z_2 + C_1^2C_2T_2eR_1I_0)] \\
&+ F_1F_2C_1^3C_2^2T_2e^2R_1R_2kI_0\Delta I\sin[k(C_1C_2z_2 + C_1^2C_2T_2eR_1I_0)]
\end{aligned} \tag{A21}$$

The average energy of electrons at coordinate z_2, $\varepsilon_2(z_2)$, obeys $\varepsilon_2(z_2)I_2(z_2) = \int d\delta\varepsilon_2(z_2,\delta)I_2(z_2,\delta)$. To first order in ΔI, this gives

$$\begin{aligned}
&\varepsilon_2(z_2) = E_2 - eR_1C_1I_0 - eR_2C_1C_2I_0 + (S_1C_1 + S_2)(C_2z_2 + C_1C_2T_2eR_1I_0) \\
&- F_1F_2C_1C_2eR_1\Delta I\cos[k(C_1C_2z_2 + C_1^2C_2T_2eR_1I_0)] \\
&- F_3C_1C_2eR_2\Delta I\cos[k(C_1C_2z_2 + C_1^2C_2T_2eR_1I_0)] \\
&+ F_1F_2C_1^3C_2^2T_2e^2R_1R_2kI_0\Delta I\sin[k(C_1C_2z_2 + C_1^2C_2T_2eR_1I_0)] \\
&+ G_3C_1C_2(\Delta I/I_0)\sin[k(C_1C_2z_2 + C_1^2C_2T_2eR_1I_0)] \\
&+ F_1G_2C_1^3C_2^2T_2eR_1k\Delta I\cos[k(C_1C_2z_2 + C_1^2C_2T_2eR_1I_0)]
\end{aligned} \tag{A22}$$

where

$$G_2 = \int \sin(kC_1^2C_2T_2\delta)\delta\, f(\delta)d\delta, \quad G_3 = \int \sin[k(C_1T_1 + C_1^2C_2T_2)\delta]\delta\, f(\delta)d\delta\ . \tag{A23}$$

For two-stage compression, eqs. (28) and (29) are modified by the energy spread to become

$$\frac{\Delta I/I_{out}}{\Delta I/I_{in}} = F_3 + iF_1F_2C_1^2C_2eR_1I_0kR_{56}^{(2)}/E_2 \tag{A24}$$

$$\begin{aligned}
&\frac{\Delta E/E_{out}}{\Delta I/I_{in}} = -C_1C_2e(F_1F_2R_1 + F_3R_2)I_0/E_2 + F_1G_2C_1^3C_2^2eR_1I_0kR_{56}^{(2)}/E_2^2 \\
&- iF_1F_2C_1^3C_2^2e^2R_1R_2I_0^2kR_{56}^{(2)}/E_2^2 - iG_3C_1C_2/E_2
\end{aligned} \tag{A25}$$

B. Energy modulation

Consider an initial symmetric distribution of energies $f(\delta)$, where δ is the initial energy deviation from that of a cold beam with energy modulation. For constant current

$$I(z) = I_0 \tag{A26}$$

At the entrance of BC1, let $\varepsilon(z,\delta)$ equal the energy at coordinate (z,δ), while the average energy at longitudinal position z is denoted $\varepsilon(z)$. Then,

$$\varepsilon(z,\delta) = E_1 + S_1z + \Delta E\cos(kz) + \delta, \quad \varepsilon(z) = \int \varepsilon(z,\delta)f(\delta)d\delta = E_1 + S_1z + \Delta E\cos(kz) \tag{A27}$$

The compression in BC1 gives the transformation

$$z_1(z,\delta) = z + T_1[\varepsilon(z,\delta) - E_1] = z/C_1 + T_1\delta + T_1\Delta E\cos(kz) \tag{A28}$$

with derivative

$$\partial z_1 / \partial z = 1/C_1 - T_1 k \Delta E \sin(kz) \tag{A29}$$

When this derivative is zero, an upright bunch region and current spike occur after BC1, as in the case without energy spread. The following equations are valid to first order in ΔE. The inverse of eq. (A28) is

$$z(z_1, \delta) = C_1 z_1 - C_1 T_1 \delta - C_1 T_1 \Delta E \cos[k(C_1 z_1 - C_1 T_1 \delta)] \tag{A30}$$

After BC1, the current density in coordinates (z_1, δ) is

$$I_1(z_1, \delta) = I(z(z_1, \delta), \delta)/(\partial z_1 / \partial z) = C_1 I_0 \{1 + C_1 T_1 k \Delta E \sin[k(C_1 z_1 - C_1 T_1 \delta)]\} f(\delta) \tag{A31}$$

Therefore, the current is

$$I_1(z_1) = \int I_1(z_1, \delta) d\delta = C_1 I_0 [1 + F_1 C_1 T_1 k \Delta E \sin(k C_1 z_1)] \tag{A32}$$

After passing through the resistive impedance R_1,

$$\begin{aligned} &\varepsilon_1(z_1, \delta) = \varepsilon(z(z_1, \delta), \delta) - eR_1 I_1(z_1) = E_1 + S_1 C_1 z_1 + C_1 \delta + C_1 \Delta E \cos[k(C_1 z_1 - C_1 T_1 \delta)] \\ &- eR_1 C_1 I_0 [1 + F_1 C_1 T_1 k \Delta E \sin(k C_1 z_1)] \end{aligned} \tag{A33}$$

The average electron energy at coordinate z_1, $\varepsilon_1(z_1)$, obeys $\varepsilon_1(z_1) I_1(z_1) = \int d\delta \varepsilon_1(z_1, \delta) I_1(z_1, \delta)$, so that

$$\varepsilon_1(z_1) = E_1 + S_1 C_1 z_1 + F_1 C_1 \Delta E \cos(k C_1 z_1) - eR_1 C_1 I_0 [1 + F_1 C_1 T_1 k \Delta E \sin(k C_1 z_1)] - G_1 C_1^2 T_1 k \Delta E \cos(k C_1 z_1) \tag{A34}$$

According to eqs. (A32) and (A34), eq. (24) for single-stage compression is modified to become:

$$\frac{\Delta I / I_{\text{out}}}{\Delta E / E_{\text{in}}} = -iF_1 C_1 k R_{56}^{(1)}, \quad \frac{\Delta E / E_{\text{out}}}{\Delta \text{E/E}_{in}} = F_1 C_1 - G_1 C_1^2 k R_{56}^{(1)} / E_1 + iF_1 C_1^2 eR_1 I_0 k R_{56}^{(1)} / E_1 \tag{A35}$$

After the linac section between BC1 and BC2,

$$\begin{aligned} &\varepsilon_L(z_1, \delta) = \varepsilon_1(z_1, \delta) + E_2 - E_1 + S_2 z_1 \\ &= E_2 + (S_1 C_1 + S_2) z_1 + C_1 \delta + C_1 \Delta E \cos[k(C_1 z_1 - C_1 T_1 \delta)] \\ &- eR_1 C_1 I_0 [1 + F_1 C_1 T_1 k \Delta E \sin(k C_1 z_1)] \end{aligned} \tag{A36}$$

The compression in BC2 gives the transformation

$$\begin{aligned} &z_2(z_1, \delta) = z_1 + T_2 [\varepsilon_L(z_1, \delta) - E_2] \\ &= z_1 / C_2 - C_1 T_2 eR_1 I_0 + C_1 T_2 \delta + C_1 T_2 \Delta E \cos[k(C_1 z_1 - C_1 T_1 \delta)] - F_1 C_1^2 T_1 T_2 eR_1 I_0 k \Delta E \sin(k C_1 z_1) \end{aligned}, \tag{A37}$$

with inverse

$$\begin{aligned} &z_1(z_2, \delta) = C_2 z_2 + C_1 C_2 T_2 eR_1 I_0 - C_1 C_2 T_2 \delta \\ &- C_1 C_2 T_2 \Delta E \cos\{k[C_1 C_2 z_2 + C_1^2 C_2 T_2 eR_1 I_0 - (C_1 T_1 + C_1^2 C_2 T_2)\delta)]\} \\ &+ F_1 C_1^2 C_2 T_1 T_2 eR_1 I_0 k \Delta E \sin[k(C_1 C_2 z_2 + C_1^2 C_2 T_2 eR_1 I_0 - C_1^2 C_2 T_2 \delta)] \end{aligned} \tag{A38}$$

Using eqs. (A28) and (A37) to relate z_2 and z gives

$$\begin{aligned} &z_2(z, \delta) = z / C_1 C_2 - C_1 T_2 eR_1 I_0 + (T_1 / C_2 + T_2 C_1)\delta + (T_1 / C_2 + T_2 C_1) \Delta E \cos(kz) \\ &- F_1 C_1^2 T_1 T_2 eR_1 I_0 k \Delta E \sin[k(z + C_1 T_1 \delta)] \end{aligned} \tag{A39}$$

The inverse of eq. (A39) is

$$\begin{aligned} z(z_2,\delta) &= C_1C_2z_2 + C_1^2C_2T_2eR_1I_0 - (C_1T_1 + C_1^2C_2T_2)\delta \\ &- (C_1T_1 + C_1^2C_2T_2)\Delta E\cos\{k[C_1C_2z_2 + C_1^2C_2T_2eR_1I_0 - (C_1T_1 + C_1^2C_2T_2)\delta]\} \\ &+ F_1C_1^3C_2T_1T_2eR_1I_0k\Delta E\sin[k(C_1C_2z_2 + C_1^2C_2T_2eR_1I_0 - C_1^2C_2T_2\delta)] \end{aligned} \tag{A40}$$

while its derivative is

$$\partial z_2/\partial z(z,\delta) = (C_1C_2)^{-1}\{1 - (C_1T_1 + C_1^2C_2T_2)k\Delta E\sin(kz) - F_1C_1^3C_2T_1T_2eR_1I_0k^2\Delta E\cos[k(z + C_1T_1\delta)]\} \tag{A41}$$

Therefore,

$$\begin{aligned} &I_2(z_2,\delta) = I[z(z_2,\delta),\delta]/(\partial z_2/\partial z) \\ &= C_1C_2I_0f(\delta)\{1 + (C_1T_1 + C_1^2C_2T_2)k\Delta E\sin[kz(z_2,\delta)] + F_1C_1^3C_2T_1T_2eR_1I_0k^2\Delta E\cos[kz(z_2,\delta) + kC_1T_1\delta]\} \\ &= C_1C_2I_0f(\delta)\begin{pmatrix} 1 + (C_1T_1 + C_1^2C_2T_2)k\Delta E\sin\{k[C_1C_2z_2 + C_1^2C_2T_2eR_1I_0 - (C_1T_1 + C_1^2C_2T_2)\delta]\} \\ + F_1C_1^3C_2T_1T_2eR_1I_0k^2\Delta E\cos[k(C_1C_2z_2 + C_1^2C_2T_2eR_1I_0 - C_1^2C_2T_2\delta)] \end{pmatrix} \end{aligned} \tag{A42}$$

Substituting eq. (A40) in eq. (A42) gives

$$\begin{aligned} I_2(z_2) &= \int I_2(z_2,\delta)d\delta \\ &= C_1C_2I_0\{1 + (C_1T_1 + C_1^2C_2T_2)F_3k\Delta E\sin[k(C_1C_2z_2 + C_1^2C_2T_2eR_1I_0)] \\ &+ F_1F_2C_1^3C_2T_1T_2eR_1I_0k^2\Delta E\cos[k(C_1C_2z_2 + C_1^2C_2T_2eR_1I_0)]\} \end{aligned} \tag{A43}$$

so that

$$\begin{aligned} &\varepsilon_2(z_2,\delta) = \varepsilon_L(z_1(z_2,\delta),\delta) - eR_2I_2(z_2) \\ &= E_2 - eR_1C_1I_0 - eR_2C_1C_2I_0 + (S_1C_1 + S_2)(C_2z_2 + C_1C_2T_2eR_1I_0) + C_1C_2\delta \\ &+ C_1C_2\Delta E\cos\{k[C_1C_2z_2 + C_1^2C_2T_2eR_1I_0 - (C_1T_1 + C_1^2C_2T_2)\delta]\} \\ &- F_1C_1^2C_2T_1eR_1I_0k\Delta E\sin[k(C_1C_2z_2 + C_1^2C_2T_2eR_1I_0 - C_1^2C_2T_2\delta)] \\ &- F_3C_1C_2(C_1T_1 + C_1^2C_2T_2)eR_2I_0k\Delta E\sin[k(C_1C_2z_2 + C_1^2C_2T_2eR_1I_0)] \\ &- F_1F_2C_1^4C_2^2T_1T_2e^2R_1R_2I_0^2k^2\Delta E\cos[k(C_1C_2z_2 + C_1^2C_2T_2eR_1I_0)] \end{aligned} \tag{A44}$$

The average electron energy of at coordinate z_2, $\varepsilon_2(z_2)$, obeys $\varepsilon_2(z_2)I_2(z_2) = \int d\delta\varepsilon_2(z_2,\delta)I_2(z_2,\delta)$. This gives

$$\begin{aligned} &\varepsilon_2(z_2) = E_2 - eR_1C_1I_0 - eR_2C_1C_2I_0 + (S_1C_1 + S_2)(C_2z_2 + C_1C_2T_2eR_1I_0) \\ &+ F_3C_1C_2\Delta E\cos[k(C_1C_2z_2 + C_1^2C_2T_2eR_1I_0)] \\ &- F_1F_2C_1^2C_2T_1eR_1I_0k\Delta E\sin[k(C_1C_2z_2 + C_1^2C_2T_2eR_1I_0)] \\ &- F_3C_1C_2(C_1T_1 + C_1^2C_2T_2)eR_2I_0k\Delta E\sin[k(C_1C_2z_2 + C_1^2C_2T_2eR_1I_0)] \\ &- F_1F_2C_1^4C_2^2T_1T_2e^2R_1R_2I_0^2k^2\Delta E\cos[k(C_1C_2z_2 + C_1^2C_2T_2eR_1I_0)] \\ &- G_3C_1C_2(C_1T_1 + C_1^2C_2T_2)k\Delta E\cos[k(C_1C_2z_2 + C_1^2C_2T_2eR_1I_0)] \\ &+ F_1G_2C_1^4C_2^2T_1T_2eR_1I_0k^2\Delta E\sin[k(C_1C_2z_2 + C_1^2C_2T_2eR_1I_0)] \end{aligned} \tag{A45}$$

Consequently, eqs. (30) and (31) are modified by the energy spread to become

$$\frac{\Delta I / I_{\text{out}}}{\Delta E / E_{\text{in}}} = F_1 F_2 C_1^3 C_2 e R_1 I_0 k^2 R_{56}^{(1)} R_{56}^{(2)} / E_2 - i F_3 C_1 k R_{56}^{(1)} - i F_3 C_1^2 C_2 k R_{56}^{(2)} E_1 / E_2 \tag{A46}$$

$$\begin{aligned}\frac{\Delta E / E_{\text{out}}}{\Delta E / E_{\text{in}}} &= F_3 C_1 C_2 E_1 / E_2 - F_1 F_2 C_1^4 C_2^2 e^2 R_1 R_2 I_0^2 k^2 R_{56}^{(1)} R_{56}^{(2)} / E_2^2 \\ &- G_3 C_1^2 C_2 k R_{56}^{(1)} / E_2 - G_3 C_1^3 C_2^2 k R_{56}^{(2)} E_1 / E_2^2 \\ &+ i F_1 F_2 C_1^2 C_2 e R_1 I_0 k R_{56}^{(1)} / E_2 + i F_3 C_1^2 C_2 e R_2 I_0 k R_{56}^{(1)} / E_2 + i F_3 C_1^3 C_2^2 e R_2 I_0 k R_{56}^{(2)} E_1 / E_2^2 \\ &- i F_1 G_2 C_1^4 C_2^2 e R_1 I_0 k^2 R_{56}^{(1)} R_{56}^{(2)} / E_2^2\end{aligned} \tag{A47}$$

[1] J. Arthur et. al, *Linac Coherent Light Source (LCLS) Conceptual Design Report*, SLAC Report No. SLAC-R-593, 2002.

[2] M. Borland, Y. C. Chae, P. Emma, J. W. Lewellen, V. Bharadwaj, W. M. Fawley, P. Krejcik, C. Limborg, S. V. Milton, H.-D. Nuhn, R. Soliday and M. Woodley, Nucl. Instrum. Methods Phys. Res., Sect. A **483**, 268 (2002).

[3] E. L. Saldin, E. A. Schneidmiller and M. V. Yurkov, Nucl. Instrum. Methods Phys. Res., Sect. A **483**, 516 (2002).

[4] Z. Huang, M. Borland, P. Emma and K.-J. Kim, in *Proceedings of the 2003 Particle Accelerator Conference, Portland, OR* (IEEE, Piscataway, NJ, 2003), p. 3138.

[5] Z. Huang, M. Borland, P. Emma, J. Wu, C. Limborg, G. Stupakov and J. Welch, Phys. Rev. ST Accel. Beams **7**, 074401 (2004).

[6] R. A. Bosch, Phys. Rev. ST Accel Beams **10**, 050701 (2007), eq. 24.

[7] K. L. F. Bane and P. Emma, in *Proceedings of the 2005 Particle Accelerator Conference, Knoxville, TN* (IEEE, Piscataway, NJ, 2005), p. 4266.

[8] H. Grote, E. Keil, T. O. Raubenheimer and M. Woodley, in *Proceedings of the 7th European Particle Accelerator Conference, Vienna* (EPS, Geneva, 2000), p. 1390.

[9] J. Rosenzweig and L. Serafini, Phys. Rev. E **49**, 1599 (1994).

[10] M. Borland, "elegant: A flexible SDDS-compliant code for accelerator simulation," Advanced Photon Source Light Source Note LS-287, September 2000.

[11] I. S. Gradshteyn and I. M. Ryzhik, *Table of Integrals, Series, and Products* (Academic Press, San Diego, 1994), 5th ed., p. 515, Eq. 3.896.4; p. 529, Eq. 3.952.1.

[12] I. S. Gradshteyn and I. M. Ryzhik, *Table of Integrals, Series, and Products* (Academic Press, San Diego, 1994), 5th ed., p. 99, Eqs. 2.261 and 2.262.3.

[13] I. S. Gradshteyn and I. M. Ryzhik, *Table of Integrals, Series, and Products* (Academic Press, San Diego, 1994), 5th ed., p. 456, Eq. 3.752.2 ; p. 465, Eq. 3.771.10.

Table I. Properties of the bunch compressor chicanes BC1 and BC2.

property	**symbol**	**value**
BC1 energy	E_1	125 MeV
BC1 compression ratio	C_1	5
BC1 energy-to-position transfer	$R_{56}^{(1)}$	-0.0977 m
BC1 resistive impedance	R_1	1131 Ω
BC2 energy	E_2	600 MeV
BC2 compression ratio	C_2	4
BC2 energy-to-position transfer	$R_{56}^{(2)}$	-0.07349 m
BC2 resistive impedance	R_2	1131 Ω

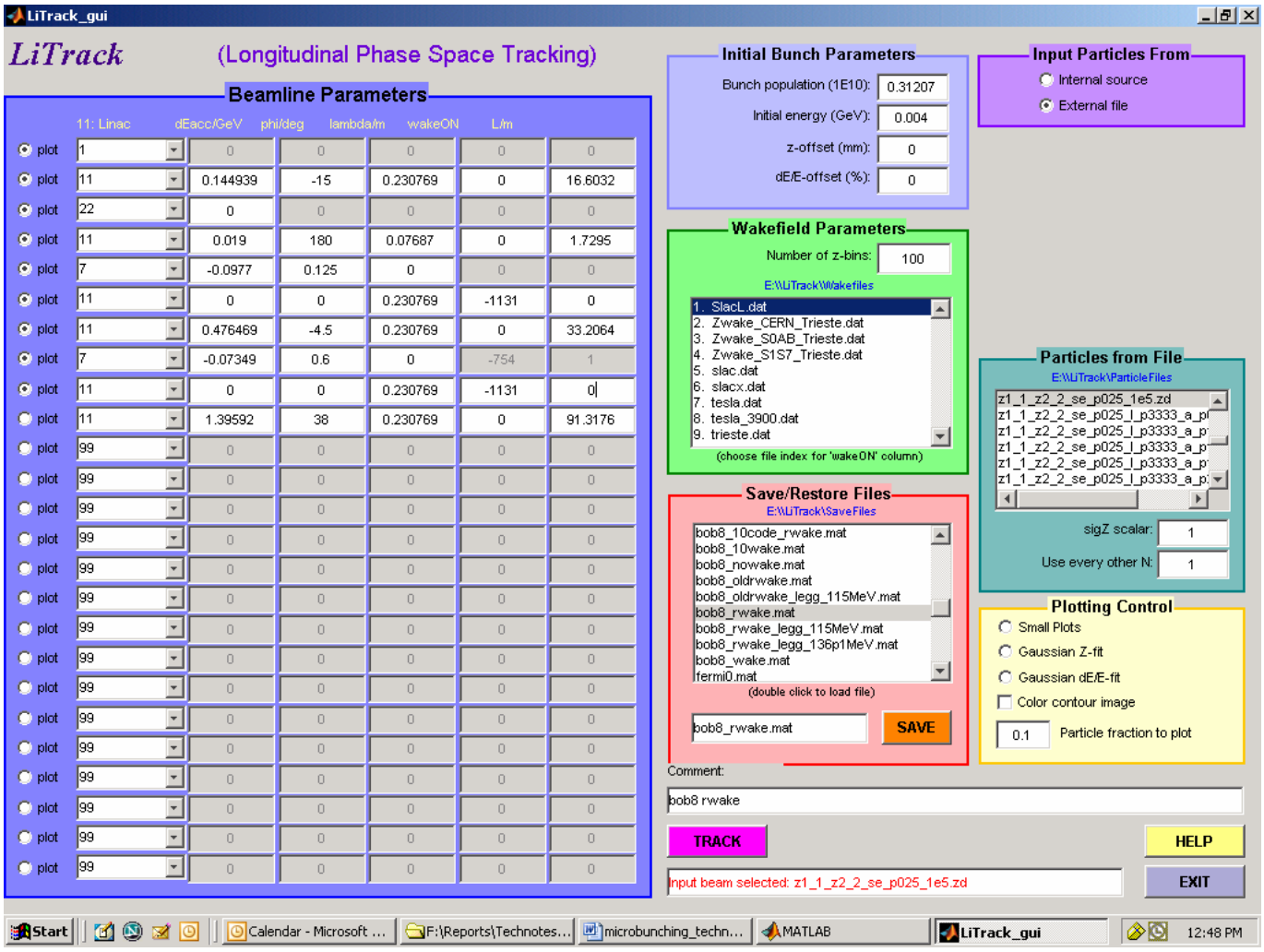

Figure 1(a). Modified-LiTrack graphical user interface for a preliminary bunch compressor design that uses two stages to compress by a factor of 20. After each chicane, a resistive impedance of 1131 Ω/m is specified with effective length of 0 m. Therefore, no wakes from CSR are computed in this case.

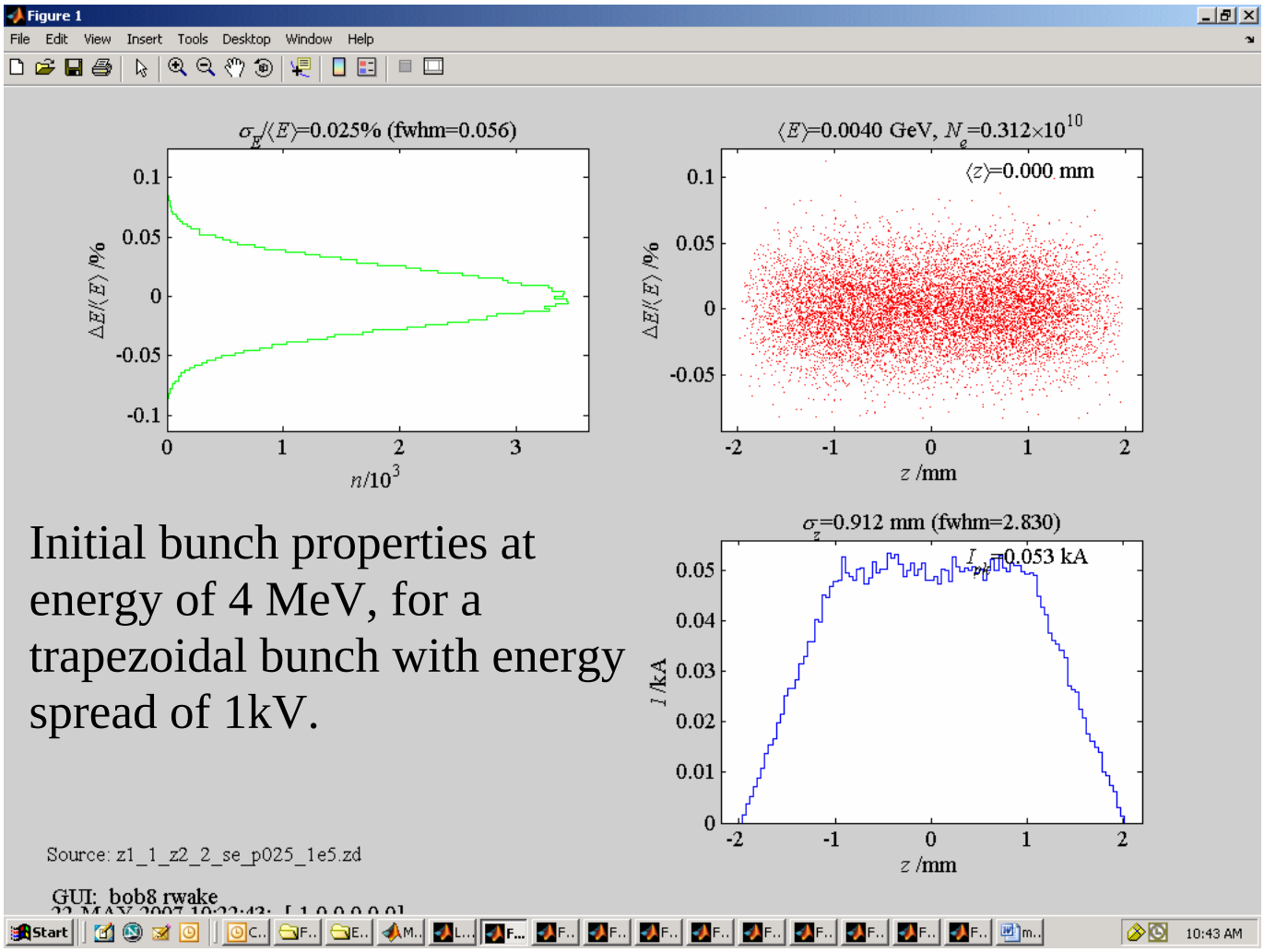

Figure 1(b). Initial bunch properties at energy of 4 MeV, for a trapezoidal bunch of 100,000 particles with flattop of 2 mm, peak current of 50 A and Gaussian energy spread of 1 kV. At the head and tail of the bunch, the current drops linearly to zero over a distance of 1 mm. Every tenth particle is plotted in this and subsequent plots.

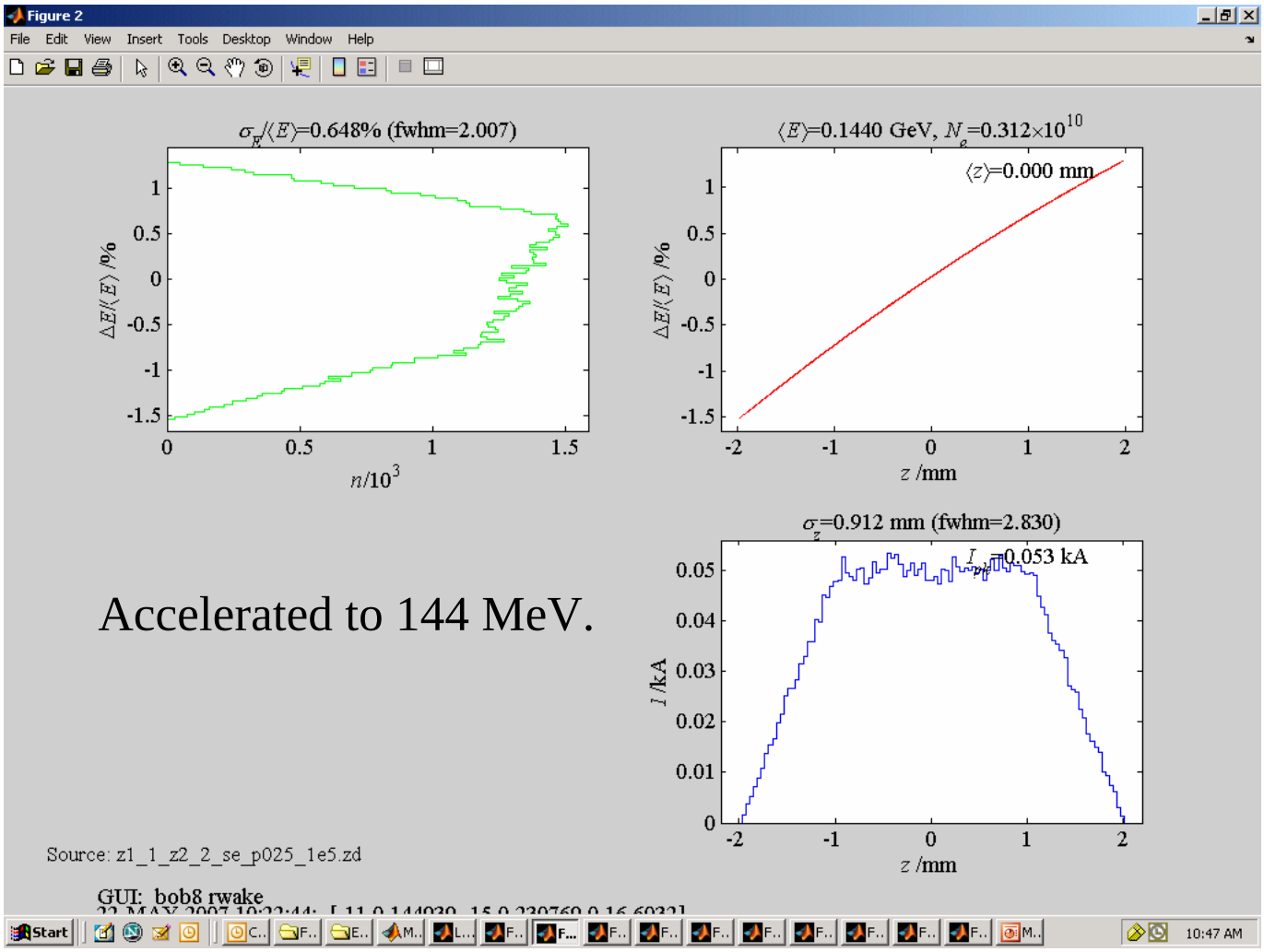

Figure 1(c). Bunch properties after being accelerated to 144 MeV through 16 superconducting 1.3-GHz TESLA cavities contained in 2 cryomodules.

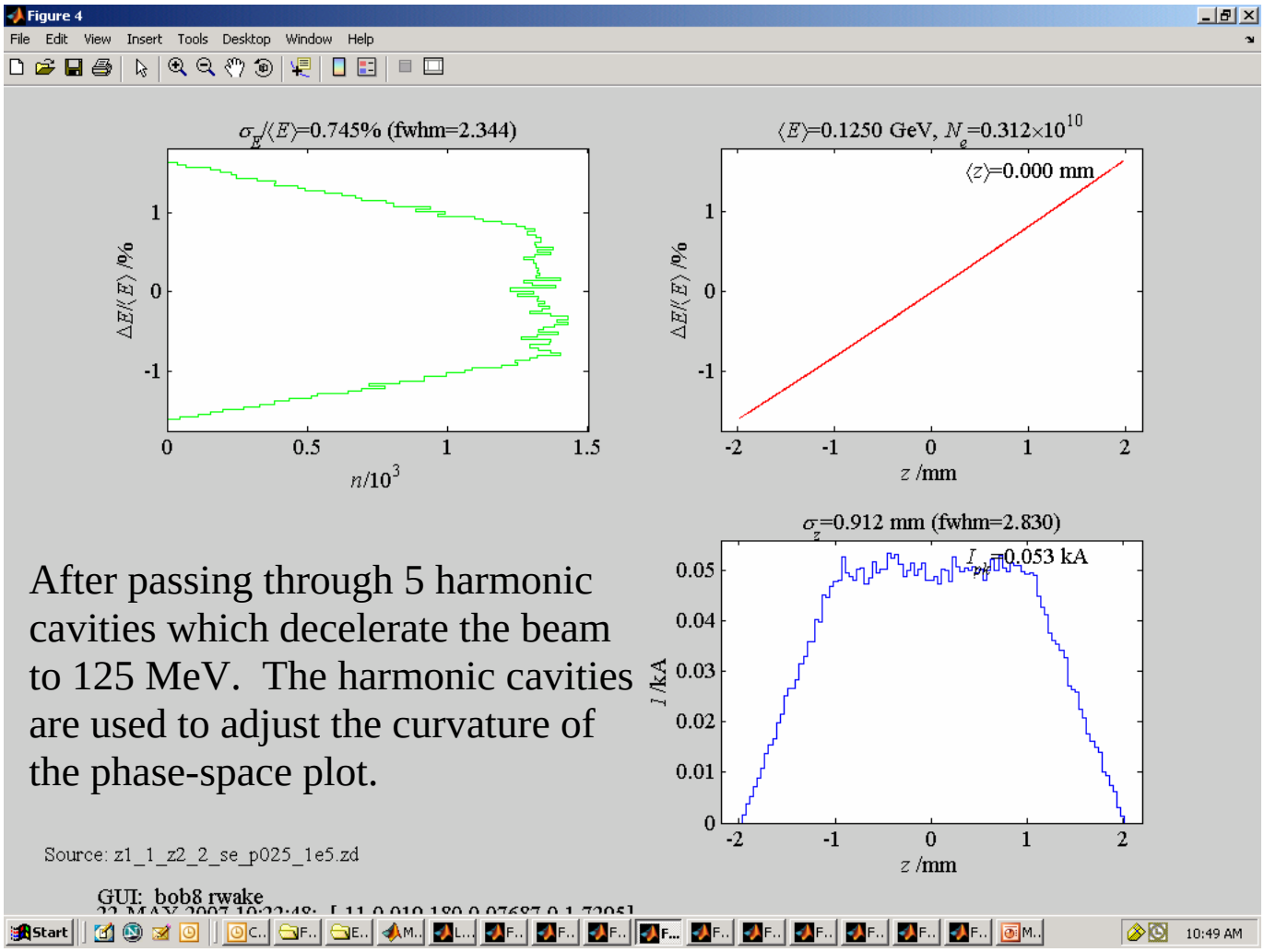

Figure 1(d). Bunch properties after passing through 5 harmonic cavities, immediately before entering the first bunch compressor chicane BC1 at energy of 125 MeV.

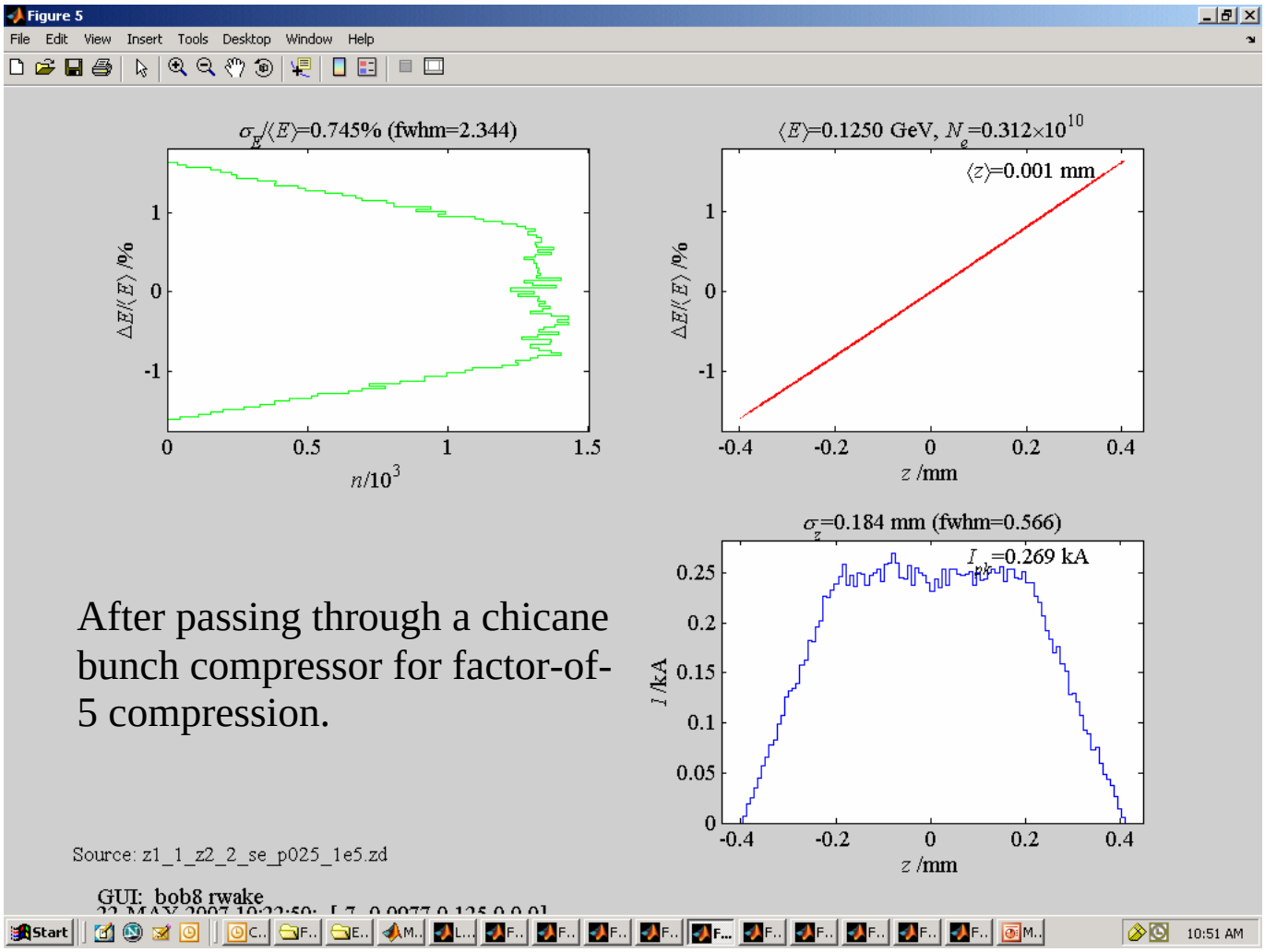

Figure 1(e). Bunch properties after passing through the first chicane BC1.

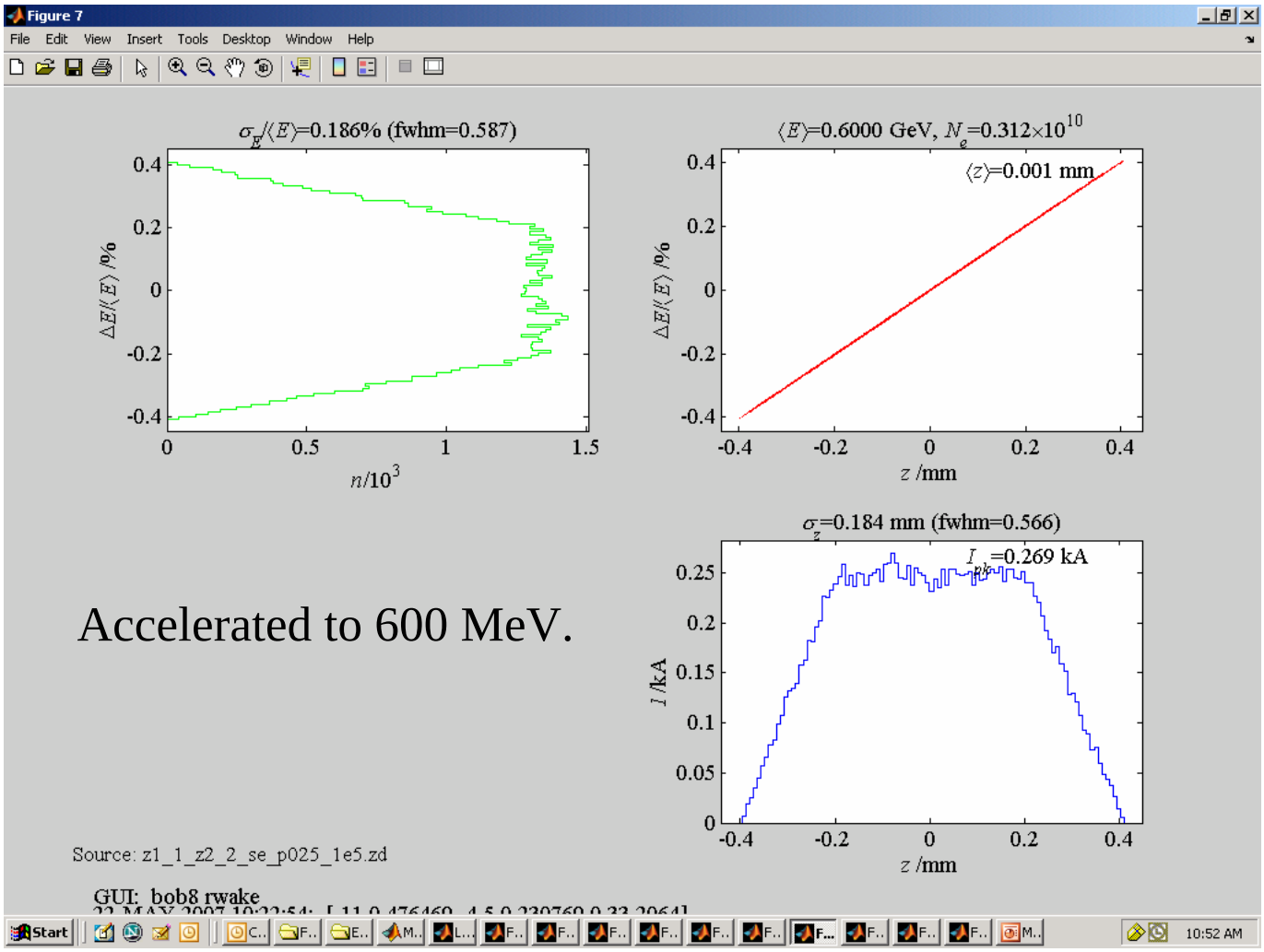

Figure 1(f). Bunch properties at 600 MeV, before entering the second bunch compressor chicane BC2.

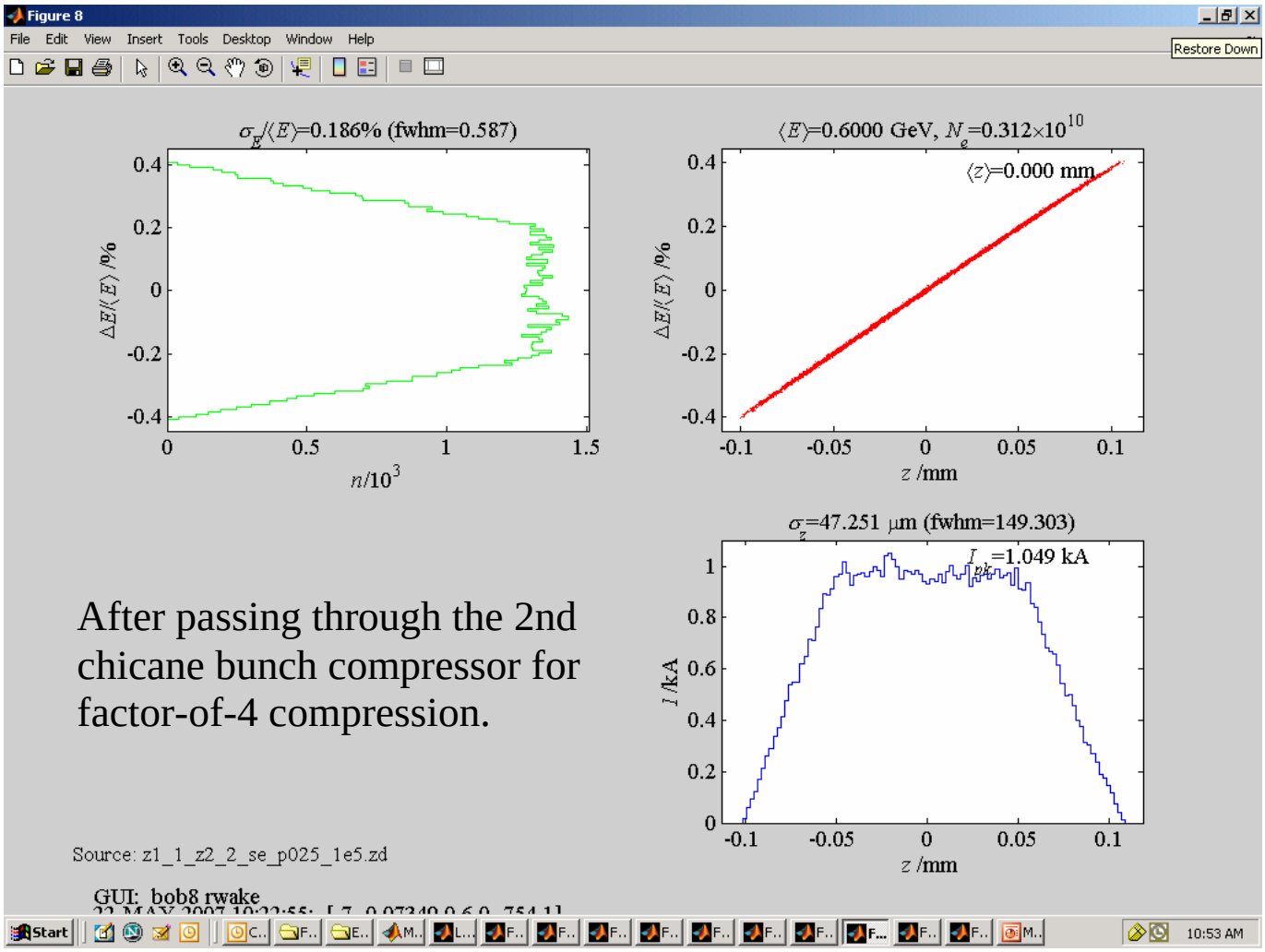

Figure 1(g). Bunch properties at 600 MeV, after passage through the second stage of bunch compression.

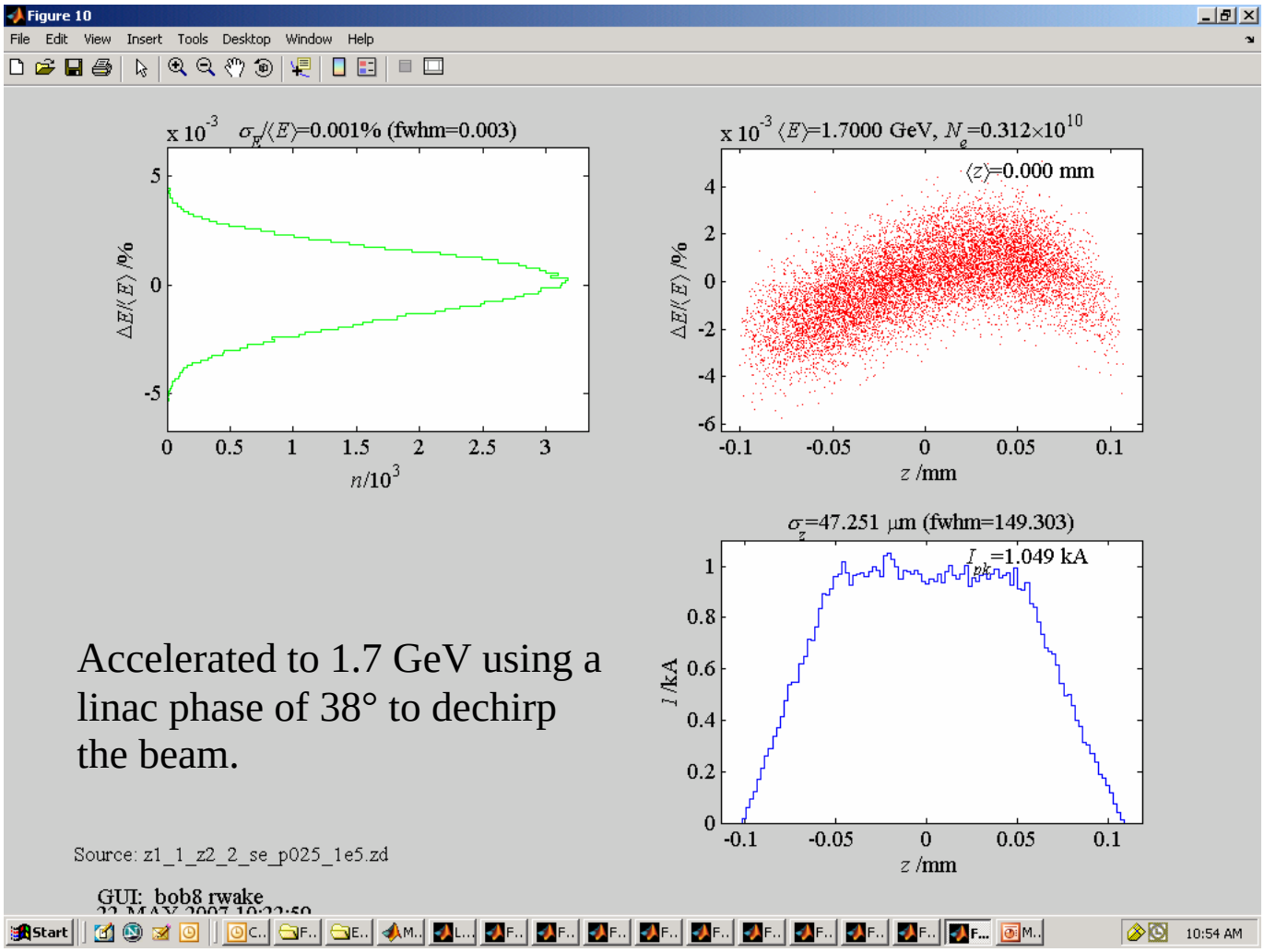

Figure 1(h). Bunch properties after acceleration to 1.7 GeV.

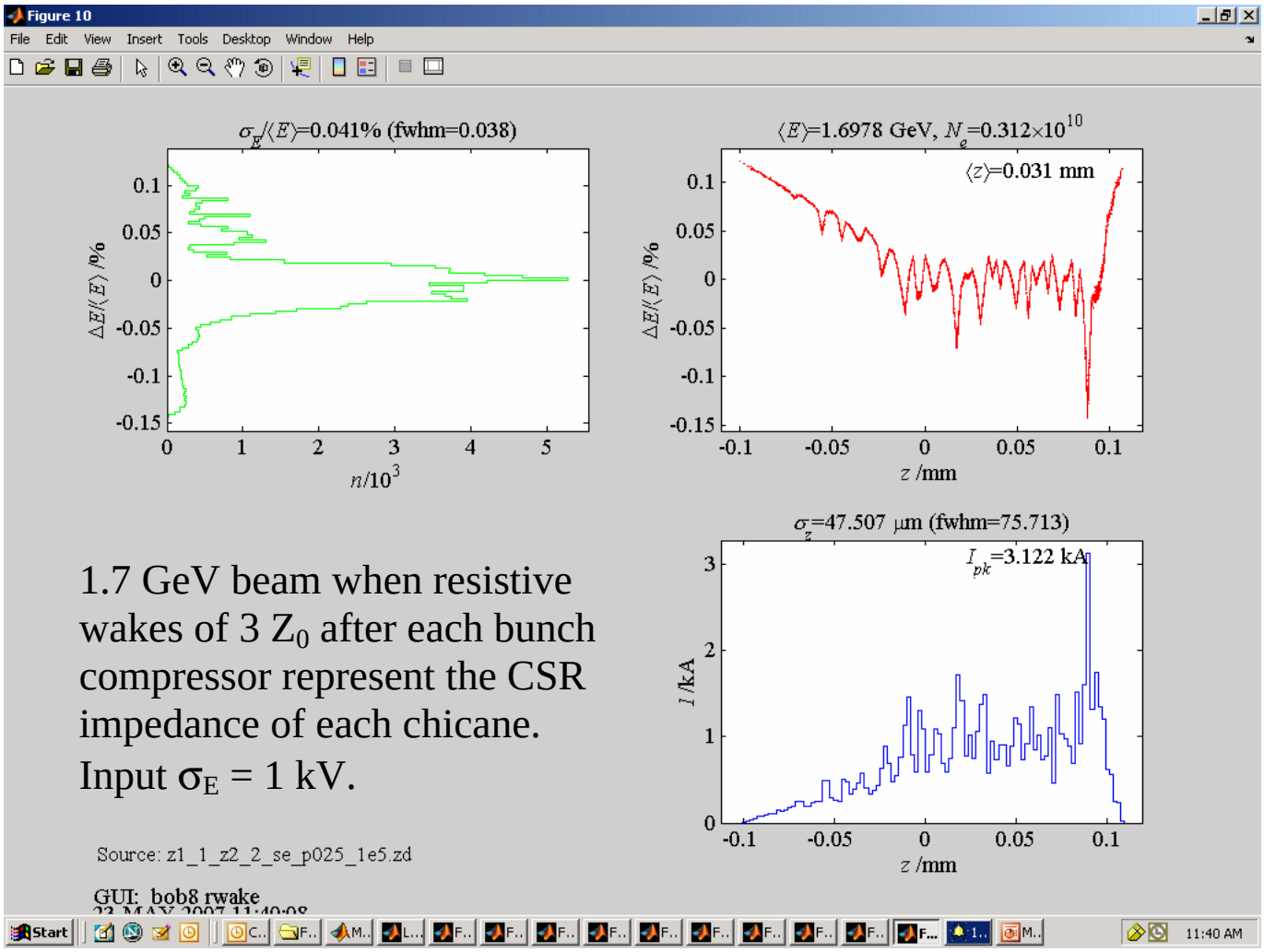

Figure 2(a). Bunch properties at 1.7 GeV when wakes from resistive impedance of $3Z_0$ are modeled after each chicane to approximate coherent edge radiation. Tracking is performed for a trapezoidal bunch of 100,000 particles with flattop current of 50 A and initial Gaussian energy spread of 1 keV.

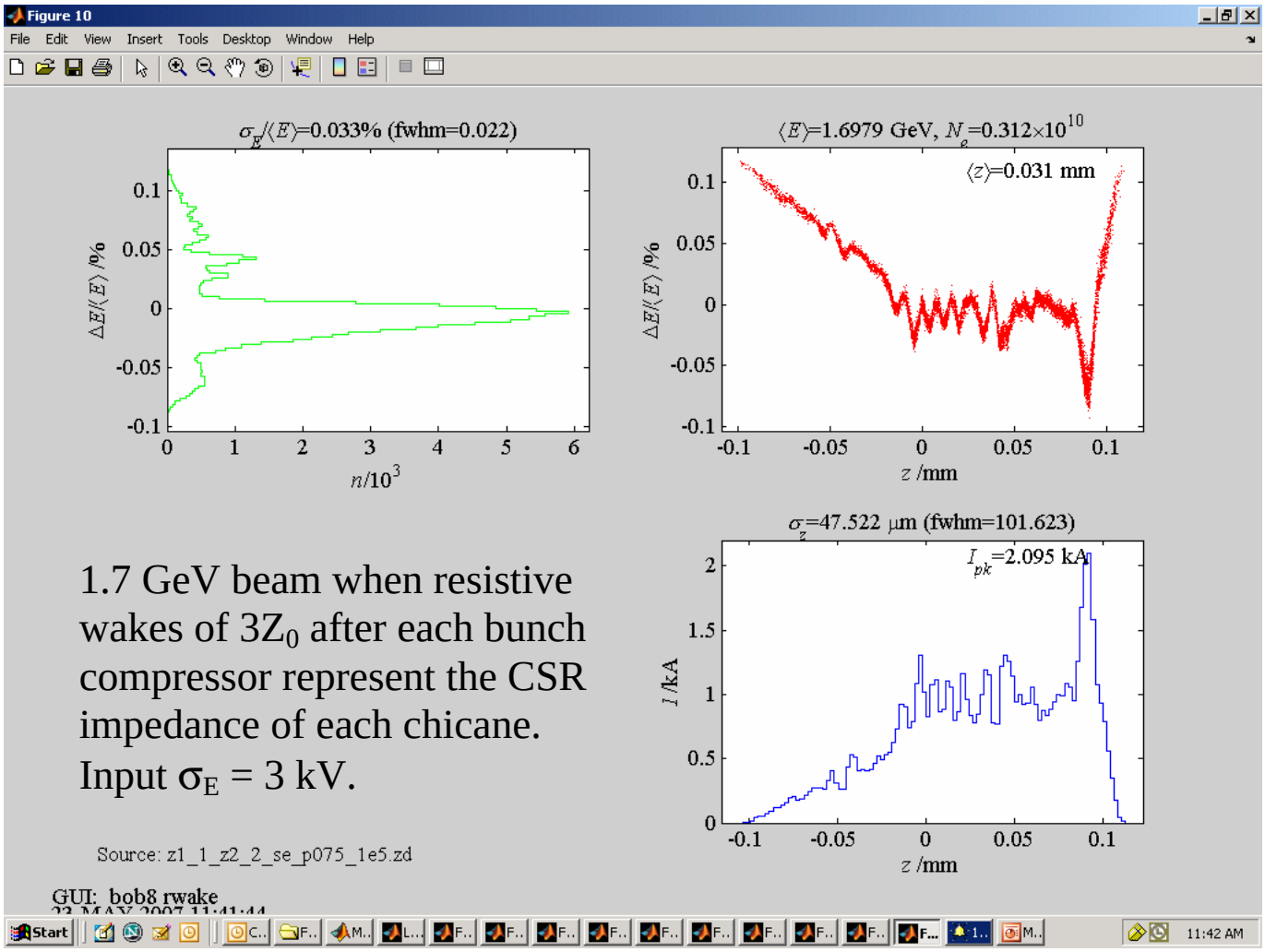

Figure 2(b). Bunch properties at 1.7 GeV when wakes from resistive impedance of $3Z_0$ are modeled after each chicane to approximate coherent edge radiation. Tracking is performed for a trapezoidal bunch of 100,000 particles with flattop current of 50 A and initial Gaussian energy spread of 3 keV.

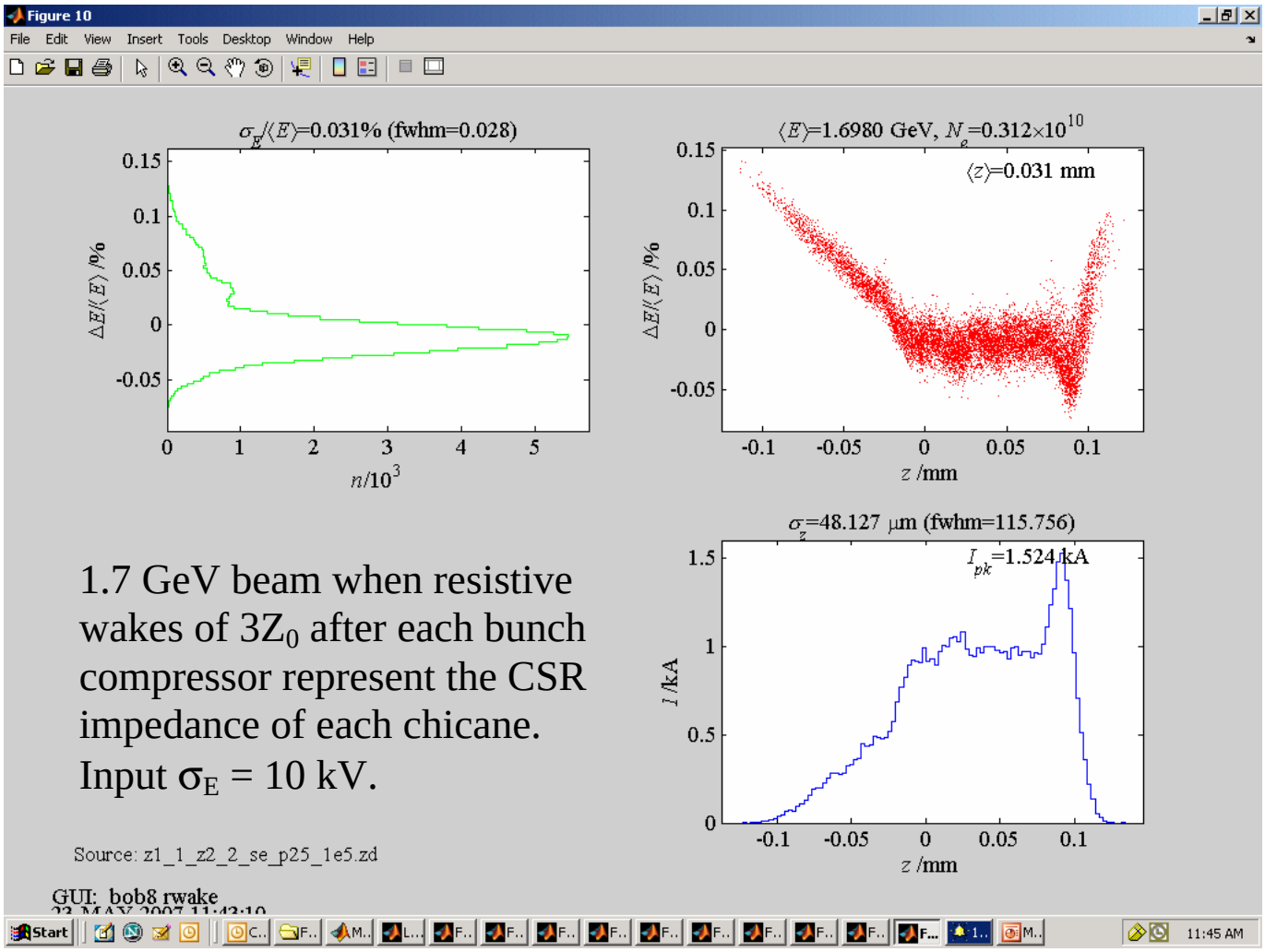

Figure 2(c). Bunch properties at 1.7 GeV when wakes from resistive impedance of $3Z_0$ are modeled after each chicane to approximate coherent edge radiation. Tracking is performed for a trapezoidal bunch of 100,000 particles with flattop current of 50 A and initial Gaussian energy spread of 10 keV.

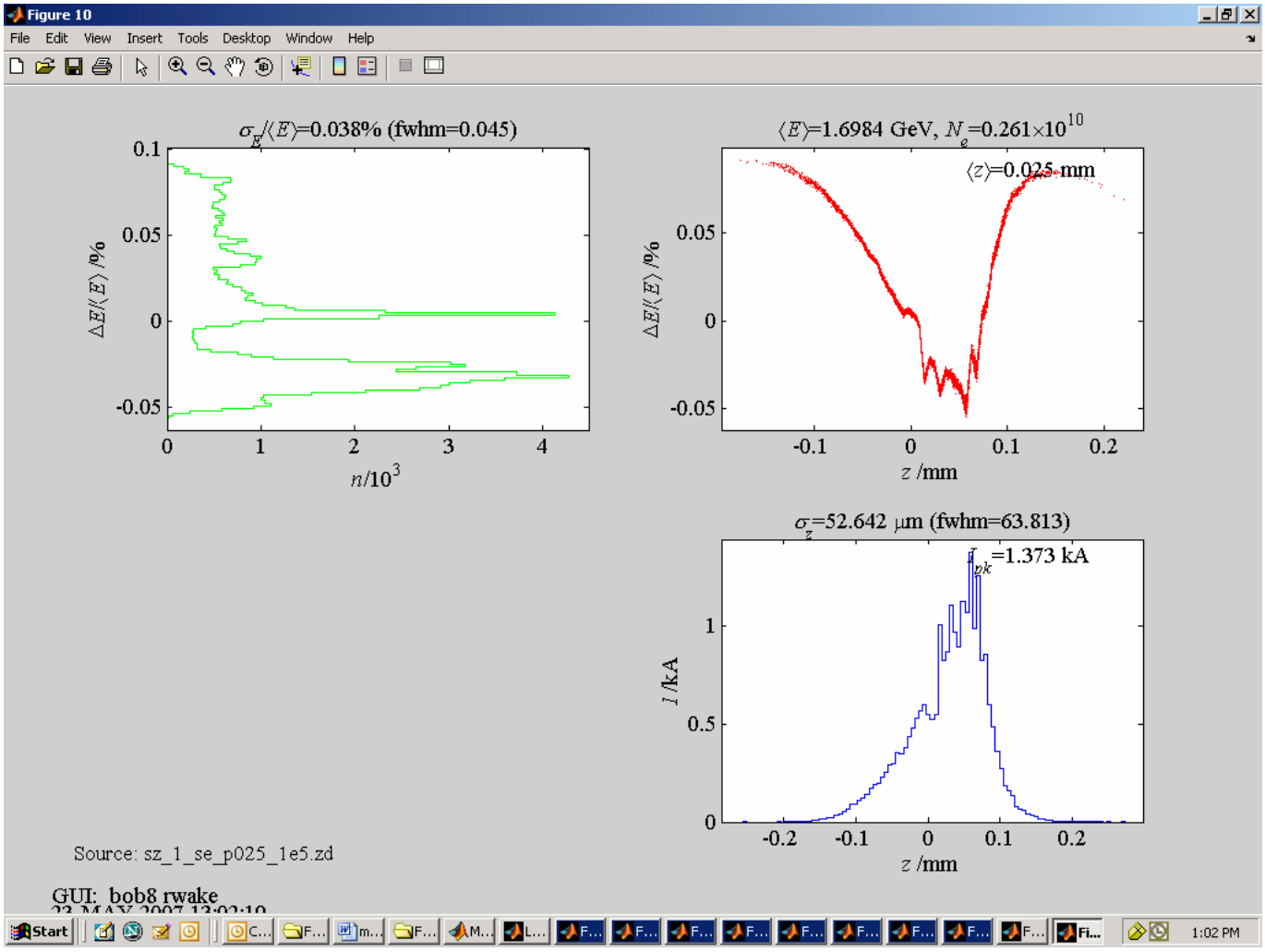

Figure 3(a). Bunch properties at 1.7 GeV when wakes from resistive impedance of $3Z_0$ are modeled after each chicane to approximate coherent edge radiation. Tracking is performed for a Gaussian bunch of 100,000 particles with peak current of 50 A, $\sigma_z = 1$ mm and initial Gaussian energy spread of 1 keV.

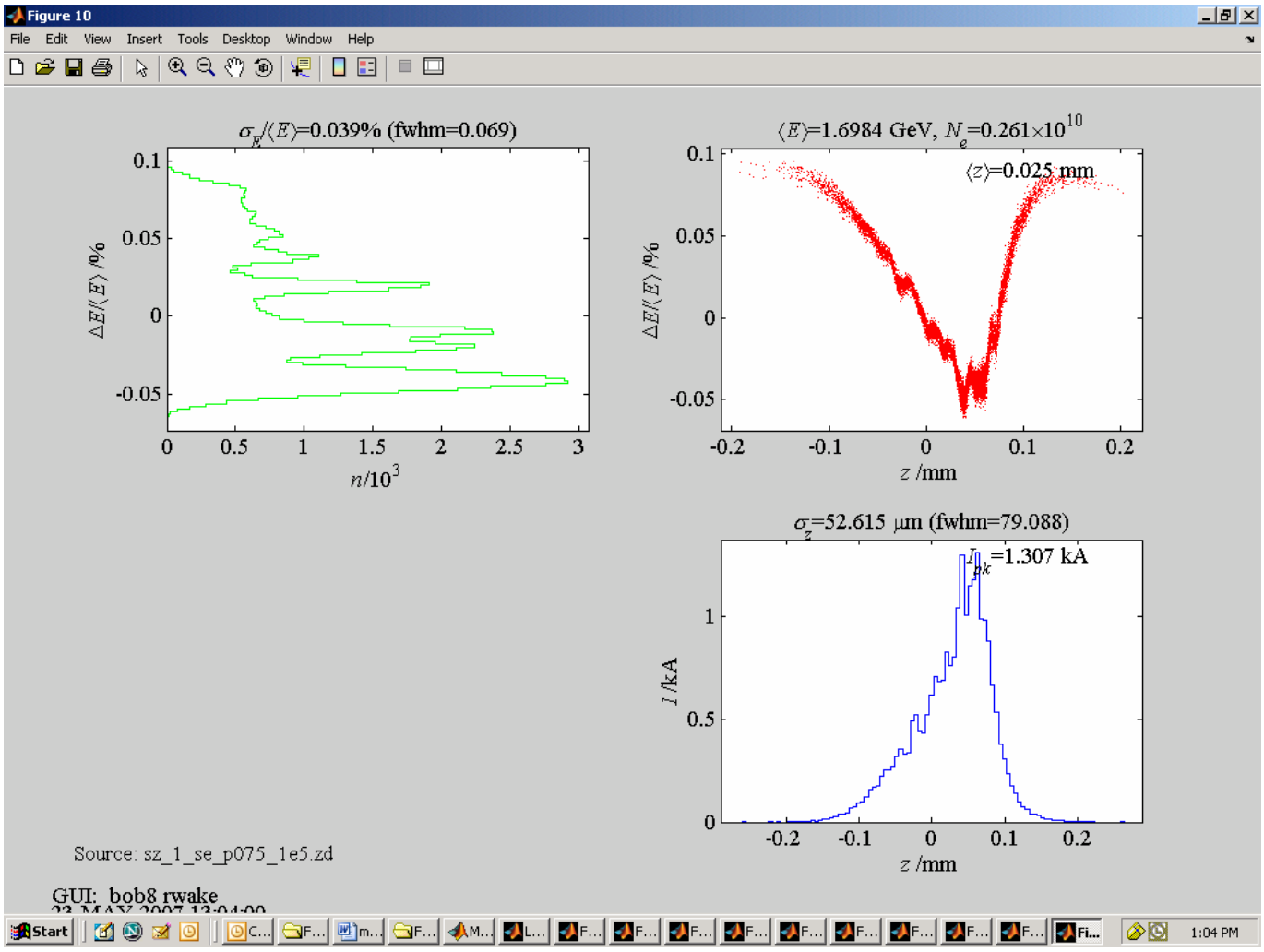

Figure 3(b). Bunch properties at 1.7 GeV when wakes from resistive impedance of $3Z_0$ are modeled after each chicane to approximate coherent edge radiation. Tracking is performed for a Gaussian bunch of 100,000 particles with peak current of 50 A, $\sigma_z = 1$ mm and initial Gaussian energy spread of 3 keV.

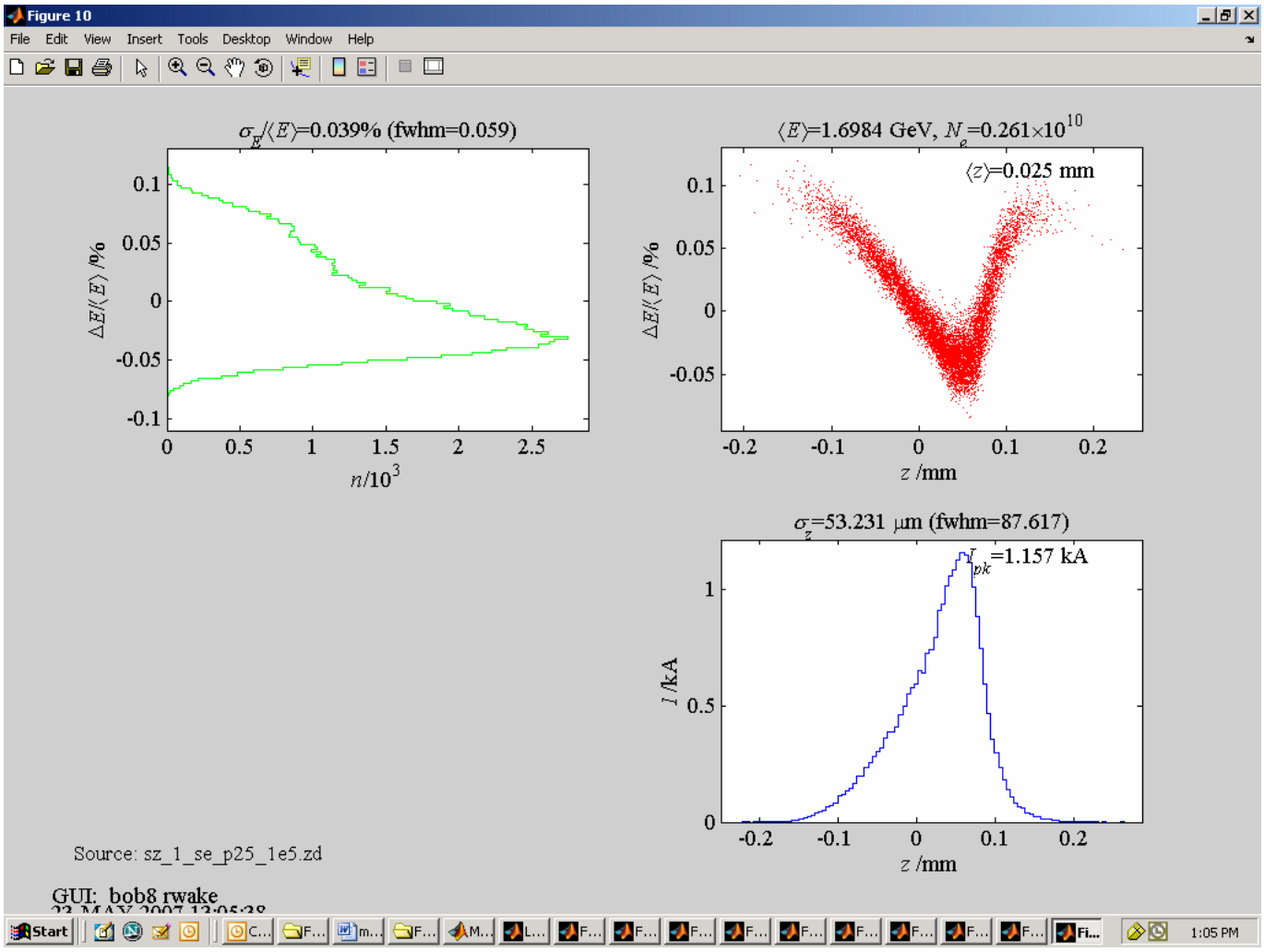

Figure 3(c). Bunch properties at 1.7 GeV when wakes from resistive impedance of $3Z_0$ are modeled after each chicane to approximate coherent edge radiation. Tracking is performed for a Gaussian bunch of 100,000 particles with peak current of 50 A, $\sigma_z = 1$ mm and initial Gaussian energy spread of 10 keV.

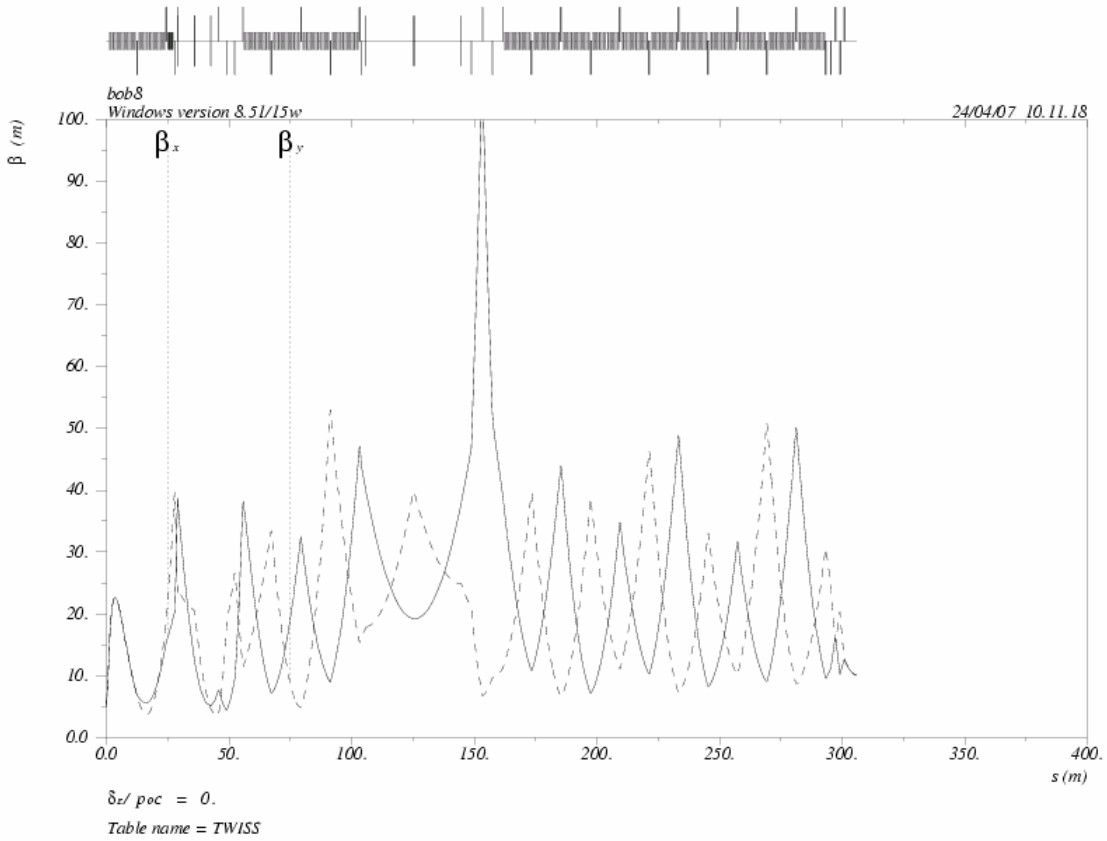

Figure 4. Lattice functions for an implementation of the preliminary bunch compressor design that uses FODO focusing in the linacs.

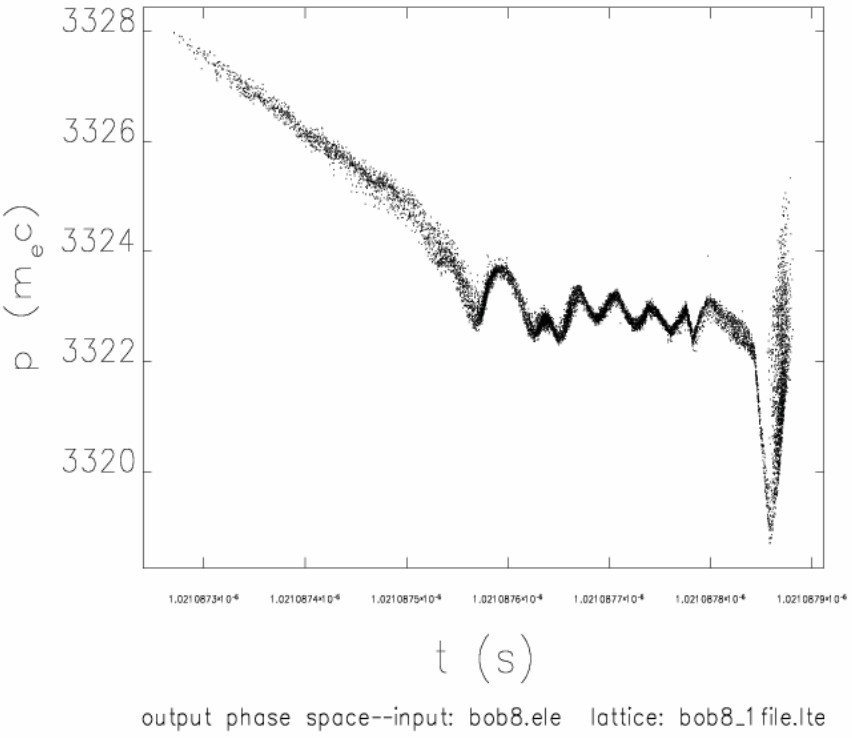

Figure 5(a). Longitudinal phase space at 1.7 GeV from tracking by the code "elegant" of a trapezoidal bunch of 100,000 particles with flattop current of 50 A, normalized emittance of 1 μm and Gaussian energy spread of 1 keV. Coherent synchrotron radiation is modeled in the chicane bending magnets and downstream drift regions. The initial longitudinal bunch properties are the same as in fig. 2(a).

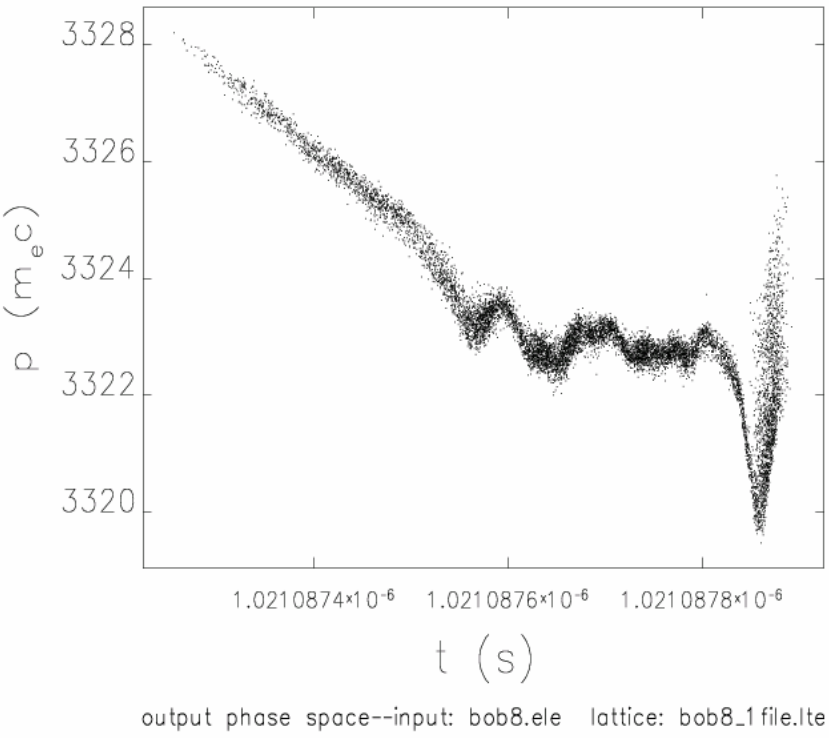

Figure 5(b). Longitudinal phase space at 1.7 GeV from tracking by the code "elegant" of a trapezoidal bunch of 100,000 particles with flattop current of 50 A, normalized emittance of 1 μm and Gaussian energy spread of 3 keV. Coherent synchrotron radiation is modeled in the chicane bending magnets and downstream drift regions. The initial longitudinal bunch properties are the same as in fig. 2(b).

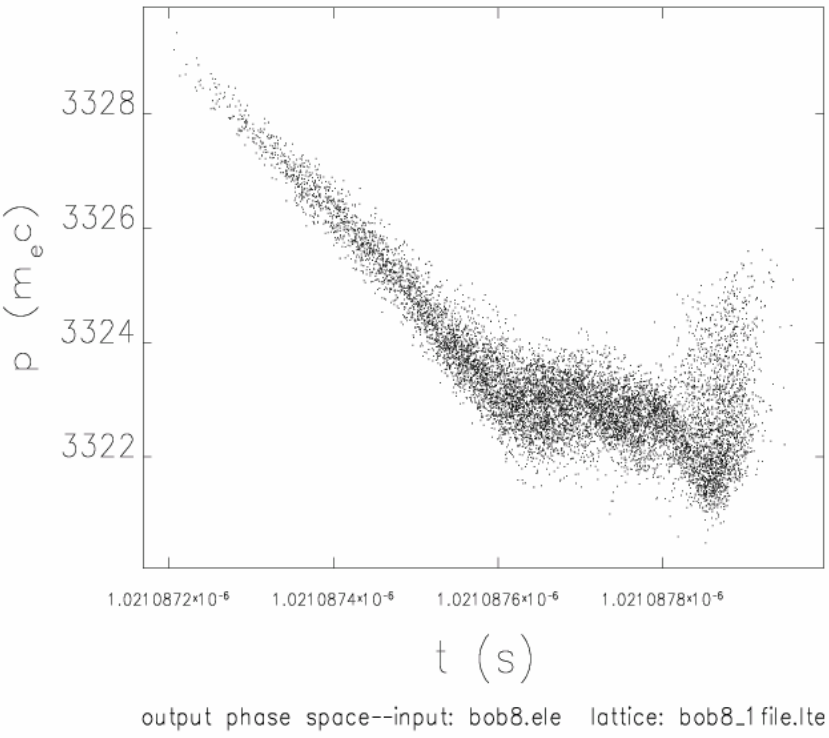

Figure 5(c). Longitudinal phase space at 1.7 GeV from tracking by the code "elegant" of a trapezoidal bunch of 100,000 particles with flattop current of 50 A, normalized emittance of 1 μm and Gaussian energy spread of 10 keV. Coherent synchrotron radiation is modeled in the chicane bending magnets and downstream drift regions. The initial longitudinal bunch properties are the same as in fig. 2(c).

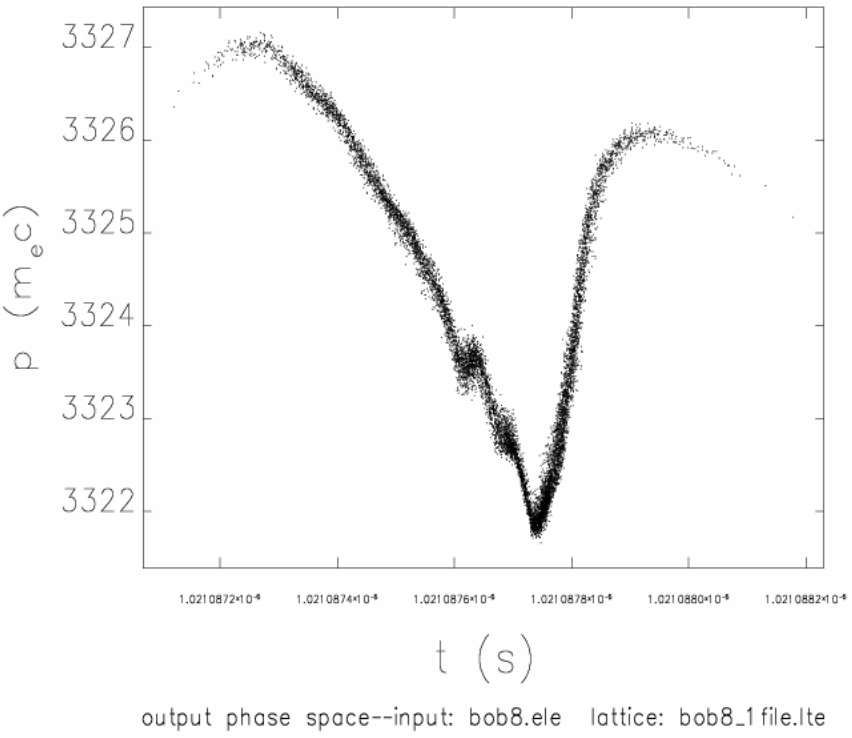

Figure 6(a). Longitudinal phase space at 1.7 GeV from tracking by the code "elegant" of a Gaussian bunch of 100,000 particles with peak current of 50 A, rms bunchlength of 1 mm, normalized emittance of 1 μm and Gaussian energy spread of 1 keV. Coherent synchrotron radiation is modeled in the chicane bending magnets and downstream drift regions. The initial longitudinal bunch properties are the same as in fig. 3(a).

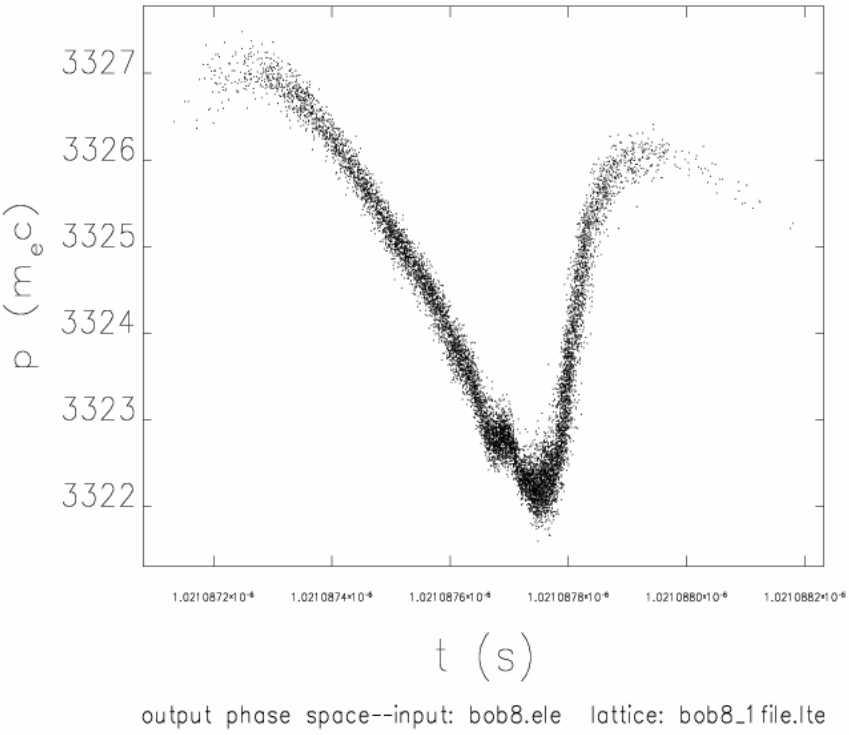

Figure 6(b). Longitudinal phase space at 1.7 GeV from tracking by the code "elegant" of a Gaussian bunch of 100,000 particles with peak current of 50 A, rms bunchlength of 1 mm, normalized emittance of 1 μm and Gaussian energy spread of 3 keV. Coherent synchrotron radiation is modeled in the chicane bending magnets and downstream drift regions. The initial longitudinal bunch properties are the same as in fig. 3(b).

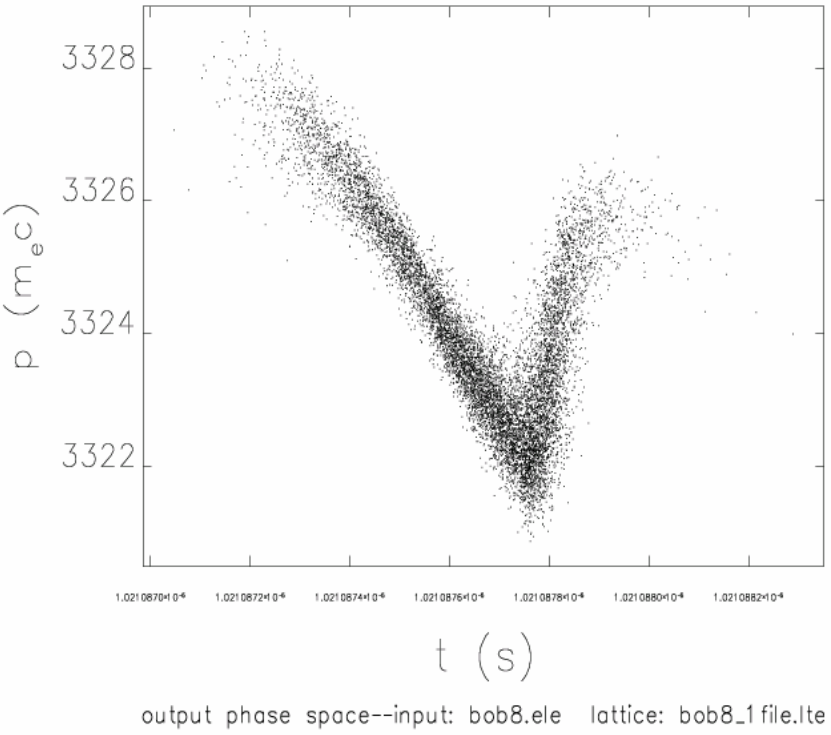

Figure 6(c). Longitudinal phase space at 1.7 GeV from tracking by the code "elegant" of a Gaussian bunch of 100,000 particles with peak current of 50 A, rms bunchlength of 1 mm, normalized emittance of 1 μm and Gaussian energy spread of 10 keV. Coherent synchrotron radiation is modeled in the chicane bending magnets and downstream drift regions. The initial longitudinal bunch properties are the same as in fig. 3(c).

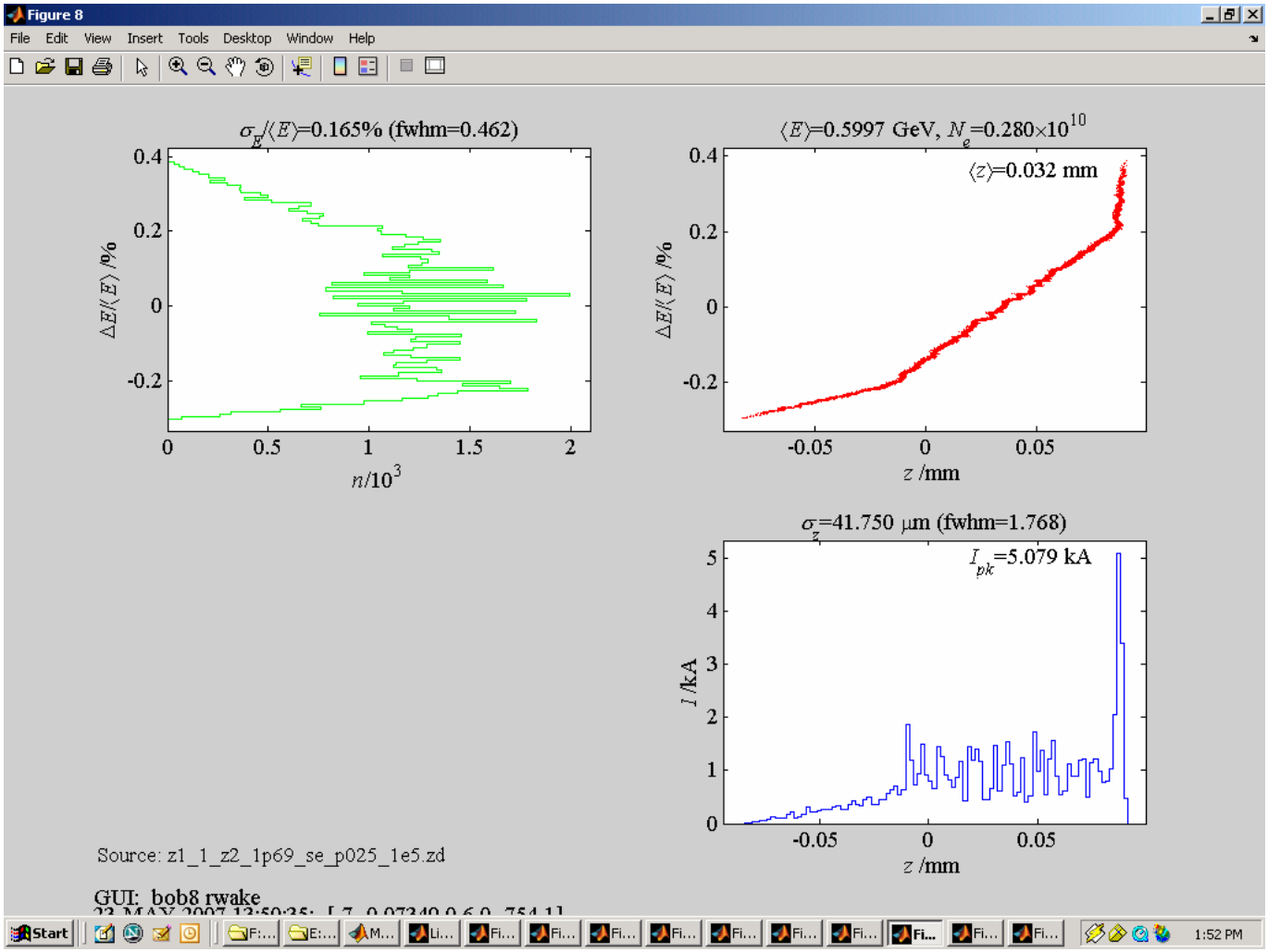

Figure 7(a). Bunch properties immediately after the second bunch compressor chicane BC2 (and prior to the resistive impedance R_2) for an initial trapezoidal bunch of 100,000 particles at 4 MeV with Gaussian energy spread of 1 keV. The initial bunch has current of 50 A over a length of 2 mm, with current dropping linearly to zero over a distance of 0.69 mm. Wakes from resistive impedance of $3Z_0$ are modeled after each chicane.

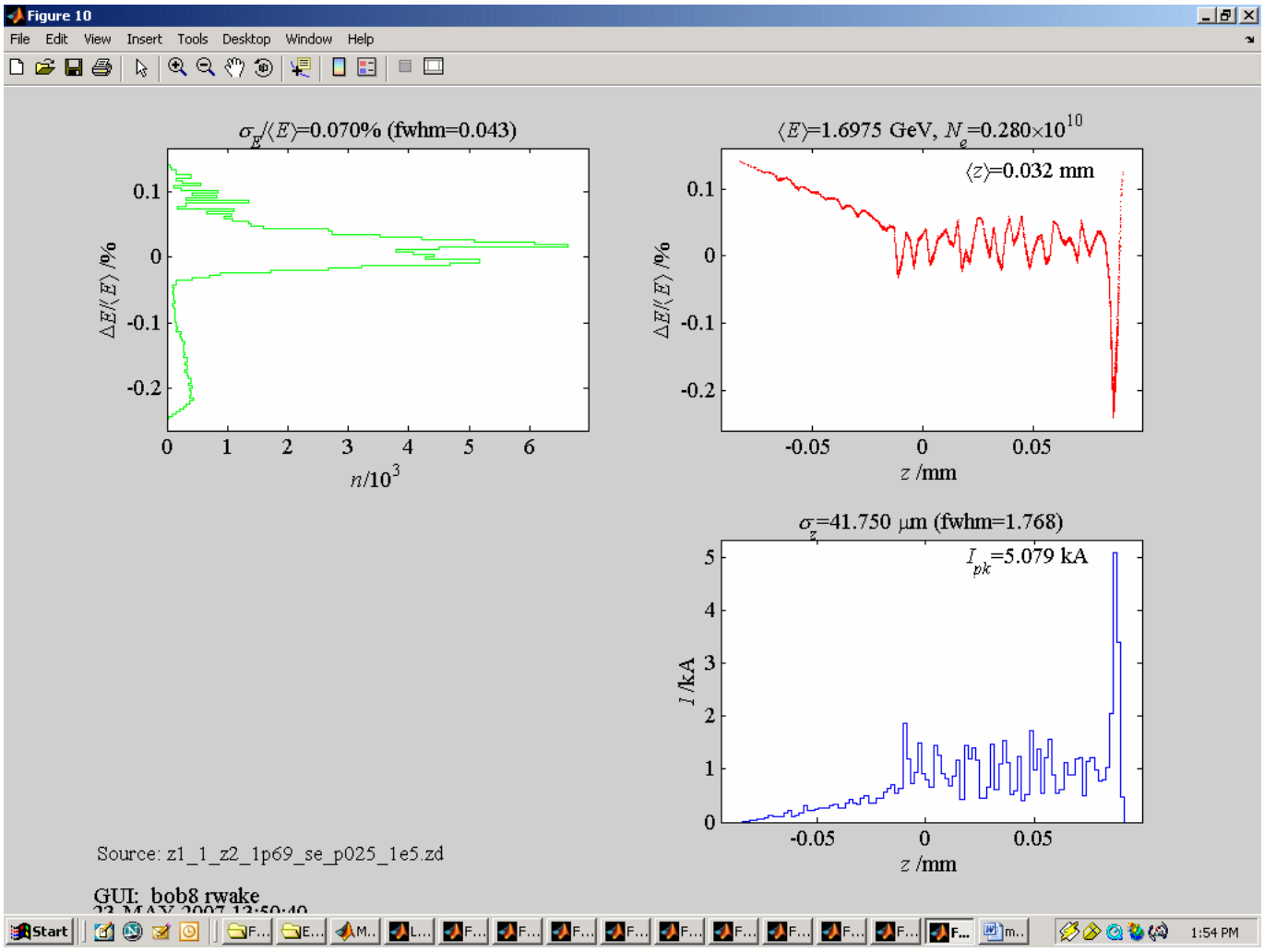

Figure 7(b). Bunch properties at 1.7 GeV for an initial trapezoidal bunch of 100,000 particles at 4 MeV with Gaussian energy spread of 1 keV. The initial bunch has current of 50 A over a length of 2 mm, with current dropping linearly to zero over a distance of 0.69 mm. Wakes from resistive impedance of $3Z_0$ are modeled after each chicane.

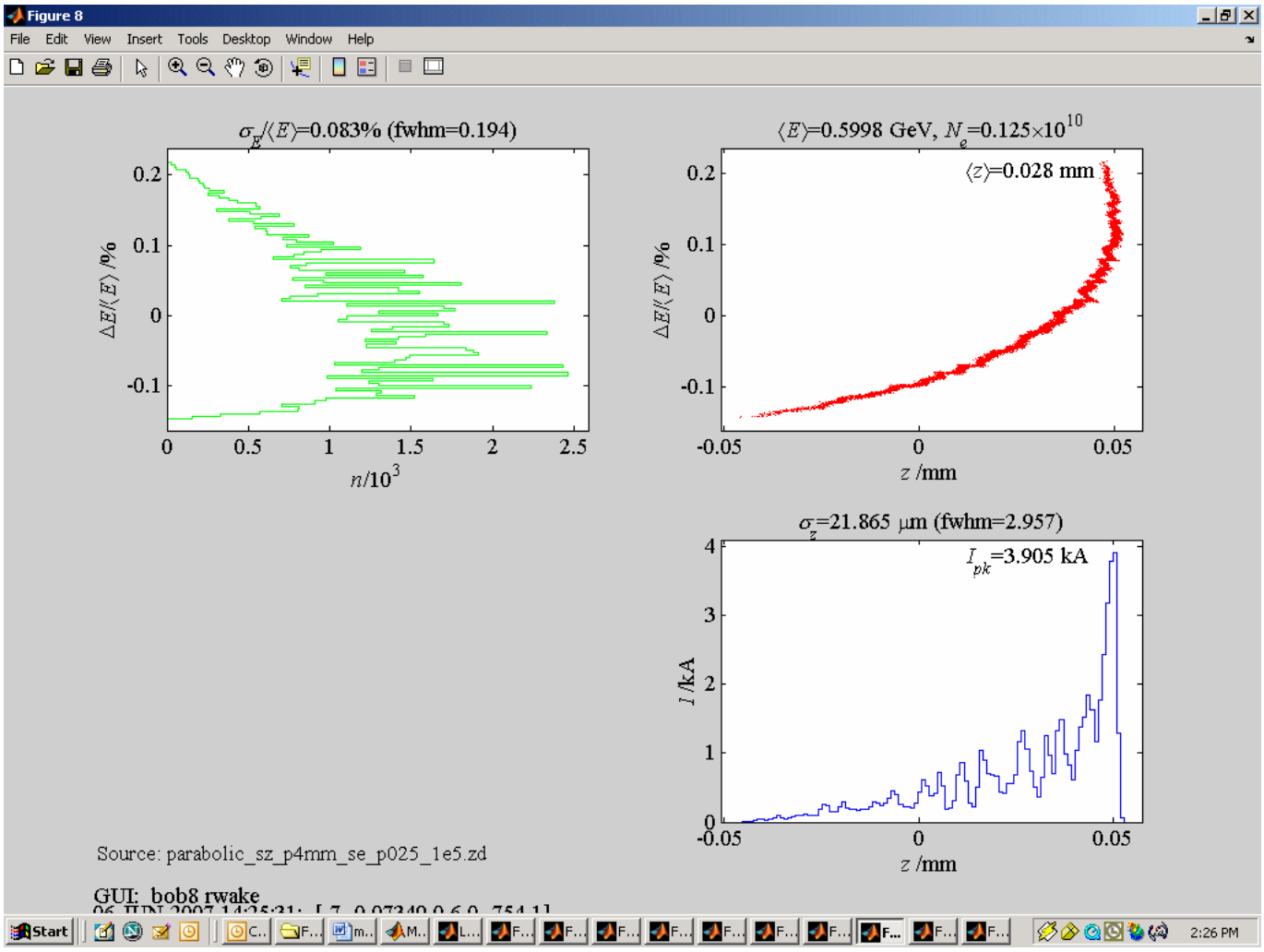

Figure 8(a). Bunch properties immediately after the second bunch compressor chicane BC2 (and prior to the resistive impedance R_2) for an initial parabolic bunch of 100,000 particles with Gaussian energy spread of 1 keV, $\sigma_z = 0.4$ mm, peak current of 50 A and bunch charge of 200 pC. Wakes from resistive impedance of $3Z_0$ are modeled after each chicane.

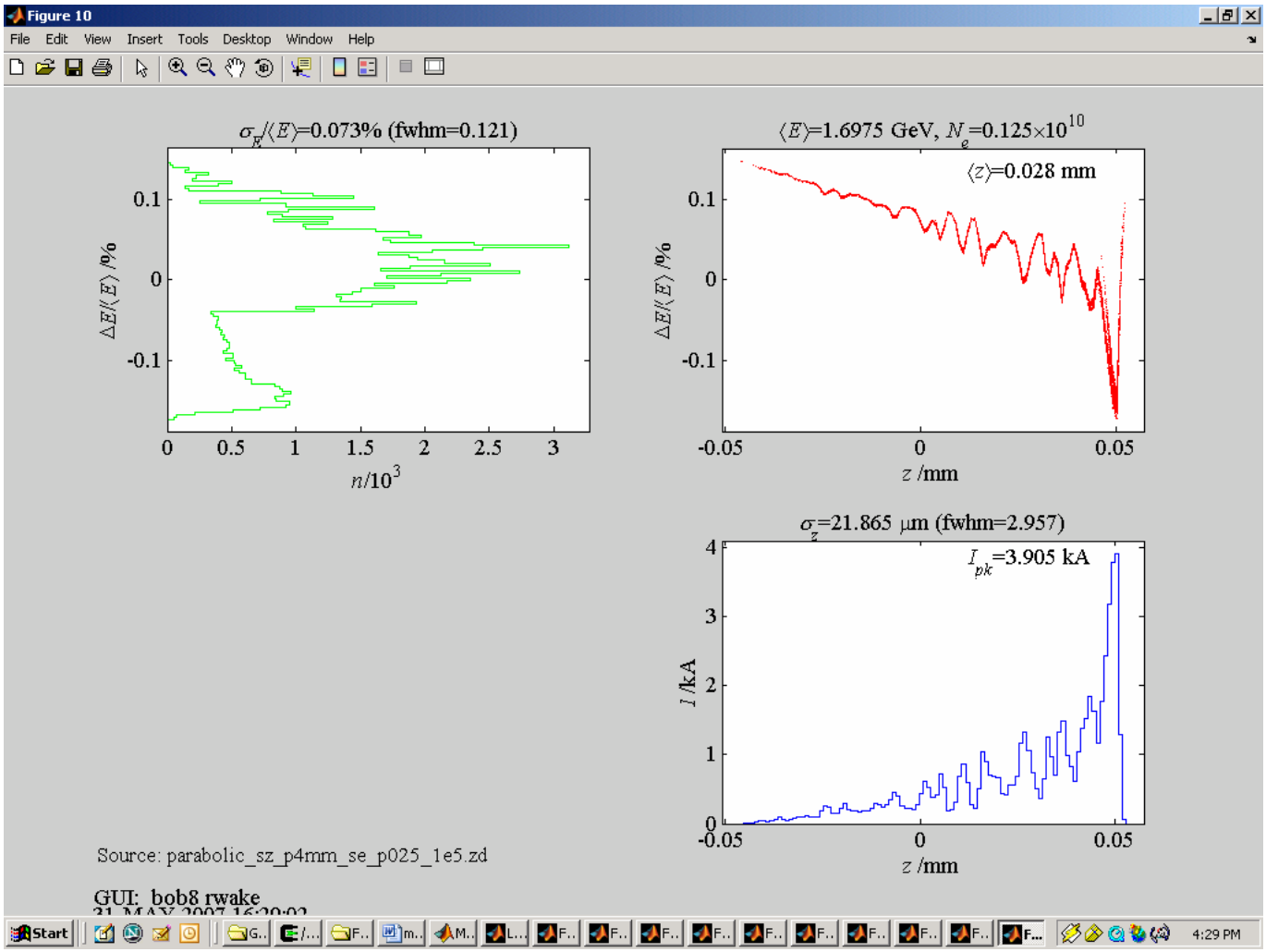

Figure 8(b). Bunch properties at 1.7 GeV for an initial parabolic bunch of 100,000 particles with Gaussian energy spread of 1 keV, $\sigma_z = 0.4$ mm, peak current of 50 A and bunch charge of 200 pC. Wakes from resistive impedance of $3Z_0$ are modeled after each chicane.

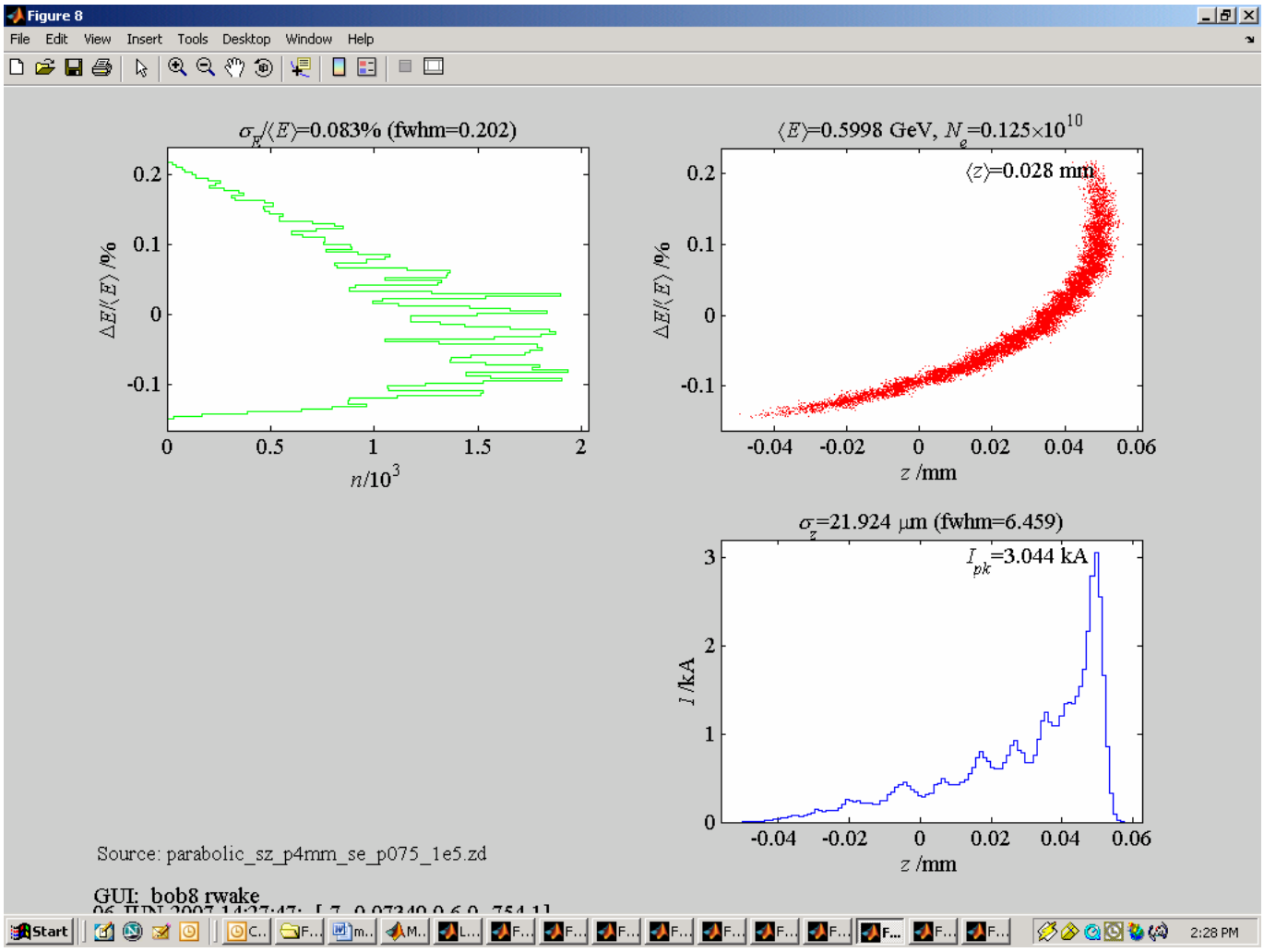

Figure 8(c). Bunch properties immediately after the second bunch compressor chicane BC2 (and prior to the resistive impedance R_2) for an initial parabolic bunch of 100,000 particles with Gaussian energy spread of 3 keV, $\sigma_z = 0.4$ mm, peak current of 50 A and bunch charge of 200 pC. Wakes from resistive impedance of $3Z_0$ are modeled after each chicane.

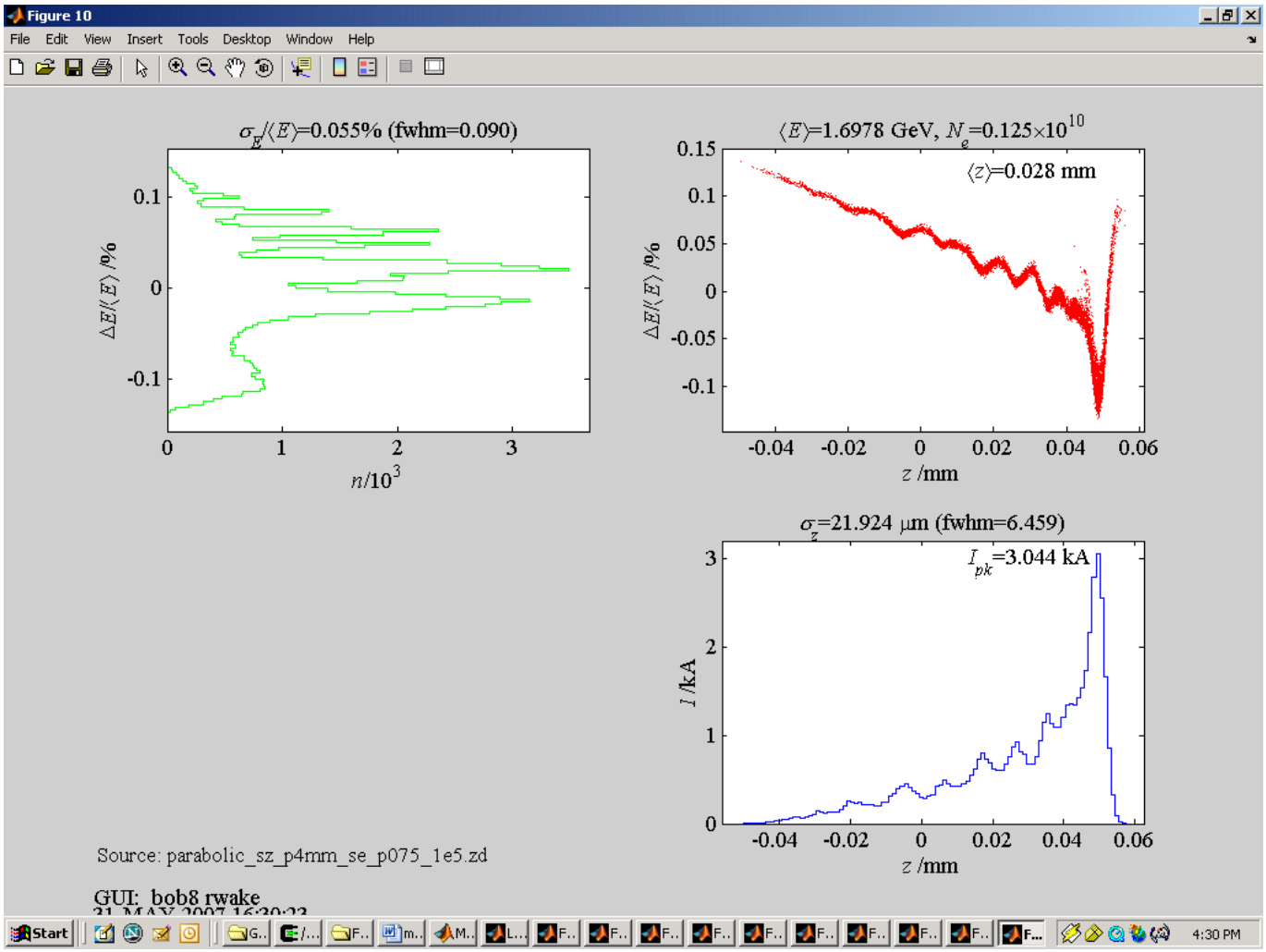

Figure 8(d). Bunch properties at 1.7 GeV for an initial parabolic bunch of 100,000 particles with Gaussian energy spread of 3 keV, $\sigma_z = 0.4$ mm, peak current of 50 A and bunch charge of 200 pC. Wakes from resistive impedance of $3Z_0$ are modeled after each chicane.

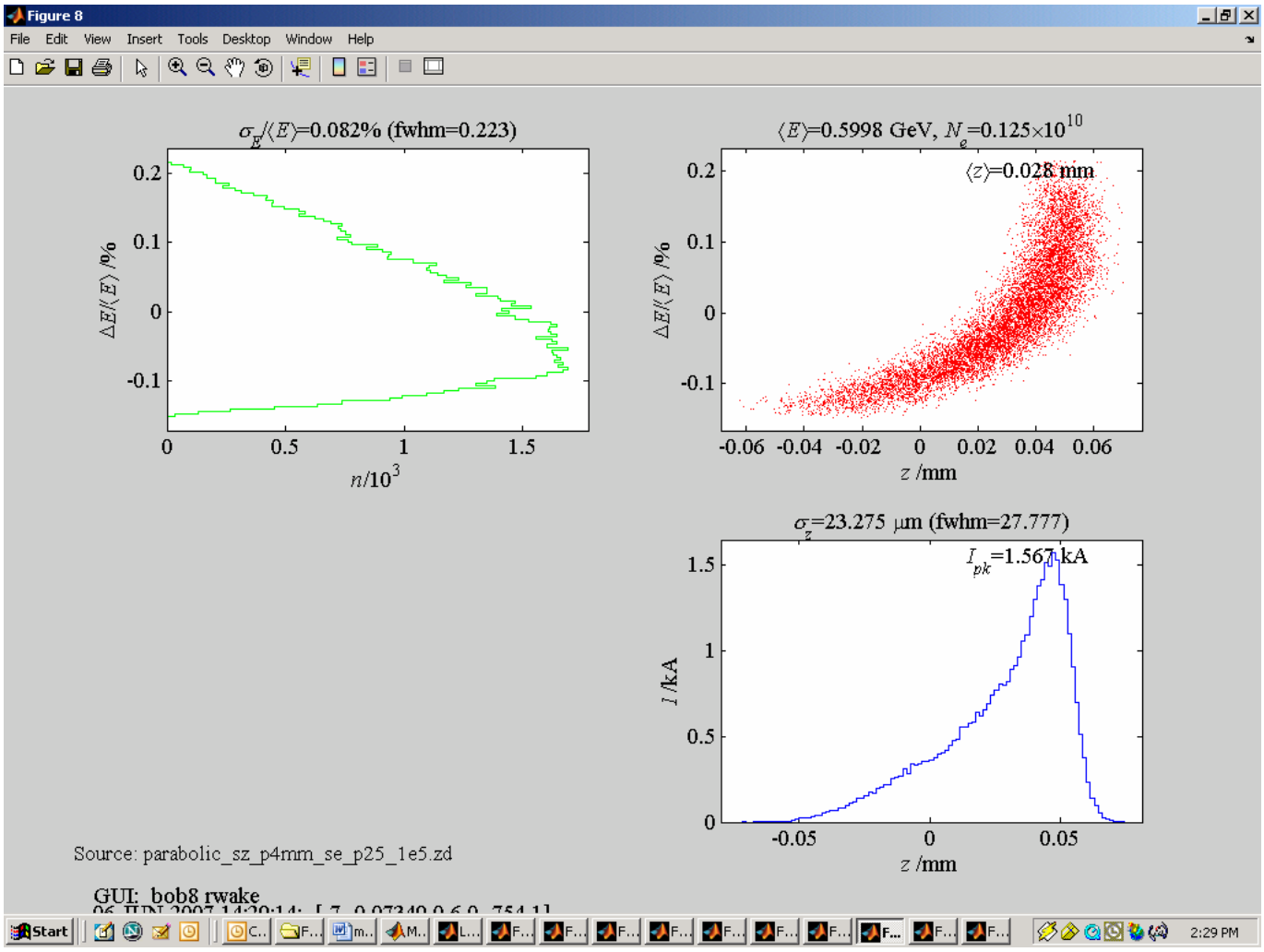

Figure 8(e). Bunch properties immediately after the second bunch compressor chicane BC2 (and prior to the resistive impedance R_2) for an initial parabolic bunch of 100,000 particles with Gaussian energy spread of 10 keV, $\sigma_z = 0.4$ mm, peak current of 50 A and bunch charge of 200 pC. Wakes from resistive impedance of $3Z_0$ are modeled after each chicane.

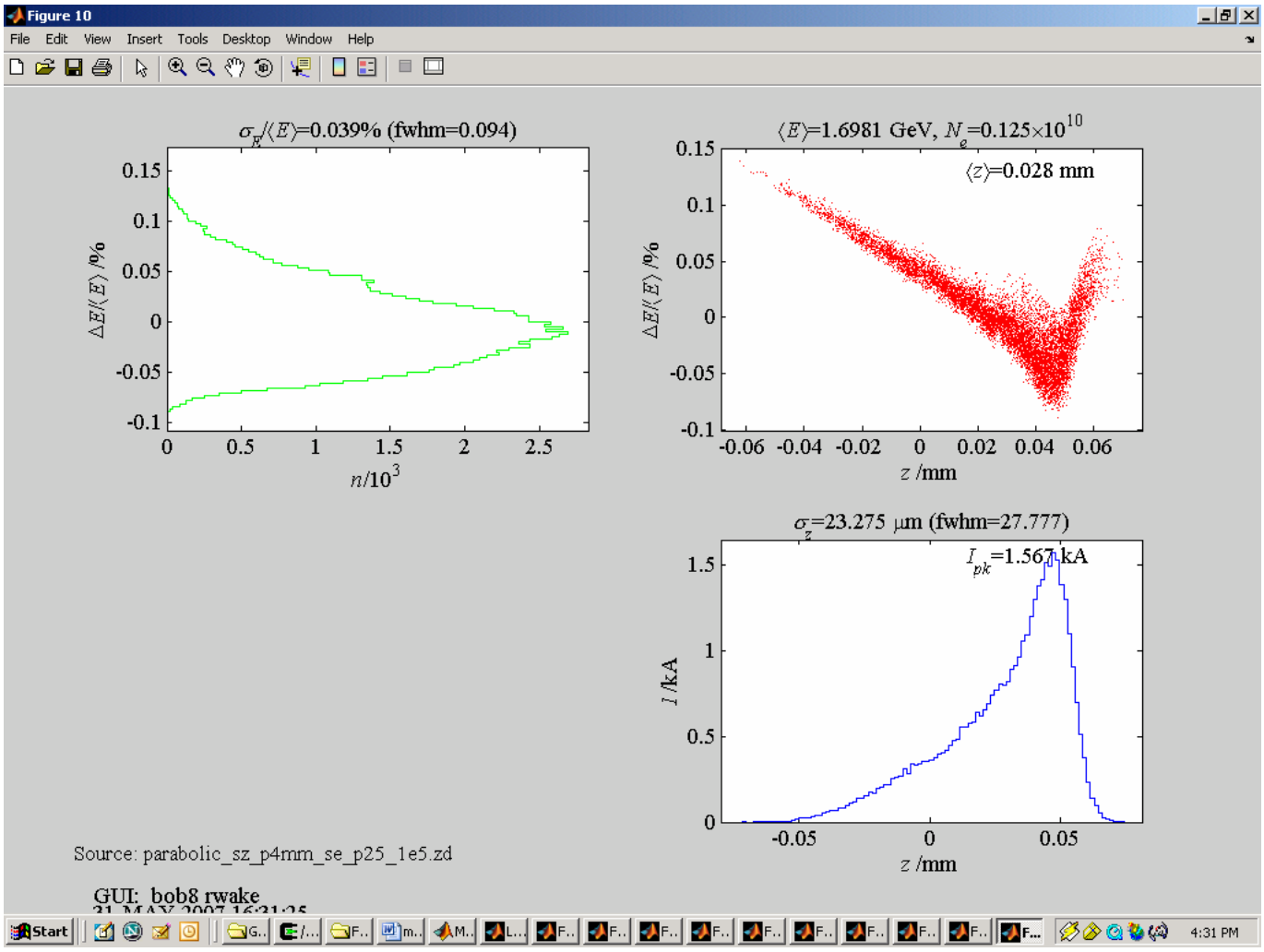

Figure 8(f). Bunch properties at 1.7 GeV for an initial parabolic bunch of 100,000 particles with Gaussian energy spread of 10 keV, $\sigma_z = 0.4$ mm, peak current of 50 A and bunch charge of 200 pC. Wakes from resistive impedance of $3Z_0$ are modeled after each chicane.

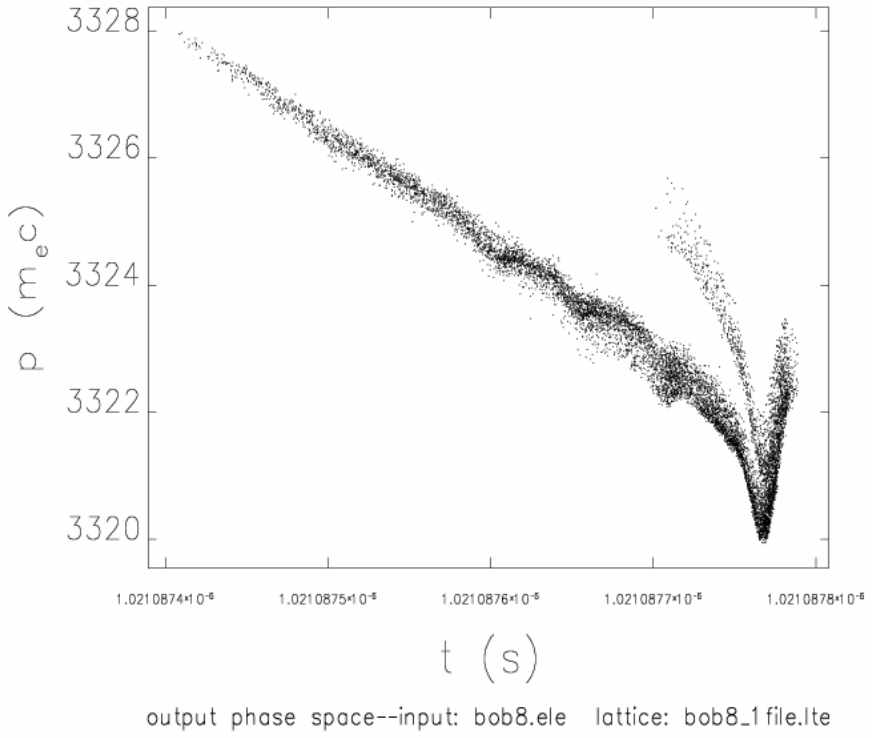

Figure 9(a). Longitudinal phase space at 1.7 GeV from tracking by the code "elegant" of a parabolic bunch of 100,000 particles with peak current of 50 A, charge of 200 pC, rms bunchlength of 0.4 mm, normalized emittance of 1 μm and Gaussian energy spread of 1 keV. Coherent synchrotron radiation is modeled in the chicane bending magnets and downstream drift regions. The initial longitudinal bunch properties are the same as in figs. 8(a)–(b).

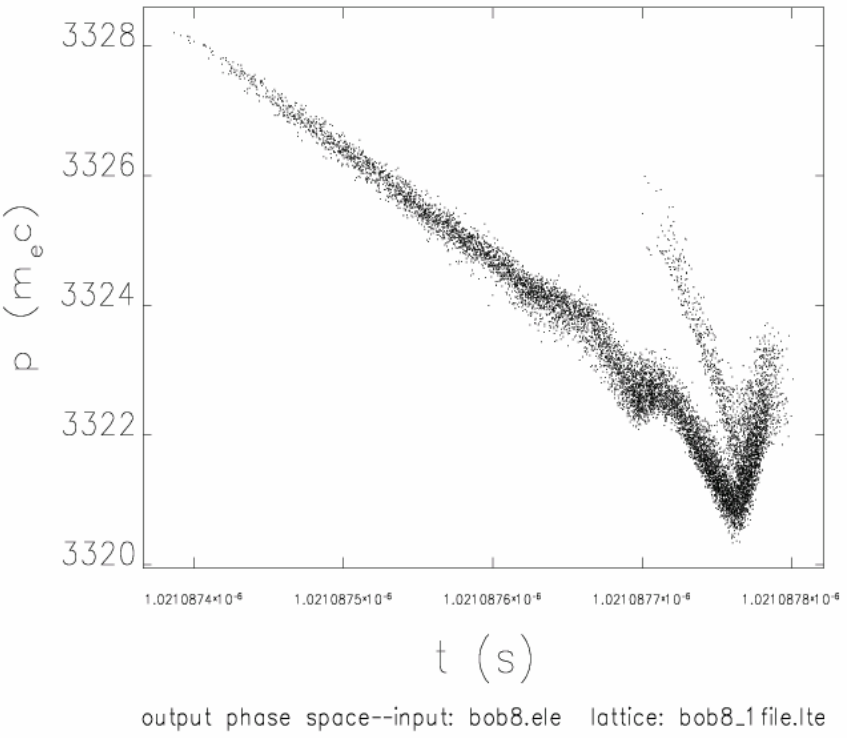

Figure 9(b). Longitudinal phase space at 1.7 GeV from tracking by the code "elegant" of a parabolic bunch of 100,000 particles with peak current of 50 A, charge of 200 pC, rms bunchlength of 0.4 mm, normalized emittance of 1 μm and Gaussian energy spread of 3 keV. Coherent synchrotron radiation is modeled in the chicane bending magnets and downstream drift regions. The initial longitudinal bunch properties are the same as in figs. 8(c)–(d).

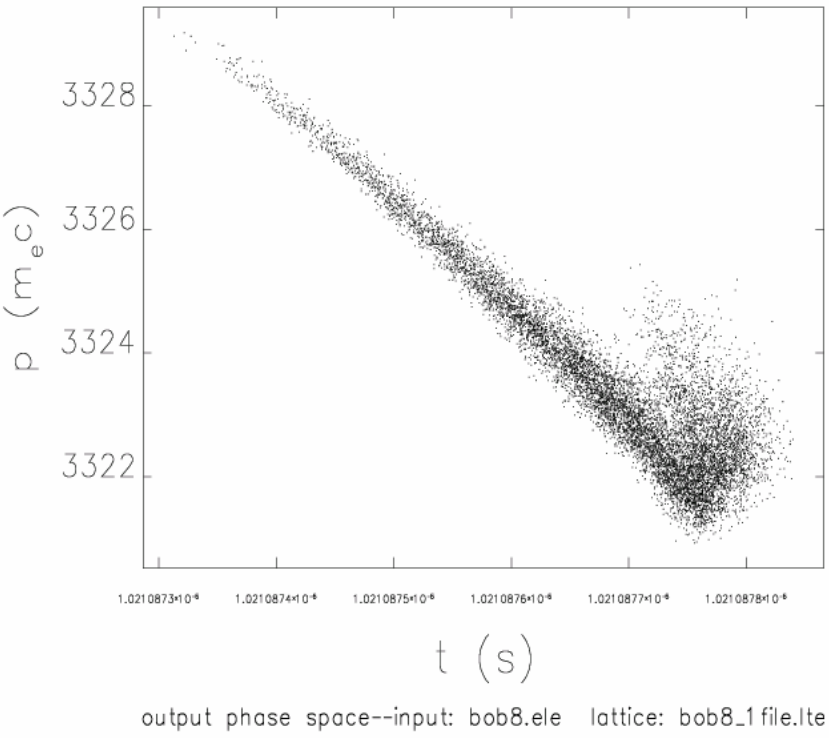

Figure 9(c). Longitudinal phase space at 1.7 GeV from tracking by the code "elegant" of a parabolic bunch of 100,000 particles with peak current of 50 A, charge of 200 pC, rms bunchlength of 0.4 mm, normalized emittance of 1 μm and Gaussian energy spread of 10 keV. Coherent synchrotron radiation is modeled in the chicane bending magnets and downstream drift regions. The initial longitudinal bunch properties are the same as in figs. 8(e)–(f).

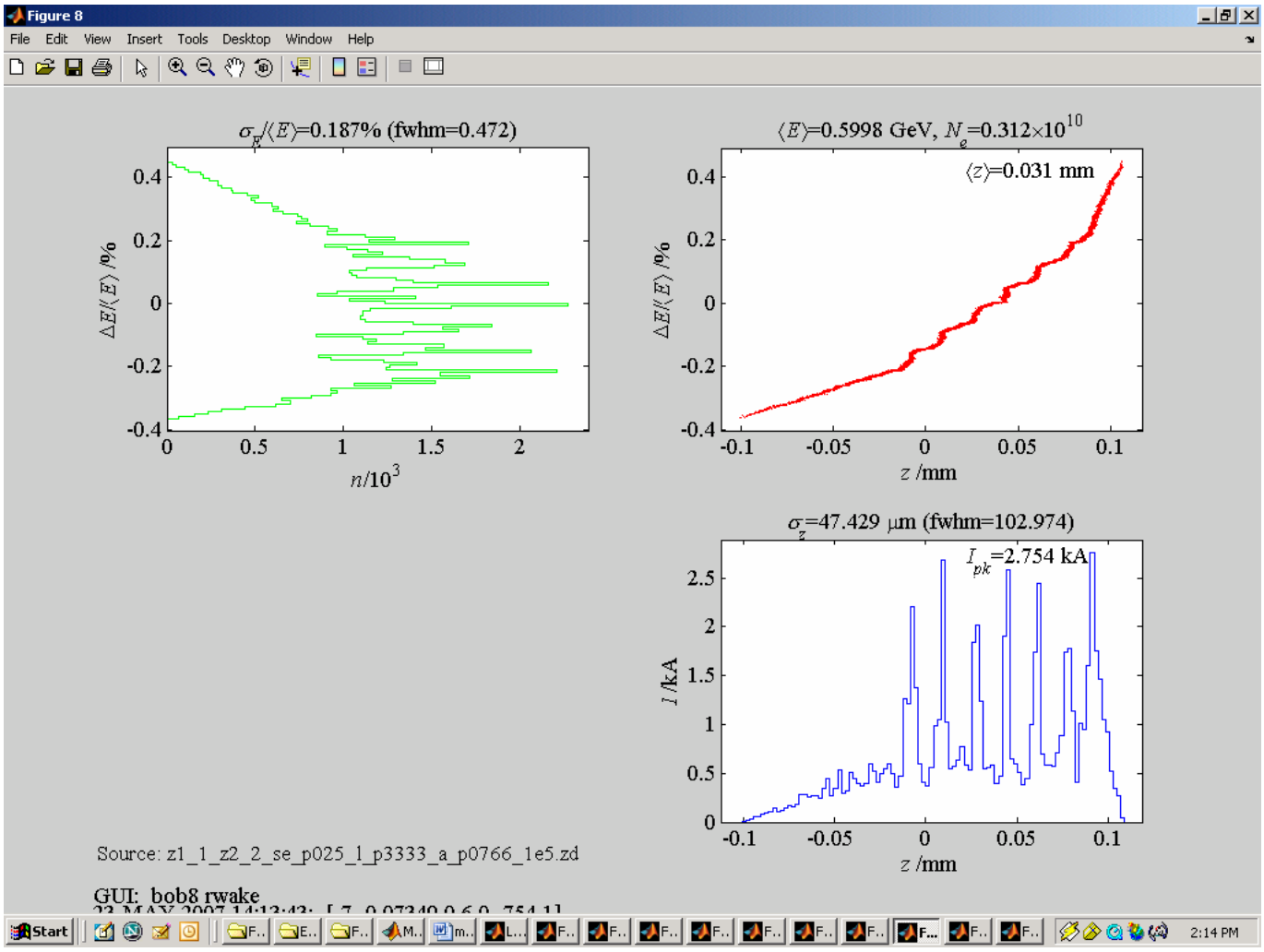

Figure 10(a). Bunch properties immediately after the second bunch compressor chicane BC2 (and prior to the resistive impedance R_2) for a trapezoidal bunch of 100,000 particles at 4 MeV with Gaussian energy spread of 1 keV and current modulation. The initial bunch has current of 50 A, and a current modulation at wavelength 0.3333 mm with $\Delta I / I = 0.0766$. Wakes from resistive impedance of $3Z_0$ are modeled after each chicane.

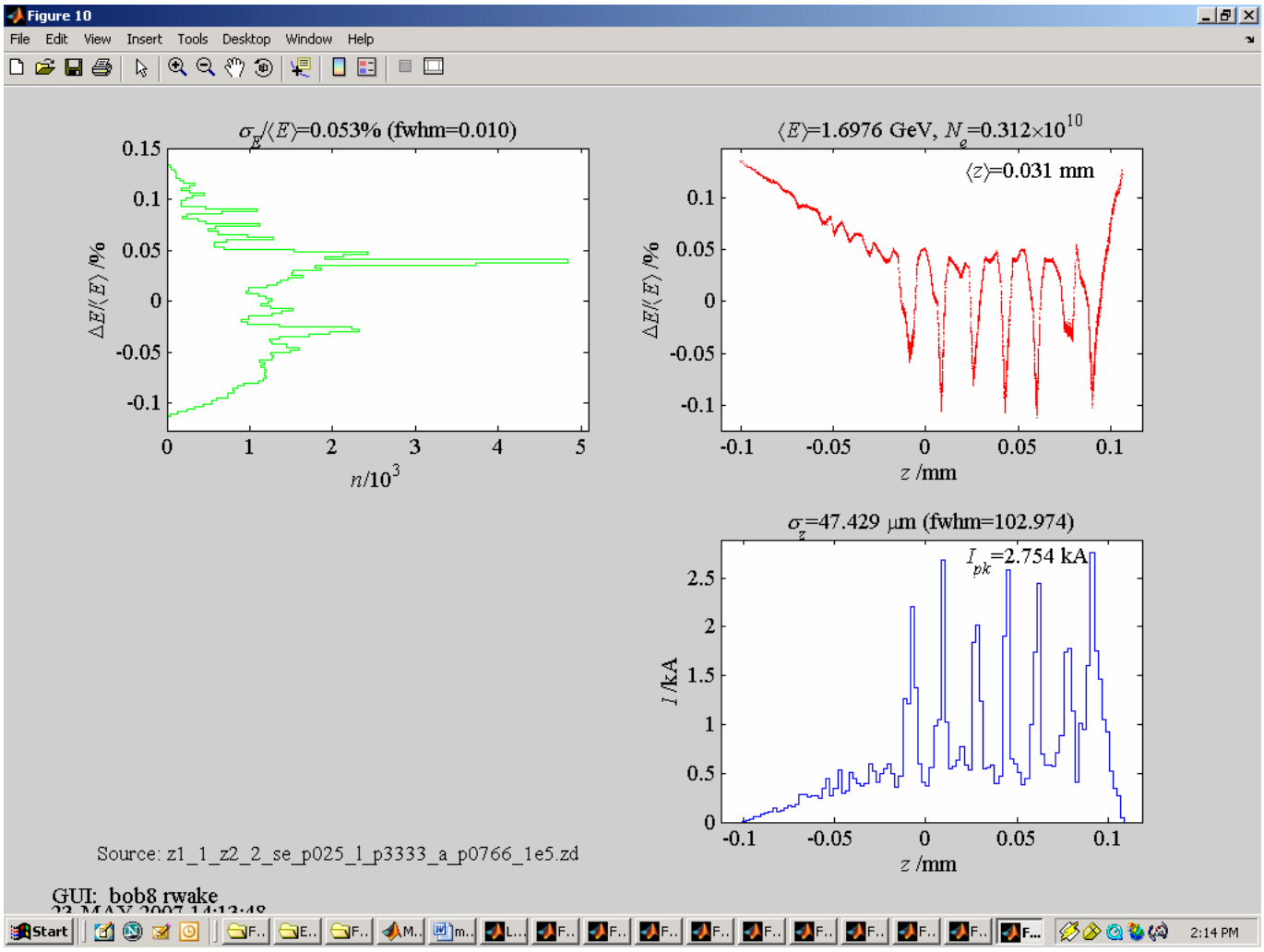

Figure 10(b). Bunch properties at 1.7 GeV for an initial trapezoidal bunch of 100,000 particles at 4 MeV with Gaussian energy spread of 1 keV and current modulation. The initial bunch has current of 50 A, with a current modulation at wavelength 0.3333 mm with $\Delta I / I = 0.0766$. Wakes from resistive impedance of $3Z_0$ are modeled after each chicane.

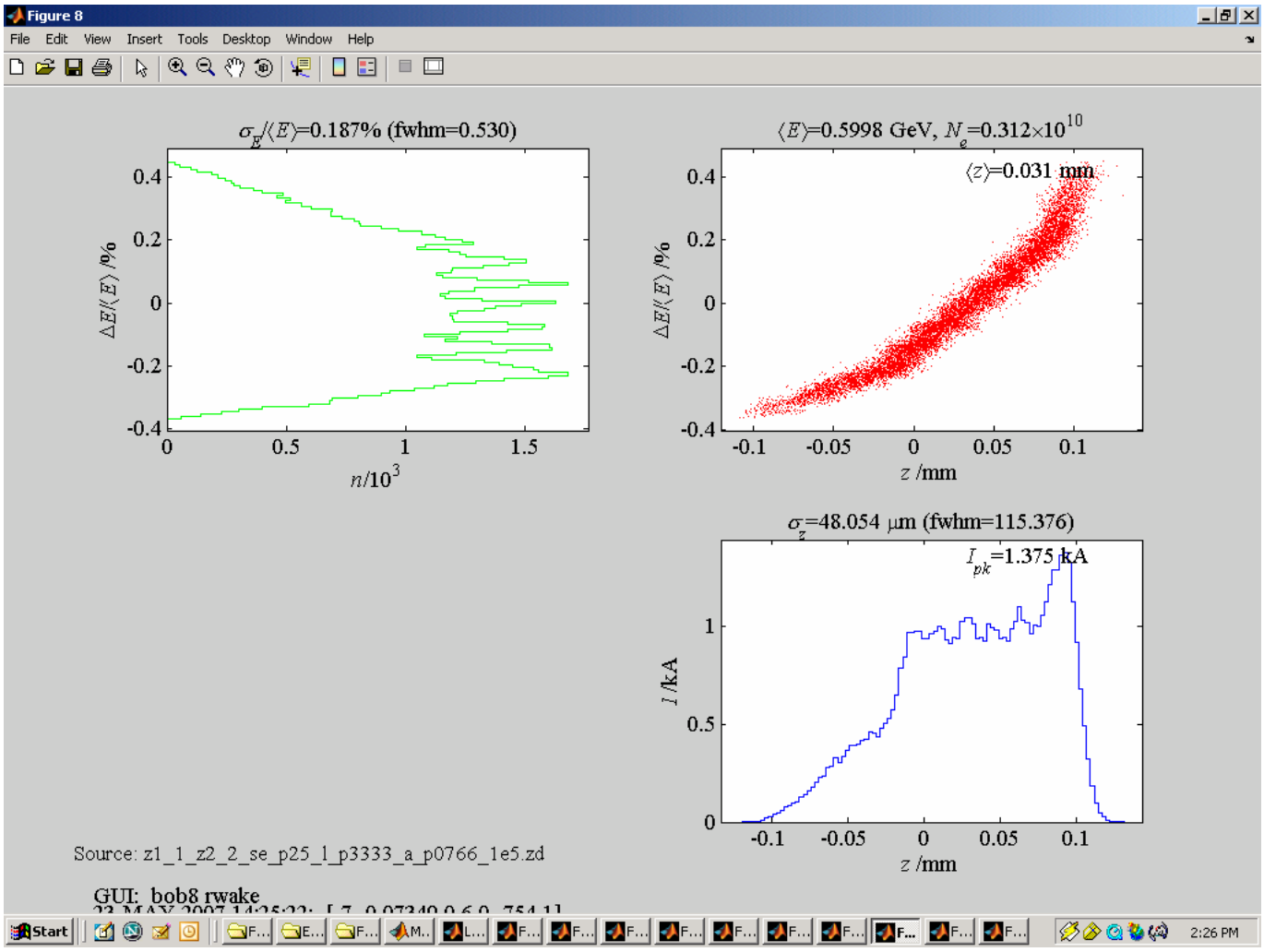

Figure 10(c). Bunch properties immediately after the second bunch compressor chicane BC2 (and prior to the resistive impedance R_2) for an initial trapezoidal bunch of 100,000 particles at 4 MeV with Gaussian energy spread of 10 keV and current modulation. The initial bunch has current of 50 A, with a current modulation at wavelength 0.3333 mm with $\Delta I / I = 0.0766$. Wakes from resistive impedance of $3Z_0$ are modeled after each chicane.

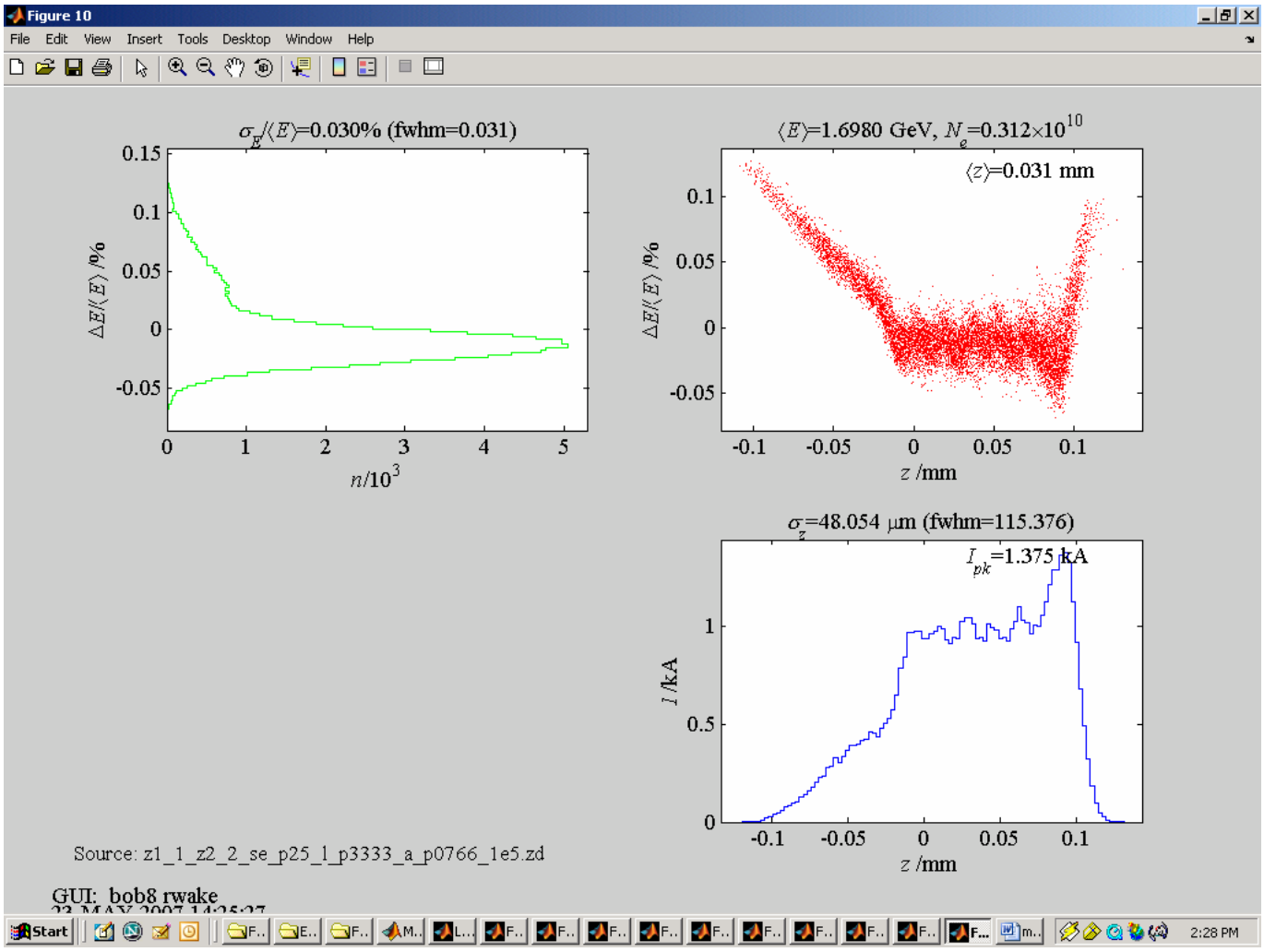

Figure 10(d). Bunch properties at 1.7 GeV for an initial trapezoidal bunch of 100,000 particles at 4 MeV with Gaussian energy spread of 10 keV and current modulation. The initial bunch has current of 50 A, with a current modulation at wavelength 0.3333 mm with $\Delta I / I = 0.0766$. Wakes from resistive impedance of $3Z_0$ are modeled after each chicane.

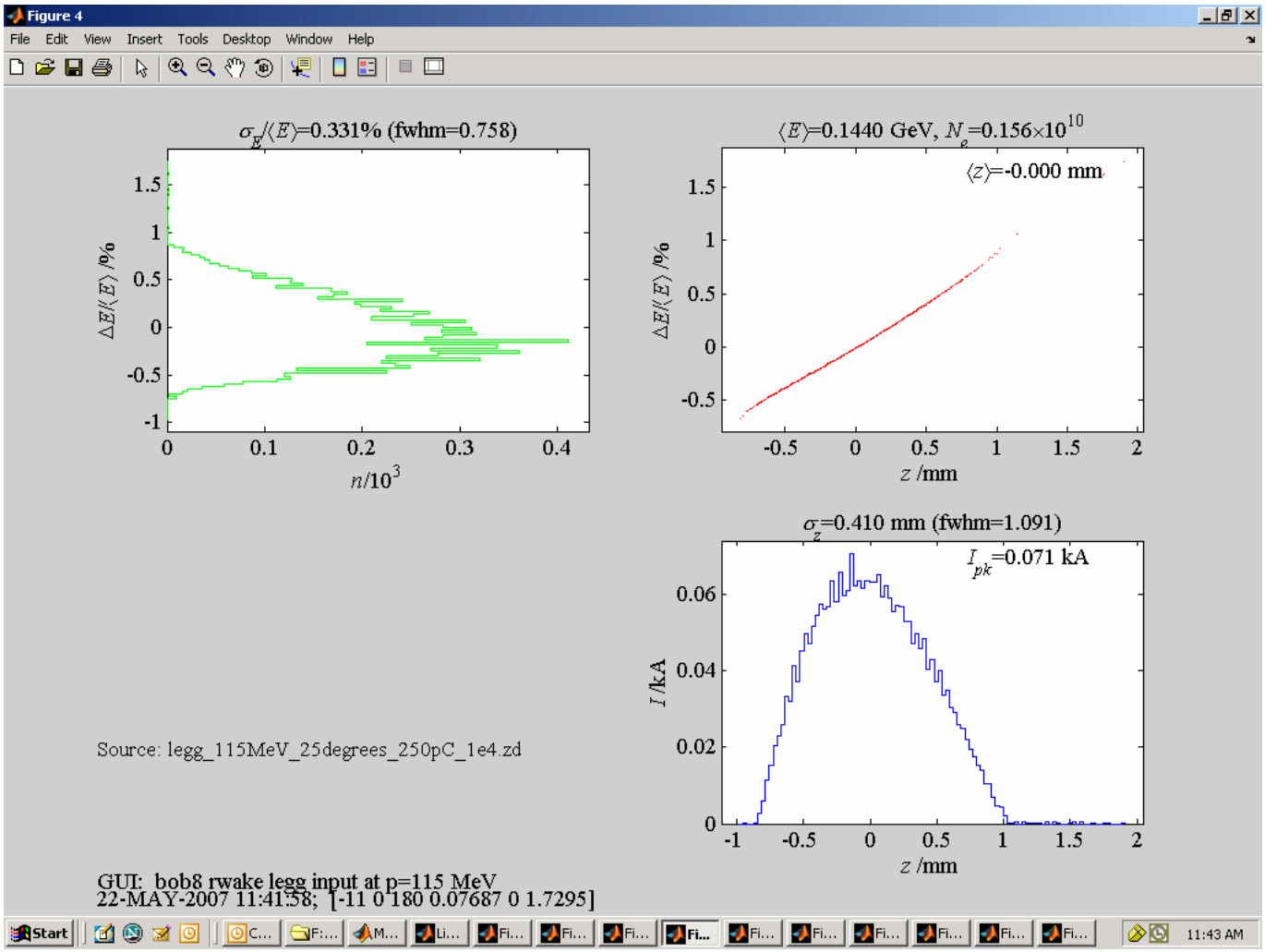

Figure 11(a). Bunch properties prior to entering the first bunch compressor chicance BC1 at energy of 144 MeV, for a 250 pC elliptical bunch obtained from a "Coulomb explosion." The bunch's initial distribution at energy of 115 MeV was given by an output file from the code ASTRA with coordinates for 10,000 particles. Linac phases and energy of compression were modified to compress this bunch by a factor of ~20 and minimize the chirp at energy of 1.7 GeV when CSR is not considered.

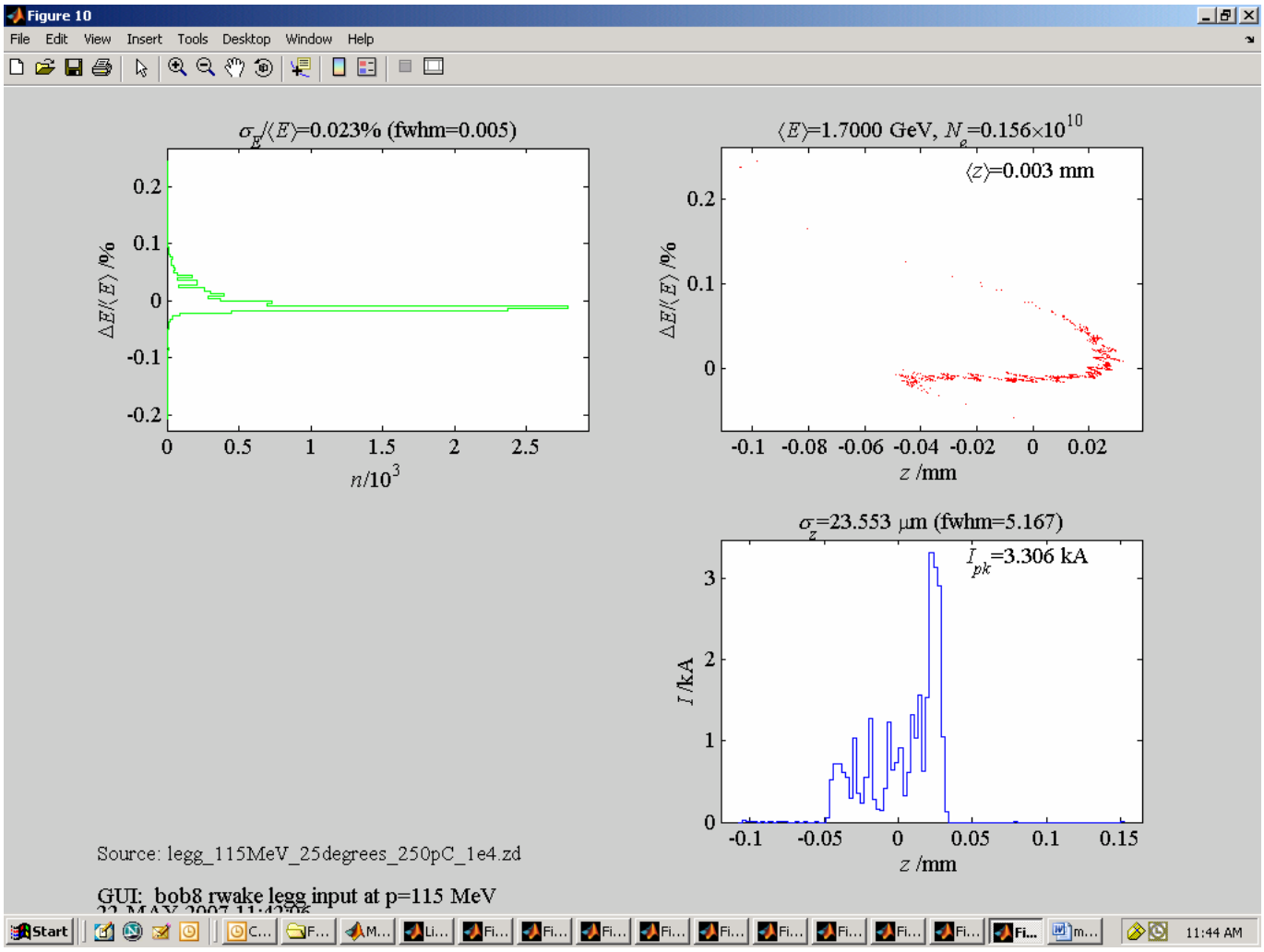

Figure 11(b). Bunch properties at 1.7 GeV from tracking an elliptical bunch of 10,000 particles without wakes.

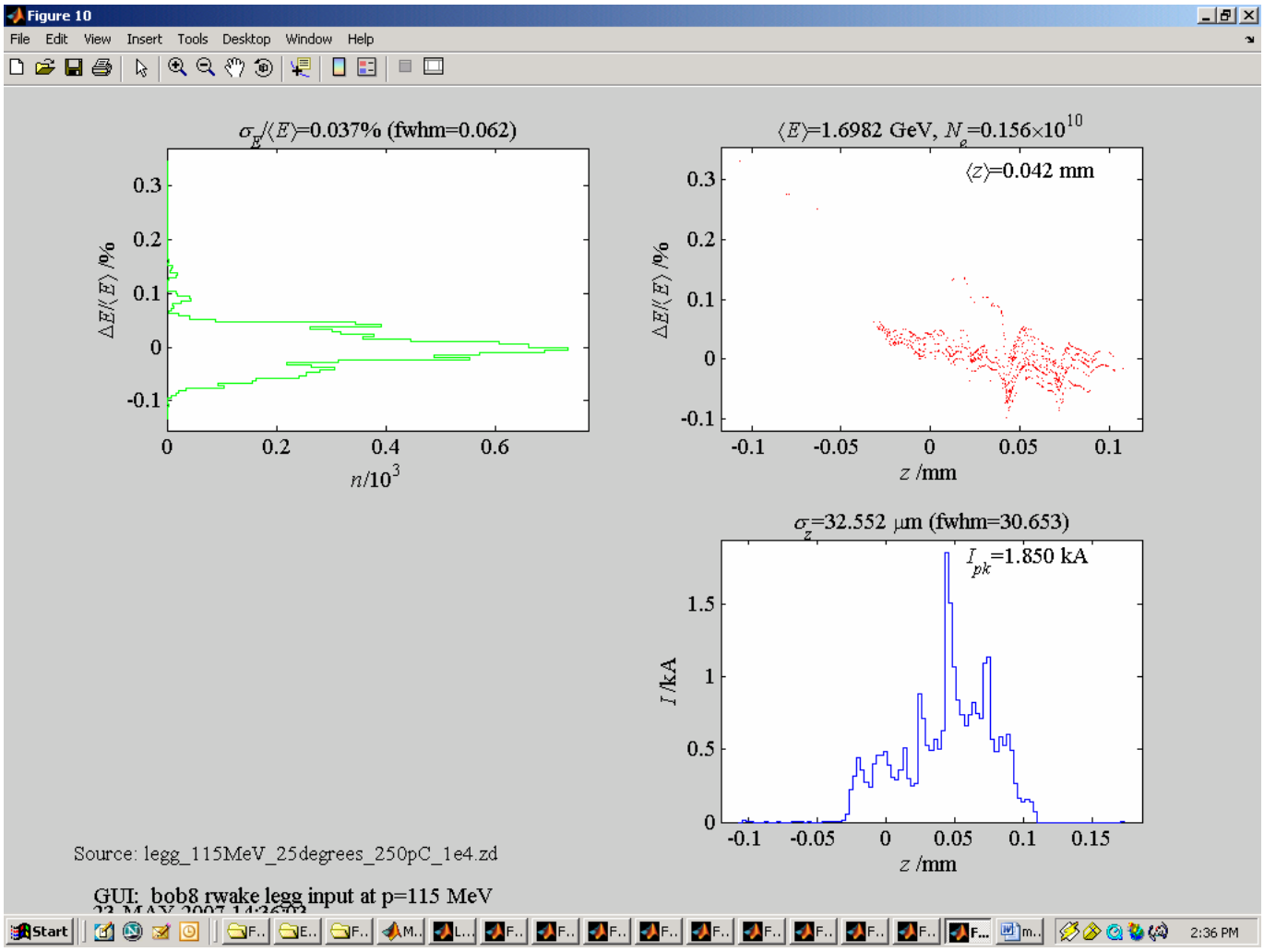

Figure 11(c). Bunch properties at 1.7 GeV when an elliptical bunch of 10,000 particles is compressed, for the case where the CSR wake after each chicane is approximated by the wake from a resistive impedance of $3Z_0 = 1131\,\Omega$.

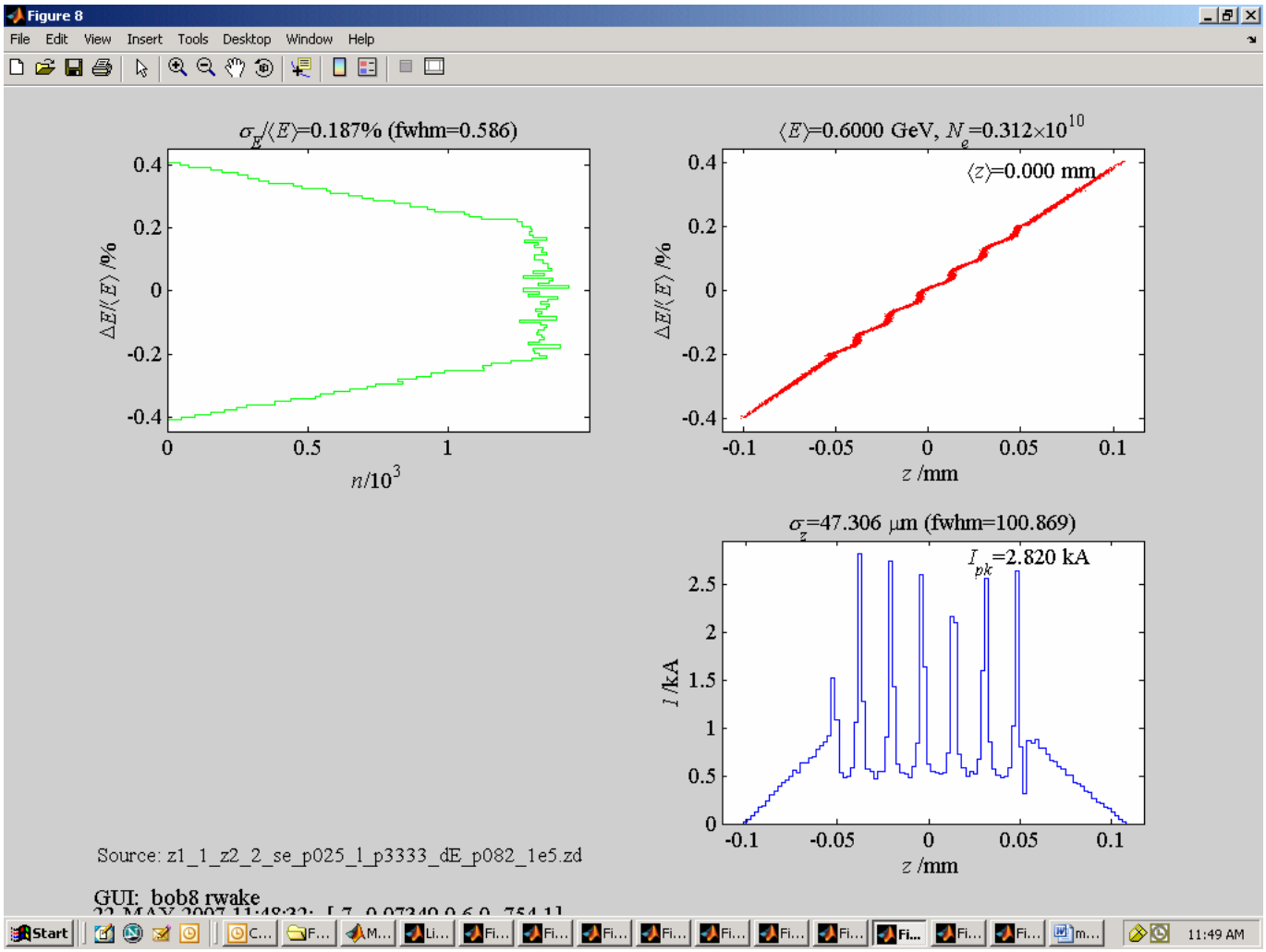

Figure 12(a). Bunch properties immediately after the second bunch compressor BC2 when an initial trapezoidal bunch of 100,000 particles with peak current of 50 A and energy spread of 1 keV has an energy modulation at wavelength 0.3333 mm of amplitude 3.28 keV. No wakes are included in the tracking.

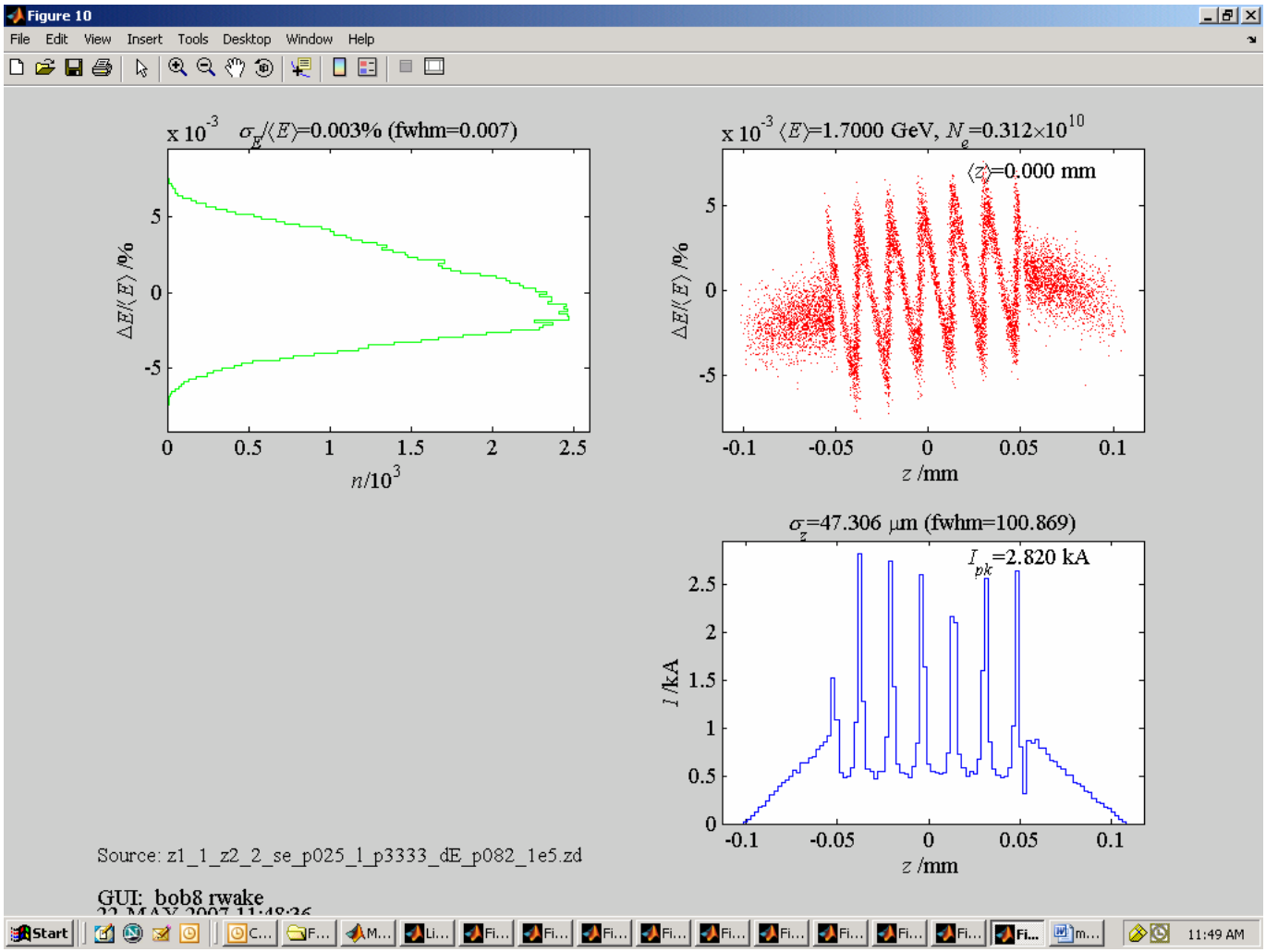

Figure 12(b). Bunch properties at 1.7 GeV when an initial trapezoidal bunch of 100,000 particles with peak current of 50 A and energy spread of 1 keV has an energy modulation at wavelength 0.3333 mm of amplitude 3.28 keV. No wakes are included in the tracking.

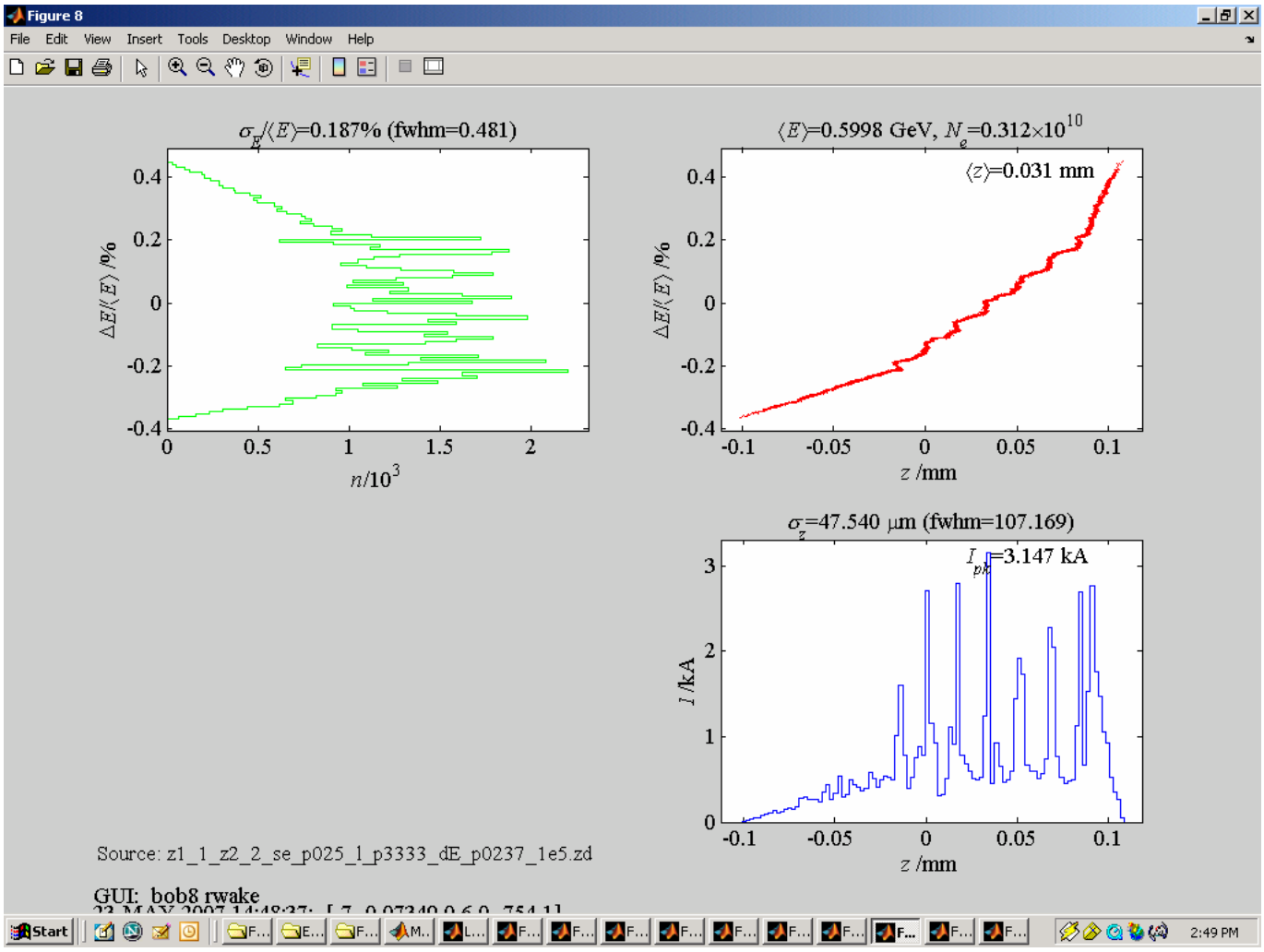

Figure 12(c). Bunch properties immediately after the second bunch compressor (and prior to the resistive impedance R_2) when an initial trapezoidal bunch of 100,000 particles with peak current of 50 A and energy spread of 1 keV has an energy modulation at wavelength 0.3333 mm of amplitude 948 eV. In this tracking, resistive impedance of $3Z_0$ after each bunch compressor chicane approximates the coherent radiation wake.

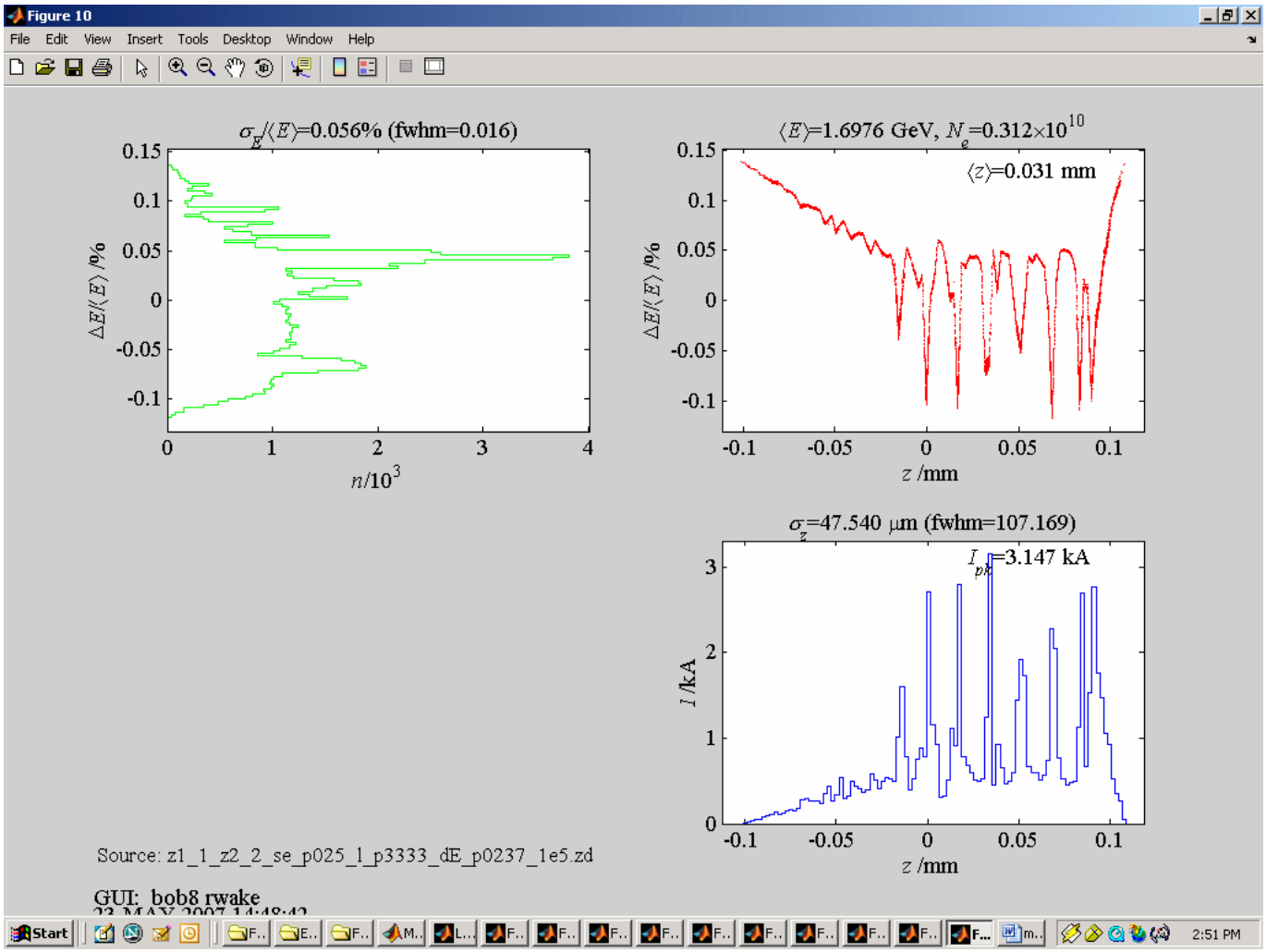

Figure 12(d). Bunch properties at 1.7 GeV when an initial trapezoidal bunch of 100,000 particles with peak current of 50 A and energy spread of 1 keV has an energy modulation at wavelength 0.3333 mm of amplitude 948 eV. In this tracking, resistive impedance of $3Z_0$ after each bunch compressor chicane approximates the coherent radiation wake.

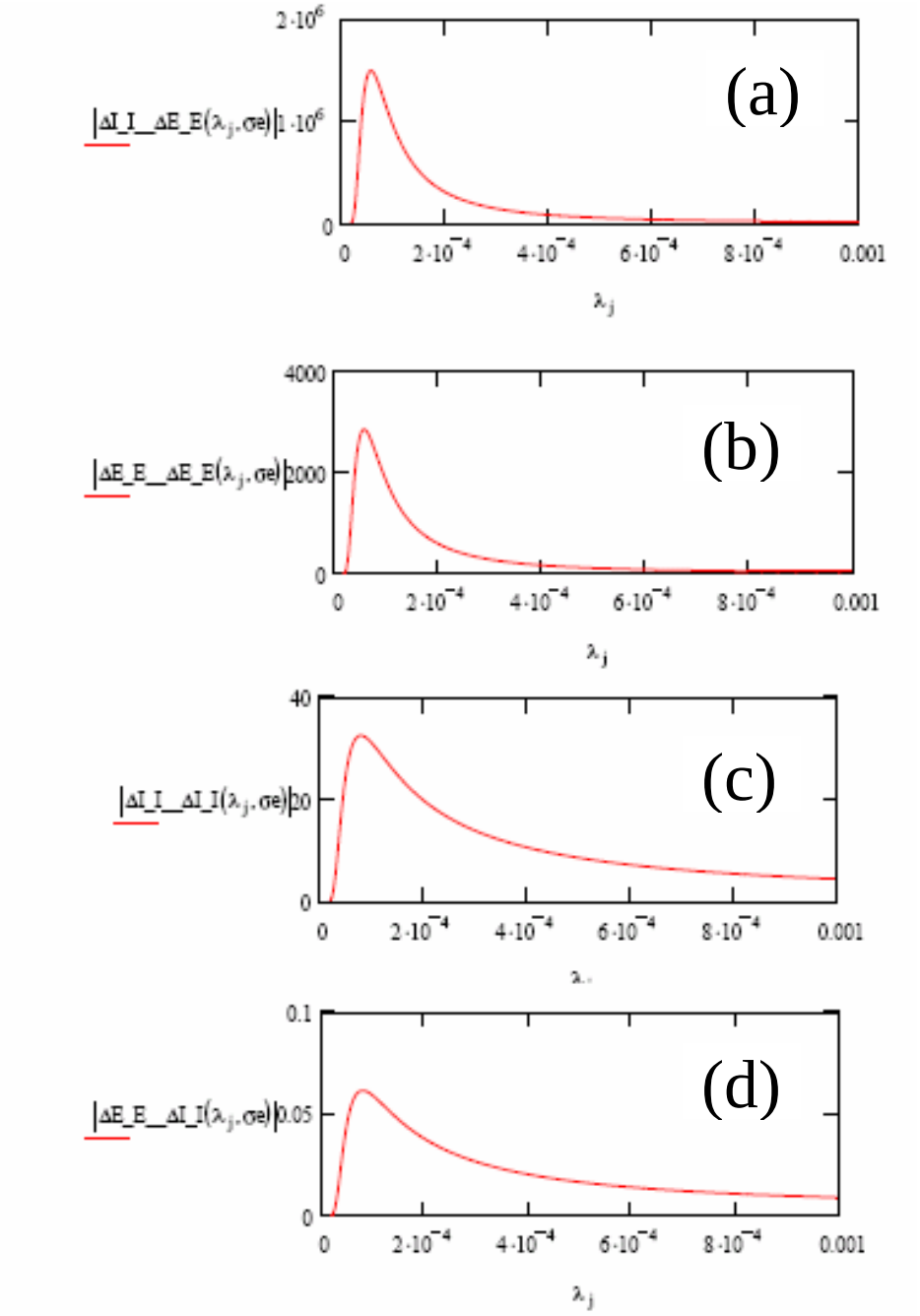

Figure 13. Microbunching gain versus wavelength in meters, for a 50-A bunch current and Gaussian energy spread of 1 keV, calculated for $R_1 = R_2 = 3Z_0$. (a) $|(\Delta I / I_{out})/(\Delta E / E)_{in}|$ (b) $|(\Delta E / E_{out})/(\Delta E / E)_{in}|$ (c) $|(\Delta I / I_{out})/(\Delta I / I)_{in}|$ (d) $|(\Delta E / E_{out})/(\Delta I / I)_{in}|$

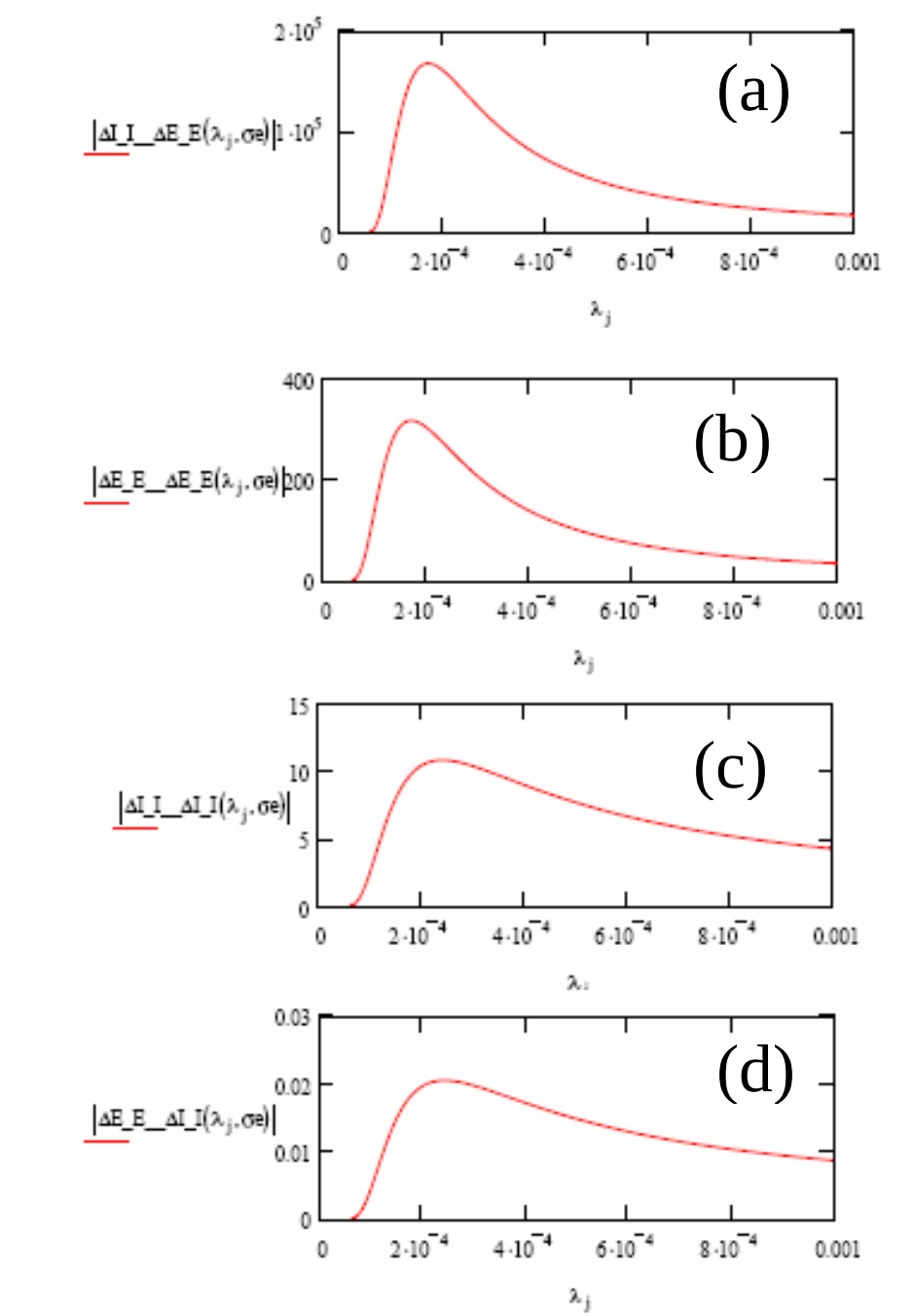

Figure 14. Microbunching gain versus wavelength in meters, for a 50-A bunch current and Gaussian energy spread of 3 keV, calculated for $R_1 = R_2 = 3Z_0$. (a) $|(\Delta I / I_{out})/(\Delta E / E)_{in}|$ (b) $|(\Delta E / E_{out})/(\Delta E / E)_{in}|$ (c) $|(\Delta I / I_{out})/(\Delta I / I)_{in}|$ (d) $|(\Delta E / E_{out})/(\Delta I / I)_{in}|$

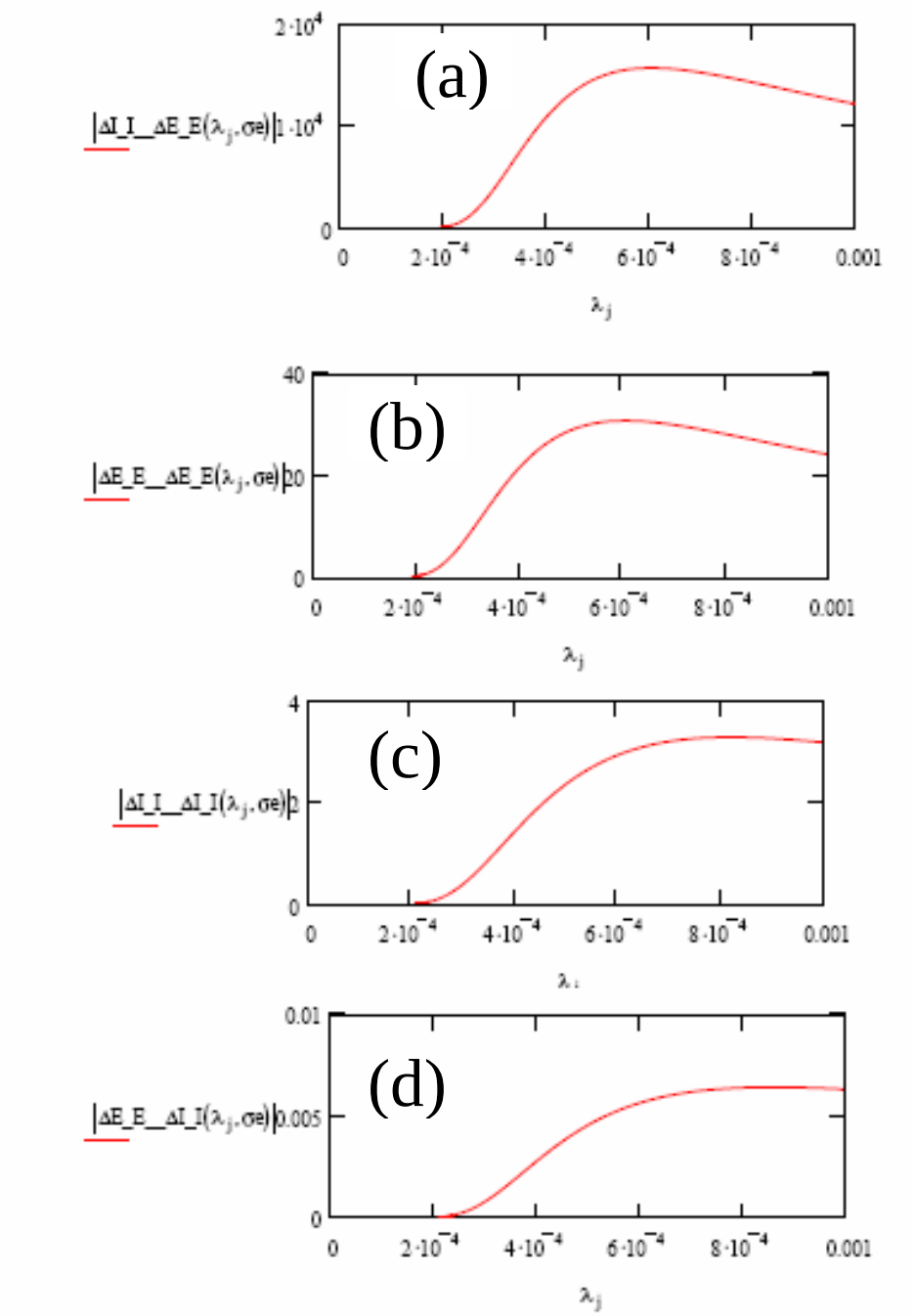

Figure 15. Microbunching gain versus wavelength in meters, for a 50-A bunch current and Gaussian energy spread of 10 keV, calculated for $R_1 = R_2 = 3Z_0$. (a) $|(\Delta I / I_{out})/(\Delta E / E)_{in}|$ (b) $|(\Delta E / E_{out})/(\Delta E / E)_{in}|$ (c) $|(\Delta I / I_{out})/(\Delta I / I)_{in}|$ (d) $|(\Delta E / E_{out})/(\Delta I / I)_{in}|$

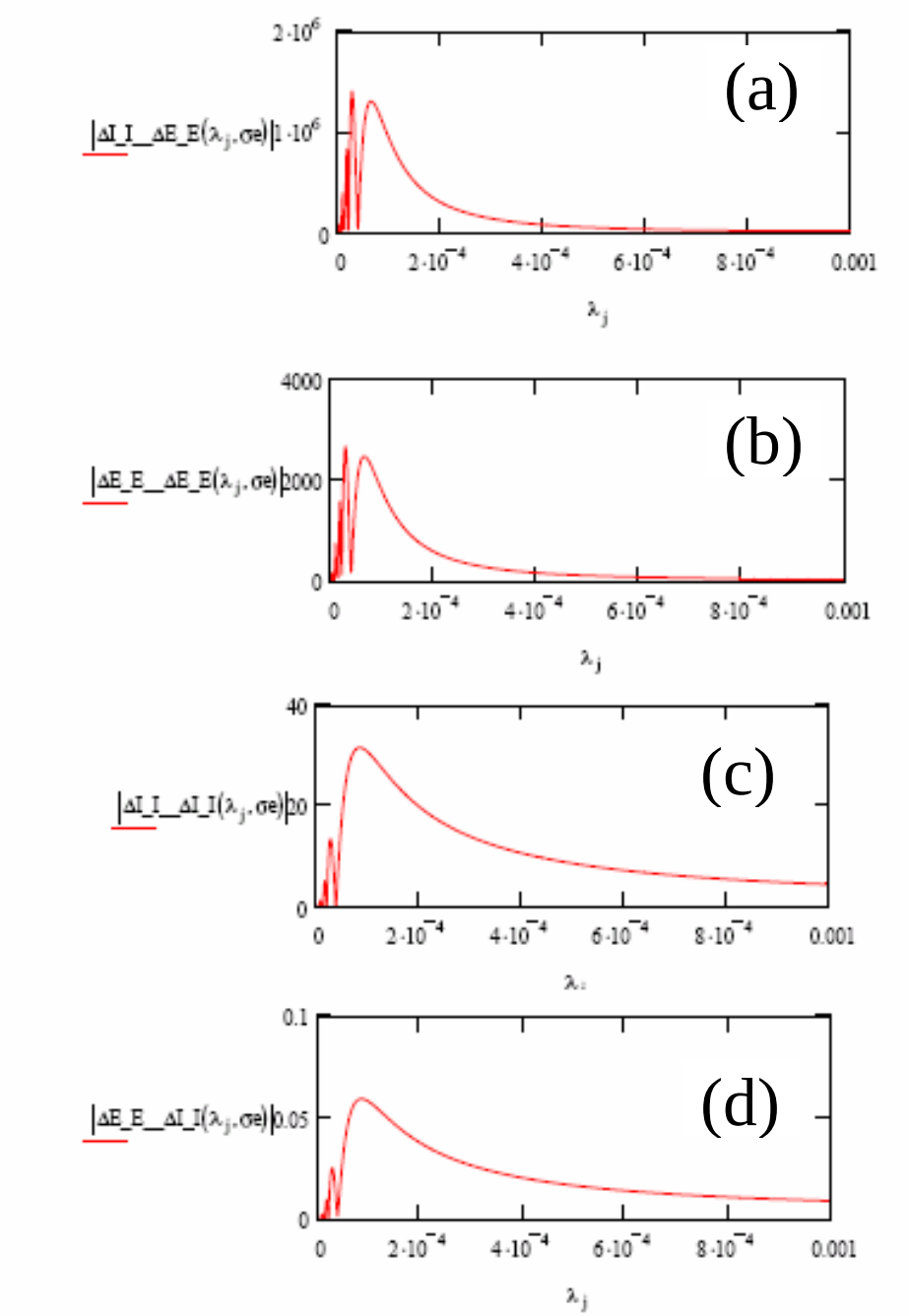

Figure 16. Microbunching gain versus wavelength in meters, for a 50-A bunch current and energy spread of 1 keV from a matched laser heater, calculated for $R_1 = R_2 = 3Z_0$. (a) $|(\Delta I / I_{out})/(\Delta E / E)_{in}|$ (b) $|(\Delta E / E_{out})/(\Delta E / E)_{in}|$ (c) $|(\Delta I / I_{out})/(\Delta I / I)_{in}|$ (d) $|(\Delta E / E_{out})/(\Delta I / I)_{in}|$

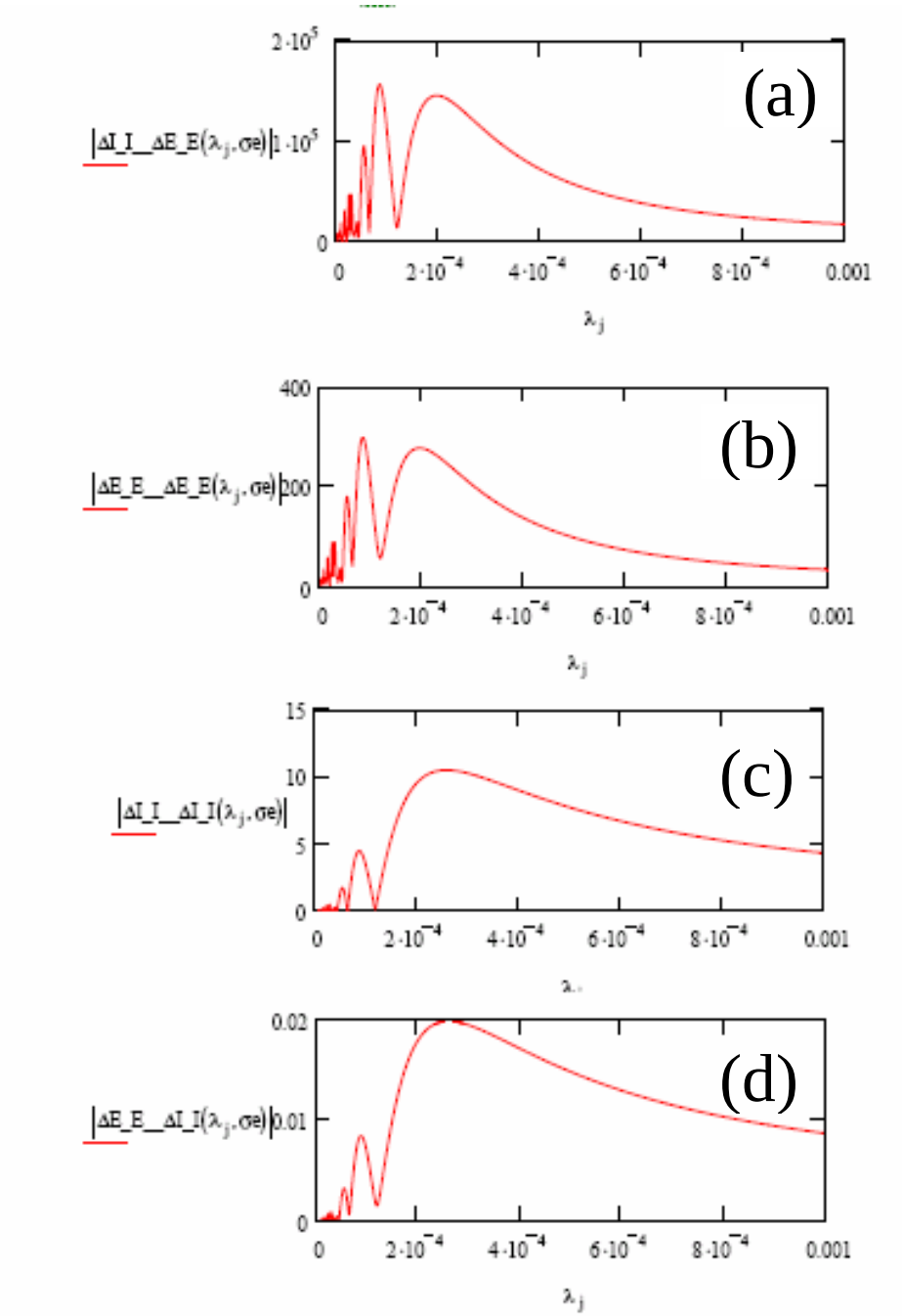

Figure 17. Microbunching gain versus wavelength in meters, for a 50-A bunch current and energy spread of 3 keV from a matched laser heater, calculated for $R_1 = R_2 = 3Z_0$. (a) $|(\Delta I / I_{out})/(\Delta E / E)_{in}|$ (b) $|(\Delta E / E_{out})/(\Delta E / E)_{in}|$ (c) $|(\Delta I / I_{out})/(\Delta I / I)_{in}|$ (d) $|(\Delta E / E_{out})/(\Delta I / I)_{in}|$

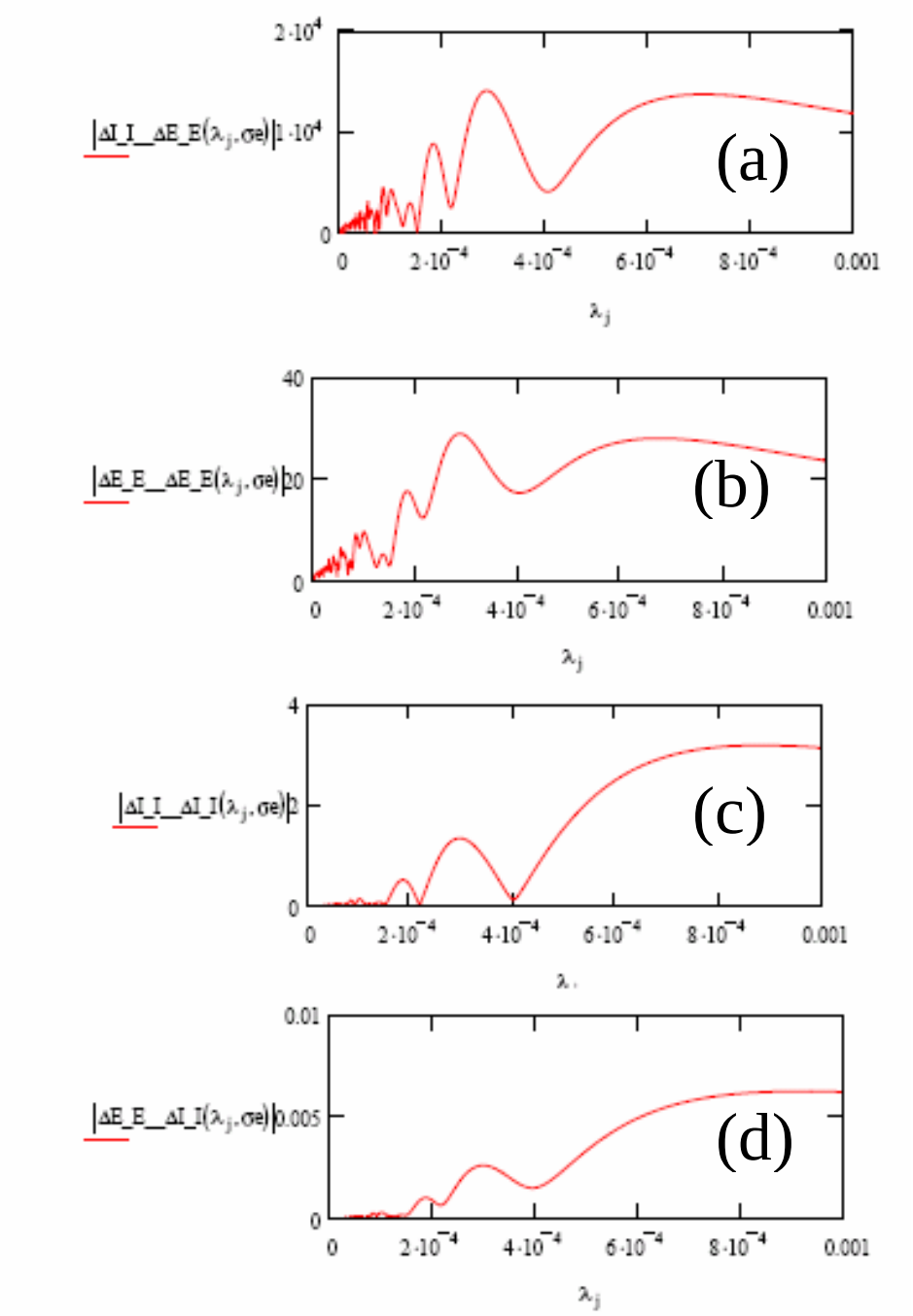

Figure 18. Microbunching gain versus wavelength in meters, for a 50-A bunch current and energy spread of 10 keV from a matched laser heater, calculated for $R_1 = R_2 = 3Z_0$. (a) $|(\Delta I / I_{out})/(\Delta E / E)_{in}|$ (b) $|(\Delta E / E_{out})/(\Delta E / E)_{in}|$ (c) $|(\Delta I / I_{out})/(\Delta I / I)_{in}|$ (d) $|(\Delta E / E_{out})/(\Delta I / I)_{in}|$